

Copyright

by

Sean Martin Maguire

2017

The Dissertation Committee for Sean Martin Maguire Certifies that this is the approved version of the following dissertation:

**SOCIAL CONTEXT AND STATUS AFFECT BEHAVIOR,
PHYSIOLOGY AND BRAIN ACTIVITY OF THE HIGHLY SOCIAL
CICHLID FISH, *ASTATOTILAPIA BURTONI***

Committee:

Johann Hofmann, Supervisor

Steve Phelps

Andrea Gore

Mike Ryan

David Crews

Kim Hoke

**SOCIAL CONTEXT AND STATUS AFFECT BEHAVIOR,
PHYSIOLOGY AND BRAIN ACTIVITY OF THE HIGHLY SOCIAL
CICHLID FISH, *ASTATOTILAPIA BURTONI***

by

Sean Martin Maguire, BS

Dissertation

Presented to the Faculty of the Graduate School of

The University of Texas at Austin

in Partial Fulfillment

of the Requirements

for the Degree of

Doctor of Philosophy

The University of Texas at Austin

May 2017

Dedication

To my parents, Bill and Chris Maguire.

Acknowledgements

This work has been vastly improved by the input from my advisor, Hans Hofmann. Hans allowed me the freedom to explore my ideas and I have learned a great deal from him in our many long conversations over the years. I would not have been able to complete the onerous project of writing this manuscript without his positive attitude and coaching throughout the last few months. I want to also thank my committee members for their help and comments as well as Rebecca Young, Caitlin Friesen, Marianna Rodriguez, Bridget Nugent and Eva Fischer for editing drafts of various portions of this manuscript. Also Dr. David Crews, Dr. Francisco Gonzalez-Lima and Ross Gillette for their assistance with the cytochrome oxidase experiments. Finally, I want to thank my collaborators, without whom I would not have been able to complete this work: Dr. Peter Dijkstra, Caleb Ellington, Sylvia Garza, and Juliette Rubin.

Thank you to everyone in the Hofmann lab, past and present for making my time in graduate school so pleasant. I could not ask for a friendlier or more collaborative group of people to work with.

I would like to thank Dr. Mark Alkema, for giving me my first taste of research and for allowing me to learn and grow so much. Also the members of his lab for their support and friendship: Jenn Pirri, Jamie Donnelly and Chris Clark.

I would like to thank the NSF and the department of integrative biology for making all of this work possible. I have been fortunate enough to receive a great deal of support, including the graduate research fellowship, DDIG and departmental funds; I am eternally grateful. I would also like to thank the NSF and the Research Council of Norway for awarding me the GROW fellowship to conduct research on Atlantic salmon in the lab of Lars Ebbesson in Norway. It was an amazingly rewarding experience.

I could not have completed this without the support of my friends and family, especially my parents. Thank you for believing in me, anything I have accomplished is because of you. I have made many life-long friends here in Austin, what follows is an incomplete list of the people who have made my time in grad school infinitely more enjoyable: Alejandro Berrío, Oscar Vargas, Rebecca Tarvin, Nathan LeClear, Anna Yu, Silu Wang, Elizabeth Milano, Sarah Sussman, Deise Gonçalves, Décio Tadeu, Lina Valencia, Serena Zhao, Patricia Salerno, Mendy Black, Mariam Okhovat, Chelsea Weitkamp, Laura Abondano, Teofil Nakov, Colin Addis, Catalina Cuellar, Sofía Rodríguez and Michael Pendergast. ¡Que se deerrame sangre, pero no trago!

I would like to thank André Williams. Finishing the Ph.D. has been an exciting but also stressful time and the most difficult project I have ever worked on. Meeting you has made the experience far more bearable and enjoyable. Thank you for your unwavering support.

Finally, I would like to thank you, dear reader. Because you're reading this I'm 99% sure that you're either my friend or family member, so know that I love and appreciate you.

Social Context and Status Affect Behavior, Physiology and Brain Activity of the Highly Social Cichlid Fish, *Astatotilapia burtoni*

Sean Martin Maguire, Ph.D.

The University of Texas at Austin, 2017

Supervisor: Johann A. Hofmann

Group living confers many benefits while at the same time exposing group members to intense competition for resources and status within the group. Monitoring the social environment involves not only participating in many fast paced social interactions but also monitoring the relationships and status of other group members. In chapter 1, we use a network analysis approach to study replicate communities of the cichlid fish, *Astatotilapia burtoni*, which live in fast-paced social groups with a complex dominance hierarchy among males. We found several correlations between an individual's behavior, their position in the social hierarchy and the social environment. In addition, we found that community properties are a key parameter that predicts both cortisol and testosterone levels. In chapter 2 we extend this paradigm and look at the effects of social status within a community on brain activity as measured by cytochrome oxidase histochemistry. In addition, we examined brain activity in transitioning animals as measured by cytochrome oxidase and *egr-1* induction. We find that social status has a variety of subtle effects on brain activity. Finally, we tested the role of the sex steroid hormones estradiol and testosterone on social transition using an aromatase inhibitor as well as an androgen receptor antagonist. We found very few effects of blocking the nuclear androgen pathway. Blocking aromatase resulted in a hyperaggressive phenotype suggesting that estradiol plays an important role in the transition process in this species.

Table of Contents

List of Tables	xii
List of Figures	xiv
Introduction:.....	1
Chapter 1: Social network dynamics predict hormone levels and behavior in the highly social cichlid fish <i>A. burtoni</i>	7
Abstract	7
Introduction.....	7
Materials and Methods.....	13
Animals	13
Behavioral Observations	13
Tissue Collection and Hormone Measurements	14
Statistical Analysis.....	14
Social Network Analysis.....	14
Individual level analysis	15
Analysis of Hormone Measurements	16
Community-Level Analyses	17
Results.....	17
Social Networks of <i>A. burtoni</i>	17
Effects of Social Network Position on Behavior	18
Individual-Level Analysis of Hormones and Behavior	19
Community level regulation of hormones and behavior.....	19
Discussion	21
Individual-level analyses	21
Dyad-level analyses	22
Community-level analyses.....	23
Conclusions.....	25
Acknowledgements.....	25

Chapter 2: The Effects of Social Status on Neural Activity Patterns in Stable and Ascending Males.....	34
Abstract	34
Introduction.....	34
Methods.....	40
Animal care	40
Behavior Studies	40
Hormone assays	42
Brain Sectioning.....	43
Cytochrome oxidase histochemistry	43
Nissl stain.....	44
Brain Homogenate Standards	44
Validation studies.....	45
Quantification	45
Egr-1 <i>in situ</i> hybridization	46
Cloning of <i>A. burtoni</i> egr-1 gene fragment	46
Detection of egr-1 mRNA.....	47
Quantification	49
Statistical analysis.....	50
Behavior.....	50
Growth and GSI.....	50
Hormone data.....	50
COX data	51
Egr-1 data.....	51
Principal components analysis.....	51
Covariance Analyses.....	51
Results.....	53
Discussion	57
Conclusion	61
Acknowledgements.....	62

Chapter 3: Influences of an androgen receptor antagonist and aromatase inhibitor on social transition, physiology and brain activity.	86
Abstract	86
Introduction.....	86
Methods.....	91
Animal care	91
Pharmacology	92
Flutamide	92
Fadrozole.....	93
Behavior Studies	93
Behavioral scoring	95
Hormone assays	95
Brain Sectioning.....	95
Cytochrome oxidase histochemistry	96
Nissl stain	96
Brain Homogenate Standards	97
COX Quantification	98
Egr-1 in situ hybridization	98
Cloning of <i>A. burtoni</i> egr-1 gene fragment	98
Detection of egr-1 mRNA.....	99
Egr-1 Quantification	101
Statistical analysis	102
Behavior.....	102
Growth and Gonad size.....	102
Hormone data.....	103
COX and egr-1 mean differences	103
Correlations between COX, egr-1 and behavior.....	103
Principal components analysis	104
Analysis of receptor densities	104
Covariance Analyses.....	104

Results	106
Discussion	109
The antiandrogen treatment did not affect behavior or physiology:	110
Inhibiting aromatase causes transitioning males to become hyperaggressive and dramatically affected hormone levels	112
Antiandrogen treatment did not affect cytochrome oxidase levels throughout fore- and midbrain	115
Inhibiting aromatase affected cytochrome oxidase in select fore- and midbrain areas	116
Antiandrogen treatment affected egr-1 activity in several areas	117
Hyperaggression in fadrozole treated animals may be related to reduced activity of the lateral septum	118
Covariance analysis suggests possible functional circuits for future studies	119
Conclusion	119
Acknowledgements	120
Conclusion:	154
Chapter 1: <i>A. burtoni</i> social interaction networks	154
Chapter 2: Brain activity patterns in DOM, SUB and Ascending males....	156
Chapter 3: Perturbing androgen and estrogen signaling during social ascension	157
The neuromodulatory patterning hypothesis and alternative frameworks..	159
From social context to neuromodulatory patterning: links across the studies	162
Appendix A: Cytochrome Oxidase Atlas	165
References	169
Vita	185

List of Tables

Table 1.1: Receiving aggression from other community members correlates to the behavior that those individuals express. Results of four mixed models comparing the aggression received from DOMs (first two rows) or SUBs (last two rows) depending on the social status of the receiver. Significant effects are displayed in bold.	33
Table 2.1: Brain area abbreviations used in this paper and putative mammalian homologous (O’Connell and Hofmann 2011). Continued on the next page.	79
Table 2.1: Continued.....	80
Table 2.2: Full statistical results of least-square means comparing behavior of ascending and control males at each time point.....	81
Table 2.3: Posthoc testing of the least-square means of COX levels of each brain area compared between ascending and control males.	82
Table 2.3: Continued.....	83
Table 2.4: Loadings of the first four principal components in each dataset. PCs with a magnitude $\geq .25$ are shown in bold.....	84
Table 2.5: Significant clusters of correlated brain areas identified by multiscale bootstrapping of the correlation matrix. Clusters were ordered to highlight similarities across datasets.....	85
Table 3.1: Abbreviations of brain areas used in this paper and putative mammalian homologies (O’Connell and Hofmann 2011). Continued on the next page.	137
Table 3.1: Continued.....	138

Table 3.2: Results of ANOVA of behavior data.....	139
Table 3.3: Posthoc testing of least-squares means of the behavior data. Continued on the next page.	140
Table 3.3: Continued.....	141
Table 3.4: Full results of models testing the treatment effects on COX levels in each brain area. Continued on the next page.....	142
Table 3.4: Continued on the next page.	143
Table 3.4: Continued on the next page.	144
Table 3.4: Continued.....	145
Table 3.5: Full results of models testing the treatment effects on <i>egr-1</i> levels in each brain area.....	146
Table 3.5: Continued on the next page.	147
Table 3.5: Continued on the next page.	148
Table 3.5: Continued on the next page.	149
Table 3.5: Continued.....	150
Table 3.6: Receptor density categories of each brain area based on Munchrath and Hofmann (2010).....	151
Table 3.7: Significant clusters of correlated brain areas identified by multiscale bootstrapping of the correlation matrix. Clusters were ordered to highlight similarities across datasets.....	152
Table 3.8: Mantel test results for each covariance matrix comparison.....	153

List of Figures

- Figure 1.1: Example networks of a single *A. burtoni* community over time. DOM and SUB Individuals are depicted in the same position on each day. DOM males (dark gray squares) are depicted in the corner of the tank that they occupied, while SUB males (light gray circles) are arranged randomly. Females (white rectangles) were not identified individually and are depicted as an aggregate node representing all eight females.27
- Figure 1.2: DOM males are network hubs and networks are stable over time. A) Density plot of the distribution of in-degree (number of incoming connections) for DOM (dark gray) and SUB (light gray) males. B) Density plot of the distribution of out-degree (number of outgoing connections) in the network as a function of status. C) Correlation coefficients of the matrices representing networks of each community on consecutive days.28
- Figure 1.3: A) DOM males (dark gray) have higher testosterone levels and lower cortisol levels compared to SUB males (light gray). B) Testosterone is significantly correlated to aggression directed towards females.29
- Figure 1.4: The DOM-FEM connectedness (the average amount of aggression directed from DOM males towards females in a community) correlated to lower SUB male aggression, even controlling for direct interactions between DOM and SUB.30

Figure 1.5: The average number of DOM-DOM connections correlates to lower testosterone levels (A) and higher cortisol (B) in both DOM (dark gray) and SUB (light gray) males. C) The average number of DOM-FEM connections in the community correlates to higher levels of testosterone in DOM community members but not SUB. D) The average number of SUB-SUB connections in the community correlates to increases in SUB male testosterone.....31

Figure 1.6: The community effect on testosterone correlates to network stability. A) Average and standard error of DOM (dark gray) and SUB (light gray) testosterone levels, centered on the whole community average, plotted for each community. Communities are plotted in order of increasing stability index. B) The difference between the average DOM testosterone levels and the average SUB levels in each community correlates to the stability index.32

Figure 2.1: A) Experimental paradigm and timeline. Compartments-A side communities of one male and three females which serve as a social stimulus for all animals in the paradigm. Compartment-B suppressor male. Compartment C- Suppressor male that is removed in the social opportunity treatment. Compartment D – refuge for focal male. Compartment E – chamber that allows for the presentation of an intruder male to both transitioning animals or the subordinate controls. Stable DOM males (dark red) have more aggressive (B) and sexual behavior (C) than stable SUB males (dark blue) and less submissive behavior (D). Social opportunity males (light red) rapidly increase levels of aggression (B) and sexual behavior (C) and decrease levels of submissive behavior (D) after the opportunity to ascend in status compared to sham controls (light blue).+ = $p < 0.05$ in the comparison between Stable DOM and SUB, * = $p < 0.05$ in the comparison between ascending males and control within that time point.....63

Figure 2.2: Example micrographs of radioactive *in situ*. All photos depict the granular zone of the dorsolateral part of the pallium (dlg1). A) 5x Brightfield and corresponding darkfield (B) micrograph of a slide incubated with the sense control probe. C) 5x Brightfield and corresponding darkfield (D) micrograph of a slide incubated with the antisense probe. E) An example of the 40x magnification used for quantification. F) The result of processing the photo in (E) with our imaging processing and silver grain counting program. Numbered blue dots represent individual silver grains counted by our algorithm. All scale bars = 0.1 mm.....64

Figure 2.3: Social status influences many physiological parameters, letter codes in A-C represent statistical differences between groups. A) Stable DOM (dark red) and ascending males (light red) had a higher growth rate than control males (light blue). Stable SUB males (dark blue) were intermediate. B) DOM and ascending males had relatively larger gonads than stable SUB males. Control males were intermediate. C) DOM and ascending males had elevated testosterone levels compared to stable SUB males. Control males were lower than stable DOM males but not different from ascending males. D) Ascending males had higher levels of circulating estradiol compared to control.65

Figure 2.4: Aggression towards the intruder was not significantly different between ascending (light red) and control males (light blue). A) Latency to attack the intruder. B) Number of aggressive displays toward the intruder/ min. C) In ascending males, body weight predicted the amount of aggression displayed to the intruder but was not significant in control males. ..66

Figure 2.5: A-B) Correlations between testosterone and aggression towards the intruder (A) and total aggression (B) in ascending (light red) and control males (light blue). C-D) Correlations between estradiol and aggression towards the intruder (C) and total aggression (D).67

Figure 2.6: Calibrated optical density measurements of COX levels were centered within each individual and are depicted for each brain area measured. Brain areas are split into four panels depending on their origin. Points and error bars represent the group average +/- the standard error for each brain area. Groups within each experiment are connected by a line.68

Figure 2.7: Number of *egr-1* silver grains /mm covered by cells were centered within each individual and are depicted for each brain area measured. Brain areas are split into four panels depending on their origin. Points and error bars represent the group average +/- the standard error for each brain area. Groups within each experiment are connected by a line.69

Figure 2.8: Principal component analysis of COX datasets. A) Biplot of experiment 1, PCs 1 and 2 showing the loadings. B) Experiment 1 principal component scores as a function of social status for the first four components. C) Biplot of experiment 2, PCs 1 and 2 showing the loadings. D) Experiment 2 principal component scores as a function of social status for the first four components.....70

Figure 2.9: Principal component analysis of *egr-1* in experiment 2. A) Biplot of PCs 1 and 2 showing the loadings. B) Principal component scores as a function of social status for the first four components.....71

Figure 2.10: Clustered heatmaps of all pairwise correlations between brain areas. Color represents Pearson correlation coefficients. Experiment 1 COX dataset (top left), Experiment 2 COX dataset (top right) and Experiment 2 *egr-1* dataset (bottom left). Bootstrap resampling was used to identify significant clusters which are depicted with black boxes.72

Figure 2.11: Correlations of the covariance matrices comparing across datasets. Each point represents the Pearson correlation coefficient between a pair of brain areas in one dataset, compared to the correlation coefficient of that pair in another dataset. A) Experiment 1 COX compared to Experiment 2 COX. B) Experiment 2 *egr-1*, compared to Experiment 2 COX. C) Experiment 2 *egr-1* compared to experiment 1 COX.....73

Figure 2.12: Staining density as a function of incubation time across the brain areas measured in this study. Staining density approximately doubled on average with each 30 min increment of incubation time (X axis). Tissue thickness was a less important factor ($16\mu\text{M}$ in red, $30\mu\text{M}$ in green), at least at this level of examination.....74

Figure 2.13: Optical density of increasingly thick cichlid brain homogenate. Slides were processed in two batches (line type) and at three incubation times: 30, 60 and 90 min (Panels). R-squared values are calculated from linear models that include both batches with the batch effect as a parameter.75

Figure 2.14: Correlations between brain areas measured on adjacent sections. Each panel shows the correlations between two incubation times. Panel 1: 30 - 60 min, Panel 2: 60 - 90 min, Panel 3: 30 - 90 min. $16\mu\text{M}$ sections are shown in red, $30\mu\text{M}$ sections are shown in green.....76

Figure 2.15: Optical density was measured in each brain area and then normalized to the internal tissue homogenate standard for that time point. The panels are arranged by incubation time (columns) and tissue thickness (rows, $16\mu\text{M}$ in red, $30\mu\text{M}$ in green).77

Figure 2.16: Permutation of covariance matrices. A) Permutations comparing similarities (matrix correlations) of the covariance matrix of each group. Violin plots show the distribution of correlation coefficients of the matrices after random permutation of the group labels. Points are the real correlation coefficient between the two matrices. B) For each covariance matrix we calculated the sum of the square of the Pearson correlation coefficients which is a measure of the overall strength of correlations across the matrix and compared that to random sampling (preserving sample size of each group) of the full dataset. Violin plots show the distribution of the sum of r^2 of the randomly permuted data while points show the sum of r^2 of the real data. C) For each pair of correlation matrices we calculated the sum of the absolute value of the differences between each off-diagonal element of the matrices. Violin plots show the distribution of the difference scores of the randomly permuted data while points show the difference score of the real data.

.....78

Figure 3.1: A) Experimental paradigm and timeline. Compartments-A: side communities of one male and three females which serve as a social stimulus for all animals in the paradigm. Compartment-B: suppressor male. Compartment-C: Suppressor male that is removed at time point 0. Compartment-D: refuge for focal male. Compartment-E: chamber that allows for the presentation of an intruder male. B-D) Mean and standard error of each group of aggressive (B), sexual (C) and submissive behavior (D) across the time points. * = $p < 0.05$ in the comparison between treatment and control. Flutamide control = pink, flutamide = orange, fadrozole control = blue, fadrozole = green.....121

Figure 3.2: A) Growth rate differed between experiments but not treatment. B) Relative gonad size was not different among groups. C) FAD males had elevated testosterone levels. D) FAD males had decreased estradiol levels. Letter codes indicate significant differences between groups. Flutamide control = pink, flutamide = orange, fadrozole control = blue, fadrozole = green.122

Figure 3.3: Treatment did not affect intruder directed aggression. A) Latency to attack the intruder. B) Number of aggressive displays directed toward intruder. Flutamide control = pink, flutamide = orange, fadrozole control = blue, fadrozole = green.123

Figure 3.4: A-B) Correlations between aggression towards the intruder and testosterone (A) and estradiol (B). C-D) Correlations between total aggressive displays and testosterone (C) and estradiol (D). Combined controls = blue, flutamide = orange, fadrozole = green.....124

Figure 3.5: Calibrated optical density measurements of COX levels were centered within each individual and are depicted for each brain area measured. For the purposes of the plot we scaled the scores within each experiment using z-scores. Brain areas are split into four panels depending on their origin. Points and error bars represent the group average +/- the standard error for each brain area. Groups within each experiment are connected by a line.....125

Figure 3.6: Number of *egr-1* silver grains /mm covered by cells were centered within each individual and are depicted for each brain area measured. Brain areas are split into four panels depending on their origin. Points and error bars represent the group average +/- the standard error for each brain area. Groups within each experiment are connected by a line.126

Figure 3.7: Example micrographs of the VL in a control animal (top row) and FAD treated animal (bottom row). Micrographs are presented with the brightfield on the left and the corresponding darkfield photo on the right.127

Figure 3.8: Example micrographs of the VSL in a control animal (top row) and FLUT treated animal (bottom row). Micrographs are presented with the brightfield on the left and the corresponding darkfield photo on the right.128

Figure 3.9: A) Correlation between *egr-1* levels in VL and total aggression in the fadrozole dataset. B) Correlation between *egr-1* levels and aggression to the intruder (measured as the time spent displaying) in the flutamide dataset.129

Figure 3.10: A) *Egr-1* effect sizes covaried with androgen receptors in the flutamide dataset, but not in the fadrozole dataset. B) COX effect sizes covaried with estrogen receptor beta levels in the flutamide dataset but not in the fadrozole dataset.130

Figure 3.11: Principal component analysis of COX datasets. A) Biplot of the flutamide experiment, PCs 1 and 2 showing the loadings. B) Flutamide principal component scores as a function of treatment for the first four components. C) Biplot of fadrozole experiment, PCs 1 and 2 showing the loadings. D) Fadrozole principal component scores as a function of treatment for the first four components.131

Figure 3.12: Principal component analysis of *egr-1* datasets. A) Biplot of the flutamide experiment, PCs 1 and 2 showing the loadings. B) Flutamide principal component scores as a function of treatment for the first four components. C) Biplot of fadrozole experiment, PCs 1 and 2 showing the loadings. D) Fadrozole principal component scores as a function of treatment for the first four components.132

Figure 3.13: Clustered heatmaps of all pairwise correlations between brain areas. Color represents Pearson correlation coefficients. A) Flutamide COX dataset, B) Flutamide *egr-1* dataset. C) Fadrozole COX dataset, D) Fadrozole *egr-1* dataset. Bootstrap resampling was used to identify significant clusters which are depicted with black boxes.133

Figure 3.14: Preliminary testing of coconut oil implant technology. Aggression levels prior to receiving the implant was subtracted from the aggression on each day post implant.134

Figure 3.15: Permutation of COX covariance matrices. A) Permutations comparing similarities (matrix correlations) of the covariance matrix of each group. Violin plots show the distribution of correlation coefficients of the matrices after random permutation of the group labels. Points are the real correlation coefficient between the two matrices. B) For each covariance matrix we calculated the sum of the square of the Pearson correlation coefficients which is a measure of the overall strength of correlations across the matrix and compared that to random sampling (preserving sample size of each group) of the full dataset. Violin plots show the distribution of the sum of r^2 of the randomly permuted data while points show the sum of r^2 of the real data. C) For each pair of correlation matrices we calculated the sum of the absolute value of the differences between each off-diagonal element of the matrices. Violin plots show the distribution of the difference scores of the randomly permuted data while points show the difference score of the real data.

.....135

Figure 3.16: Permutation of *egr-1* covariance matrices. A) Permutations comparing similarities (matrix correlations) of the covariance matrix of each group. Violin plots show the distribution of correlation coefficients of the matrices after random permutation of the group labels. Points are the real correlation coefficient between the two matrices. B) For each covariance matrix we calculated the sum of the square of the Pearson correlation coefficients which is a measure of the overall strength of correlations across the matrix and compared that to random sampling (preserving sample size of each group) of the full dataset. Violin plots show the distribution of the sum of r^2 of the randomly permuted data while points show the sum of r^2 of the real data. C) For each pair of correlation matrices we calculated the sum of the absolute value of the differences between each off-diagonal element of the matrices. Violin plots show the distribution of the difference scores of the randomly permuted data while points show the difference score of the real data.

.....136

Figure 4.1: Conceptual diagram illustrating possible links between the three chapters.

Social context (chapter 1) has effects on hormones as well as behavior of individuals and those effects depend on social status. Social status is linked to differences in brain activity and steroid hormone levels.

Blocking the nuclear androgen pathway with flutamide or estrogen signaling with fadrozole did not block social ascension. It did however have effects on circulating hormones but only weakly effected brain activity patterns. The effect of fadrozole depended on social status. All of these processes form an integrated system, whereby changes in the brain activity networks, hormones and behavior of an individual can feedback on group properties and group properties can affect individual's hormone levels and behavior.164

Appendix A: COX brain atlas. Coordinates are measured based on their distance in relation to location of the anterior commissure (AC), with negative coordinates rostral to the AC and positive coordinates caudal to the AC. Left hand sections are a schematic showing outlines of the brain areas, center sections show the Nissl stained cell bodies and right hand sections show an alternative section of the same brain stained for COX.168

Introduction:

Animals are faced with visual, acoustic, chemical, and tactile information as they navigate their environment. The central nervous system integrates these stimuli with internal information and past experience in order to guide potentially adaptive behavioral decisions (i.e. approach or avoidance of a salient stimulus). The behavioral decisions of an individual are embedded in a social interaction network and can directly and indirectly affect the behavior of their social partners by inducing neuronal and physiological responses (Rosenquist, Fowler, and Christakis 2011; Jacobs and Petit 2011; White, Gersick, and Snyder-Mackler 2012). Social cognition and social interaction networks form an integrated system, because the behavior of each actor can perturb the social network, and changes in the social network can in turn feed back on the physiological and cognitive state of the actors, thus changing their behavior (Barrett, Henzi, and Lusseau 2012). Network theory is well suited to bridge the different levels of organization in this system to begin to understand how social stimuli are processed in the brain and how behavior influences social networks.

Social cognition is a dynamic process of feedback and adjustment rather than a linear stimulus-response function (Barrett, Henzi, and Lusseau 2012). Brain circuits are recurrently and reciprocally connected and are capable of generating complex patterns spontaneously (Sporns 2009). Processing of stimuli depends on the emergent structure of this spontaneous activity in the brain: the response properties of one neural element (e.g. a single neuron, a circuit or a brain region) is effected by the activity of the network it is embedded in (Bressler and McIntosh 2007). The network state is a determinative factor in sensory processing, influencing not only the perception of stimuli but also behavioral decision-making (Fontanini and Katz 2008).

Across vertebrates, similar life history strategies and social systems have evolved independently. Even distantly related species can show similar behaviors, presumably shaped by similar selective pressures within those social systems. The neural circuits and systems underlying these behaviors can also show many convergent features. For example, several lineages of fish have evolved the ability to sense and discharge electric fields and can even use these discharges to sense their environment (Rose 2004). The neural systems underlying electrosensation have several convergent features. For example, the same paralog of the sodium channel evolved convergent mutations to be used within the electric organ. This may be due to a preadaptive mutations in the gene complex which lowered the expression level in skeletal muscle, thereby reducing purifying selection on the paralog and allowing for neofunctional evolution (Thompson et al. 2014). Also, within the brain, very similar circuits evolved to receive electrical information from the lateral line, as well as the neural mechanisms underlying the jamming avoidance responses and the cancelation of self-stimulated sensory input (Rose 2004). The convergent evolution of these circuits likely arises because existing circuits are elaborated in the evolution of new behaviors.

Another example is vocal learning which has evolved three times in distantly related mammals (humans, bats, and cetaceans) and three times in distantly related birds (songbirds, parrots and hummingbirds; Jarvis 2004). Within birds the neural circuitry has many convergent features. For example, in all three cases a prominent hypertrophied nucleus evolved in the nidopallium (parrot NLC, hummingbird VLN, and songbird HVC), which is critical for the acquisition and production of song. The connectivity profile and circuitry of this hypertrophied area is similar across the species. This evolved as an elaboration of a pre-existing vocal motor circuit that is found in non-vocal learning species (Jarvis 2004). It is clear that behavior evolves in the background of pre-existing neural

circuitry inherited from the vertebrate ancestor approximately 500 m.y.a. which can lead to convergent and parallel evolution of the circuits controlling behavior.

The process of social decision making involves integrating sensory information with internal information and experiences to make the appropriate behavioral response. Across vertebrates, social behavior is linked to a core network of brain regions called the social decision making network (SDMN; O'Connell and Hofmann 2012). The SDMN is comprised of 12 brain regions, many of which are bidirectionally connected to one another and are sensitive to sex steroid hormones (SSH) and neuropeptides. They have been linked to a large variety of social and sexual behaviors across vertebrates (Newman 1999; Crews 2003; O'Connell and Hofmann 2011; Goodson 2005). Despite substantial progress in the understanding of limbic circuitry, it is still unclear how context, experience, motivation and hormones shift the function of these circuits to shape adaptive behavioral decisions. The neuromodulatory patterning hypothesis, first proposed by Newman (1999) and expanded by Goodson and Kabelik (2009), proposes that the pattern of correlated activity (functional connectivity) across these nodes explains behavioral decisions. Furthermore, the neuromodulatory patterning hypothesis proposes that hormones and other neuromodulators can shift functional connectivity and thus change how stimuli are perceived, processed and acted upon. If functional connectivity is the primary factor that shapes phenotypic variation in behavioral decision making, then different behavioral phenotypes should have different functional connectivity. There are several studies mapping brain activity using cytochrome oxidase (COX) levels that support that relationship. COX is the terminal electron acceptor in the mitochondrial electron transport chain and is critical for energy metabolism (Wong-Riley 1989). COX levels correlate positively with the amount of neural activity. Levels of cytochrome oxidase respond to experimental changes in neural function on the order of hours to days (Wong-Riley 1989;

Gonzalez-Lima and Garrosa 1991; Liang, Ongwijitwat, and Wong-Riley 2006). In anole lizards, exposure to viewing fights between other males causes increased aggression and shifts the functional connectivity in the SDM (Yang and Wilczynski 2007). Leopard geckos have temperature dependent sex determination and developmental temperature can have effects on behavior that are dissociated from gonadal sex. For example, both males and females from a male-biased incubation temperature have increased aggression. Likewise regardless of sex, incubation at the male-biased temperature caused different patterns of correlations in the SDM, notably in the correlation between the anterior hypothalamus and lateral septum which are known to regulate aggression (Sakata et al. 2000).

Other studies using immediate early genes (IEGs) support the relevance of functional connectivity to behavior and the role of hormones. Immediate early genes respond within minutes to neural activity and can be used as a proxy for recent neural activity related to a stimulus (Hofmann 2010). In Tungara frogs, male calls cause stronger levels of correlations in limbic brain areas in females, compared to non-relevant sounds (Hoke, Ryan, and Wilczynski 2005). In white throated sparrow females, male song elicits strong responses in nodes of the SDM during the breeding season compared to control tones, but not in the non-breeding season. Implanting non-breeding season females with estrogen restores breeding season-like responses to male song (Maney et al. 2008). This indicates that hormones shape how stimuli are represented in the brain. Similarly, lactating female mice will respond aggressively to novel males to defend their offspring, while virgin females respond affiliatively (Hasen and Gammie 2005). These differences in behavior correlate to a different IEG response across nodes of the SDM, in particular intruder induced responses in the amygdala of lactating females that was absent in virgins (Hasen and Gammie 2005). While the role of hormones was not specifically addressed in

this study, it is clear that either the experience of giving birth, the hormones involved in the birthing process and postpartum hormones shifted the neural representation of the stimulus and the behavioral response.

These studies strongly suggest that sex steroid hormones mediate a patterning effect on functional connectivity and shape context dependent neural responses to stimuli. However, these studies do not directly demonstrate an effect of hormones on functional connectivity. This represents a fundamental gap in our understanding of how the social decision making network functions and how it is related to hormones. The aim of this thesis is to explore the neuromodulatory patterning hypothesis in a highly social cichlid fish, *Astatotilapia burtoni*.

A. burtoni is an ideal model system with which to address questions about social decision making. Members of this species establish complex social hierarchies and form naturalistic communities in the lab. *A. burtoni* males display two distinct phenotypes dominant (DOM) and subordinate (SUB), which are associated with a suite of hormonal, brain gene expression, and behavioral differences (Renn, Aubin-Horth, and Hofmann 2008). I hypothesized that variation in behavioral phenotype would be linked to variation in brain network states. As a general approach, I exploited the different time courses of two neural activity measures, COX and an IEG, *egr-1*, to measure in the same animals, baseline network state and evoked responses to social interactions. *Egr-1* can be used as a proxy for neural activity related to an acute social stimulus and COX can be used as a measure of the baseline metabolic activity of the brain regions, giving a pre-stimulus and longer term view of the brain networks.

My thesis takes an integrative approach to understanding social behavior in *A. burtoni*, examining social interactions between individuals and group level properties as well as examining the proximate mechanisms of hormones and brain activity within an

individual. This thesis consists of 4 experiments grouped into three chapters. In chapter 1, I examined how an individual's position in the social network affects its behavior as well as how group level properties feedback on an individual's hormone levels and behavior. Chapter 2 consists of two experiments. In the first experiment I examined COX levels in stable DOM and SUB males from communities similar to the social setting of chapter 1. In the second experiment I allowed males to transition from SUB to DOM. In both cases I looked at the effects of social status on hormones, behavior and COX levels. Additionally, in the second experiment I challenged males with an intruder stimulus and measured *egr-1* induction. Finally, in chapter 3, I examined the role of androgen and estrogen signaling in ascending males by treating with either flutamide (an androgen receptor antagonist) or fadrozole (an aromatase inhibitor) and examining the effects on COX and *egr-1* levels.

Chapter 1: Social network dynamics predict hormone levels and behavior in the highly social cichlid fish *A. burtoni*.

ABSTRACT

Group living confers many benefits while at the same time exposing group members to intense competition. Selection at the individual level to gain prominence within a group may conflict with the overall functioning of the group. There is therefore a complex and dynamic relationship between the behavioral displays that directly benefit an individual, the consequences of these actions for the community as a whole, and how they feed back on individual-level fitness. We used a network analysis approach to study replicate communities of the cichlid fish, *Astatotilapia burtoni*, which live in fast-paced social groups with a complex dominance hierarchy among males. We explore the feedback between individual level behavior and community level properties of the social network. We demonstrate that individual behavior can have direct and indirect effects on the behavior of other individuals while at the same time also affecting group level properties. In addition, we find that community membership is strongly predictive of both testosterone and cortisol levels and can be partially explained by differences in the social environment. Variance in testosterone levels is also related to group stability and in unstable groups dominant and subordinate male testosterone levels are equalized. In sum, our analyses provide novel insights into the processes by which individual-level and community-level properties interact.

INTRODUCTION

Animal societies are often characterized by complex social hierarchies (Chase and Seitz 2011; Landau 1951a; Landau 1951b). While animals derive substantial benefits from

group living (e.g. predator avoidance, shared resources, efficient foraging, and other forms of cooperation; Krause and Ruxton 2002; Clutton-Brock and Harvey 1977), they are also in constant conflict with their social partners since each individual aims to maximize their share of resources and reproductive opportunities (Hofmann et al. 2014). Awareness of the social environment allows animals to maximize opportunities while avoiding costly interactions with other group members. When making behavioral decisions, animals must integrate internal physiological information (such as condition and experience) with external social and environmental information to make context-appropriate choices (Taborsky and Oliveira 2012). Each animal inhabits a social environment composed of the overlapping networks of behavioral interactions that it participates in (e.g., aggressive or affiliative interaction networks). Perturbations to one part of the system can affect the stability and properties of other parts, potentially creating social opportunities and conflicts (Jordan et al. 2016). For example, in Pig-tail Macaques, *Macaca nemestrina*, removing the dominant males (who typically police aggressive interactions in the group) results in a destabilization of the aggressive interaction network as well as a fragmentation of affiliative behavior networks such as playing and grooming (Flack et al. 2006). In human social networks, similar peer effects have been linked to the spread of obesity, smoking cessation, and depression (Christakis and Fowler 2007; Christakis and Fowler 2008; Rosenquist, Fowler, and Christakis 2011).

Social network position also has important consequences for evolutionary fitness. For example in house finches, *Carpodacus mexicanus*, and wire-tailed manakins, *Pipra filicauda*, social network position has been linked to mating success (Ryder et al. 2008; Ryder et al. 2009; Oh and Badyaev 2010). Furthermore, in the house finch, males can modify the effects of sexual selection by choosing social environments where they are relatively more attractive (Oh and Badyaev 2010).

The African cichlid fish, *Astatotilapia burtoni*, lives in complex social hierarchies and forms naturalistic communities in the laboratory, providing a tractable model system to study the causes and consequences of social life. Males of this species can be either dominant (DOM) or subordinate (SUB), and they can transition between these phenotypes at any time depending on the social environment. DOM males are brightly colored, highly aggressive, territorial, and sexually active; SUB males are cryptically colored, less aggressive, non-territorial, and rarely show sexual behavior (Fernald and Hirata 1977; Maruska and Fernald 2013). Once established, dominance relationships remain stable for 4-8 weeks under standard laboratory conditions before individuals ascend or descend in social status, likely as a consequence of differential somatic growth (Hofmann, Benson, and Fernald 1999). Specifically, DOM males devote their energy to reproduction and slow their growth rate, while SUB males increase their growth rate. This system stabilizes social groups in the short term by reducing inter-male aggression and facilitates regular cycles of turnover in the dominance hierarchy as SUB males overtake the DOM males in size and ascend in status (Hofmann, Benson, and Fernald 1999).

Both male and female *A. burtoni* exhibit sophisticated social cognition (for review see Weitekamp and Hofmann 2014), including transitive inference of dominance rank (Grosenick, Clement, and Fernald 2007) and cooperative territory defense (Weitekamp and Hofmann 2017). Furthermore, SUB males have been shown to adjust their behavior based on whether or not DOMs are watching their behavior (Desjardins et al. 2012). Specifically, SUB males show increased courtship and aggressive behavior when DOM males are out of view. Finally, females have been shown to recognize individual males in a mate choice paradigm, and exhibit different neural responses depending on whether their initially preferred male won or lost a fight that they were allowed to view (Desjardins et al. 2010).

A number of physiological processes interact with the social environment to modulate behavior. Steroid hormones, such as androgens and glucocorticoids, respond to changes in the social environment and may help animals translate social context into appropriate behavioral responses. Testosterone, in particular, is associated with social dominance across vertebrates (Hirschenhauser and Oliveira 2006) and is known to regulate the response to aggressive challenges across vertebrates (Wingfield et al. 1990; Hirschenhauser et al. 2004). Glucocorticoids (mainly cortisol in teleost fish) mediate the stress response in vertebrates in response to both physical and psychosocial stressors (Wendelaar 1997). Exogenous cortisol can suppress testosterone levels by acting directly on the testosterone-producing Leydig cells in the testes (Welsh, Bambino, and Hsueh 1982) although many species are resistant to this effect (Sapolsky 2005). Furthermore, testosterone can impinge on the HPA axis and suppress the secretion of cortisol (Handa et al. 1994). The relationship between testosterone, glucocorticoids, and social status is variable across species and depends on the organization of the group (Sapolsky 2005). For example, in some species of primates, dominant animals have higher levels of glucocorticoids while in others the subordinates do (Sapolsky 2005). This divergence highlights the complex and dynamic nature of interactions among social environment, hierarchy, individual condition, and steroid hormones, and the need for highly quantitative experimental approaches to understand these interactions in animal groups.

In *A. burtoni*, circulating testosterone responds to changes in social status and is associated with both aggression and courtship (Maruska 2015; Maruska and Fernald 2010; Huffman et al. 2012; O'Connell and Hofmann 2012). DOM males show higher levels of circulating testosterone which is correlated with the rate of aggressive behavior (O'Connell and Hofmann 2012). Further, androgen receptor agonists increase courtship behavior in DOMs while antagonists have the opposite effect. Interestingly, androgen receptor

manipulations do not affect aggressive behavior, suggesting that testosterone is likely correlated to aggression through aromatization to estradiol (O'Connell & Hofmann 2012b). In response to an opportunity to ascend in status, SUB males show a behavioral response and a surge in testosterone levels within 10 minutes (Huffman et al. 2012; Maruska and Fernald 2013; Maruska and Fernald 2010). In DOM males, loss of status is associated with a significant decrease after 24 hrs. (Parikh, Clement, and Fernald 2006a). Cortisol levels in this species are dependent on social status and the social environment. In communities where DOM males change status very infrequently SUB males have higher cortisol levels, while in communities characterized by an unpredictable social environment cortisol levels are more variable and do not depend on social status (Fox et al. 1997). In DOM males, descent in status is associated with a significant increase in cortisol levels after 24 hours (Parikh, Clement, and Fernald 2006a; Huffman et al. 2015).

These results demonstrate the need for a quantitative measurement of social structure if we are to understand how hormones and individual behavior interact in a social context. One such approach is to use social network analysis to measure behavioral interactions and hormones across all social group members. Social network analysis (SNA) provides the tools to extract descriptive statistics from relational data. Utilizing SNA to explore animal networks has led to novel insights into: the contact structure of animal societies (Croft, Krause, and James 2004; Lusseau 2003; Lusseau et al. 2003), the influence of individuals on network structure (Flack et al. 2006; Lusseau and Newman 2004; Williams and Lusseau 2006), fitness consequences of an individual's position in the network (Oh and Badyaev 2010; Ryder et al. 2008; Ryder et al. 2009; Jordan et al. 2016), disease transmission (Craft et al. 2011; Godfrey et al. 2010; Gear, Perkins, and Hudson 2009), and collective decision making (Ward et al. 2002; Aplin et al. 2014). Despite substantial progress in applying SNA to animal societies, there are few studies using this

approach to study direct and indirect effects of behavioral interactions on individuals (but see Schürch, Rothenberger, and Heg 2010). Many social network studies are hampered by small numbers of groups and difficulties associated with uneven sampling. Thus, the links in the network are typically not quantitative, but are instead defined as present or absent using a heuristic approach that takes sampling effort into account (Whitehead 2009). In order to study the direct and indirect effects that individuals have on their social partners, quantitative measures are needed, and ideally linked with variation in individual status and condition. Furthermore, obtaining data from multiple groups allows for the use of statistical models that are more powerful and can better account for dependencies in the data than the bootstrapping approaches typically used in studies with a small number of groups (Croft et al. 2011).

Here we quantify the behavioral interactions between all males from eight naturalistic communities of *A. burtoni* over a 10-day period, examining how changes in social structure interact with individual behavior and circulating hormone levels. Specifically, we test how connectedness (in-degree and out-degree centrality) in the network is associated with aggressive and courtship behavior and levels of circulating androgens and glucocorticoids. We found that individuals can have direct and indirect effects on the behavior and physiology of their social partners and that group level properties also influence these variables. Our results provide a compelling experimental framework for understanding community behavioral dynamics that will facilitate group manipulation experiments on this and other species in the future.

MATERIALS AND METHODS

Animals

Animals used in this study were adult *A. burtoni* (males were between 5.1-8.0 cm in standard length, females were not measured) from a laboratory population originally derived from Lake Tanganyika, Africa (Fernald and Hirata 1977). Fish were fed cichlid flakes (Omega Sea Ltd.) every morning before behavioral observations, and were maintained at 28°C on a 12:12 hour light/dark cycle. The present study comprises eight communities, each consisting of eight males and ten females. All aquaria (110 l) contained a sufficient number of terra cotta pots to serve as territorial shelters for up to four males, although in some communities only three males became dominant. Communities were established and allowed to acclimate for two weeks prior to the start of observations. All males were individually tagged through the dorsal musculature with plastic beads of varying colors; females were not tagged. All procedures were approved by The University of Texas at Austin Institutional Animal Care and Use Committee.

Behavioral Observations

Communities were filmed at 09:30 hours for 30 minutes each on days 1, 3, 6, 7, 8, 9, and 10 using a Sony digital Handycam. We conducted 5-minute focal observations of each male from these video recordings (i.e., 7 observations per individual); the identities of the recipients of all behaviors were recorded as well. In total, this study includes 210 observations on 30 individual DOM males and 238 observations on 34 individual SUB males. Males were identified as individuals based on their tag colors and females were identified by sex, but not as individuals. Behavioral patterns were scored according to (Fernald and Hirata 1977), including aggressive behaviors (chasing, biting, threat displays, territorial displays), courtship behaviors (lateral display, leading and quivering),

submissive behaviors (fleeing), and non-social behaviors (digging, shelter visits and foraging). Behavior was scored by a naïve observer (PD).

Tissue Collection and Hormone Measurements

After behavioral observations on the 10th day, males were weighed and measured, and blood was drawn through the dorsal aorta using heparinized 26-gauge butterfly needles (Surflo). Plasma was separated by centrifugation (3000 rpm for 15 min) and stored at -80°C until further processing. Animals were euthanized immediately following blood collection. Gonads were removed and weighed to ascertain the gonadal somatic index (gonad weight/body weight *100). Finally, brain and skin tissue were collected for use in a separate study (Dijkstra et al. 2017).

We measured circulating testosterone (n=59) and cortisol (n=61) using ELISA (Assay Designs). Plasma samples were diluted 1:30 following Kidd et al. (2010) and the manufacturer's instructions. The coefficient of variation within the testosterone and cortisol assay plates averaged 1.91% and 2.58%, respectively. Across testosterone and cortisol assay plates the coefficient of variation was 4.44% and 4.33%, respectively.

Statistical Analysis

All statistical analyses were conducted in R (R Core Team 2016).

Social Network Analysis

Social networks were constructed using the R package, igraph (Csárdi and Nepusz 2006). Networks were created for each tank on each day separately. Nodes represent individuals while edges represent the sum of aggressive interactions directed from one individual to another. The width of each edge is weighted by the rate they occurred. Females are represented by a single aggregate node, comprising the sum total of aggressive interactions between males and females during the observation period. Female to female

aggressive interactions are rare and were not scored (Renn et al. 2009). Using these networks, we extracted indices of node importance: in-degree and out-degree centrality (defined as the sum of the weights of incoming and outgoing ties for each node, respectively). We conducted analyses at the individual and community level using linear mixed models (LMM) and generalized linear mixed models (GLMM), created with the R package lme4 (Bates et al. 2015). The distribution of in-degree and out-degree centralities were compared between DOM and SUB males with a GLMM that included status as a fixed effect and random effects to control for community membership and fish identity.

We analyzed autocorrelation patterns across time, correlating all sequential time point combinations of each network (Hobson, Avery, and Wright 2013). We calculated product moment correlation coefficients and assessed their significance using 1000 replicates of the quadratic assignment procedure (QAP) implemented in the SNA R package (Butts 2014). This procedure iteratively re-labels the nodes of the network, repeating the correlation calculation each time. Nodes were swapped randomly without regard for social status. P-values are given as the proportion of those randomized replicates that have a greater correlation coefficient than the observed correlation coefficient, with the null hypothesis that the two matrices are unrelated. We calculated a stability index by averaging the Pearson correlation coefficient of each network compared between sequential time points.

Individual level analysis

To examine the effects of behavior received by individuals on their behavior towards others, we used GLMMs with a Poisson error structure and a log link function. We created four separate models, using behavior received from DOMs and behavior received from SUBs as the response variables. DOM and SUB individuals were modeled

separately. We included random effects to account for repeated observations of individuals and communities. Furthermore, we included a random effect at the level of each observation to account for over-dispersion (zero-inflation) in our count data using the method described by (Elston et al. 2001). To avoid over-parametrization, we used a forward fitting procedure, fitting each parameter and all two-way interactions one at a time. In each round we chose the parameter that improved the model the most, based on a chi square test and Akaike Information Criterion (AIC) score, until the model could no longer be significantly improved. The covariates we considered in this model included all outward social behaviors (aggression towards DOM, aggression towards SUB, aggression towards FEM and courtship towards FEM), as well as non-social behaviors (foraging, shelter visitation, and digging).

Analysis of Hormone Measurements

To meet parametric assumptions testosterone data were square root transformed and cortisol measurements were log transformed. The log transformed cortisol measurements showed a significant correlation with the time elapsed during blood sampling ($r^2 = 0.29$, $p = 4.67 \times 10^{-6}$) similar to previous studies in this species (Fox et al. 1997; Dijkstra et al. 2017). To control for this sampling effect we used residuals from this regression in all of our analyses, these residuals were normally distributed. Community effects on hormones were analyzed using ANOVA with fixed effects for community and status.

Comparisons of hormones and behavior included only the behavior on day 10, when the hormones were sampled. We used LMM with random effects for community. P-values were calculated using ANOVA with Wald Chi-square tests implemented in the car R-package (Fox and Weisberg 2011).

Community-Level Analyses

Connectedness based on social status was calculated by averaging the connections between members of a particular social status (Royle et al. 2012). For analyses of connectedness and hormones we included only the day 10 networks, when the hormones were sampled. We used LMM with random effects for community. For analyses of how connectedness of DOMs affected connectedness of SUBs and vice-versa, all data were included and we used LMM with random effects for community and day. In both cases P-values were calculated using ANOVA with Wald Chi-square tests.

The stability index (average Pearson correlation coefficient of the networks over time, see above) was compared to the hormone data in two ways. In the first approach we averaged the hormone data for each social status in each community and subtracted the average DOM hormone level from the average SUB level. We then tested for a correlation using non-parametric Kendall's tau correlation. In the second approach we included all of the hormone data and used a LMM with stability, status, and their interaction as main effects and a random effect for community. The results of both methods were concordant.

RESULTS

Social Networks of *A. burtoni*

We quantified behavior in eight communities based on seven observation periods over ten days and visualized the emergent social networks based on the sum of the total aggressive behavioral interactions. A representative community is shown in Figure 1. We observed that DOMs were hubs in the network and most of the aggressive interactions are directed from DOM animals toward other DOMs, SUBs, and females, while aggressive displays from SUBs are lower in frequency and usually directed towards other SUBs or females. To formalize this observation, we examined the degree densities of incoming (in-

degree) and outgoing (out-degree) edges in the network as a function of social status. As expected, we found strong evidence that DOMs had higher aggressive in-degree than SUBs (GLMM Status: 0.255 ± 0.107 , $p = 0.0176$) and much higher aggressive out-degree than SUBs (GLMM Status: 3.278 ± 0.236 , $p < 0.001$) (Figure 2A). To assess the stability of individual associations over time, we calculated a stability index by correlating association matrices representing the networks across all eight pairwise, sequential time points and used the quadratic assignment procedure to assess significance. We found that associations between individuals were strongly correlated across sequential time points with 100% of these comparisons having a p-value < 0.05 after false discovery rate correction (Figure 2B).

Effects of Social Network Position on Behavior

We then asked how an individual's position in the social network affects its behavior. Table 1 summarizes the following results. Among DOMs, interacting aggressively with other DOMs was associated with increased courtship displays and decreased aggression towards SUBs. Among SUB males, receiving more aggressive behavior from DOMs was correlated with a reciprocal increase in aggression from those SUB males back towards DOMs. This is largely driven by SUB males that are intermediate in the dominance hierarchy challenging DOM males, since most SUB males do not show aggression towards DOMs. Looking at the DOM males that are targeted by these intermediate SUB males, receiving aggression from SUB males was positively associated with a reciprocal increase in aggression back towards those SUBs (this is the same effect seen in the previous model) and negatively associated with aggression towards other DOMs and females. Finally, among SUB males, receiving aggression from other SUB males was negatively associated with aggression to DOM males.

Individual-Level Analysis of Hormones and Behavior

Steroid hormones have long been known for their role in regulating social behavior. We therefore examined the relationship between T and CORT on the one hand and social status, aggression, and courtship behavior performed on observation day 10 (when steroid levels were assayed). Not surprisingly, we found that T was higher in DOM males (Figure 3A: 1.590 ± 0.879 , $\chi^2 = 6.343$, $p = 0.0118$) however it was not correlated to overall aggression ($\chi^2 = 2.043$, $p = 0.153$). We then partitioned aggressive displays into those directed against DOMs, SUBs, or females, respectively, finding that T levels were not associated with aggression towards DOMs ($\chi^2 = 0.222$, $p = 0.637$) or SUBs ($\chi^2 = 0.020$, $p = 0.887$). However, we found a significant association between T levels and aggression towards females, controlling for social status (Figure 3A: 0.082 ± 0.055 , $\chi^2 = 4.005$, $p = 0.045$). Testosterone was not associated with the amount of courtship displays in either DOMs or SUBs. Next we created similar models with cortisol as the response variable. We found that DOM males had lower CORT levels than SUB males (Figure 3A: -0.152 ± 0.068 , $\chi^2 = 5.000$, $p = 0.025$). We found no relationships between CORT and courtship or any aspects of aggressive behavior.

Community level regulation of hormones and behavior

We first asked whether community level behavioral variables could explain the amount of DOM and SUB aggression in these communities. Specifically, we looked at whether the aggressive output of the DOM males within the community predicted the aggressive output of SUB males and *vice versa*. We found that DOM-FEM connectedness (the average amount of DOM aggression towards females) was strongly negatively correlated to SUB male aggression in the community (Figure 4: -0.046 ± 0.018 , $\chi^2 = 6.907$, $p = 0.009$). The average amount of direct interactions between DOMs and SUBs did not

correlate with SUB aggression and neither did DOM-DOM connectedness. No aspects of SUB male behavior in the community correlated with DOM male aggression.

Steroid hormones have well known roles in individual social behaviors, but how they are related to properties of the social group is less well understood. We therefore asked whether testosterone and cortisol were regulated by community membership, using ANOVAs with social status and community membership as fixed effects. We found significant main effects for both community membership and status as well as the community by status interaction with both hormones (Testosterone ANOVA community*status: $F=3.504$, $p=0.005$; Cortisol ANOVA community*status $F=2.745$ $p=0.018$). We then used mixed models to discover which community-level behavioral variables explain this effect. Interestingly, DOM-DOM connectedness (the average connections between DOMs) strongly predicted an individual's testosterone level controlling for social status. In other words, when DOM-DOM connectedness was high, circulating testosterone levels were lower in both DOMs and SUBs (Figure 5A; -0.109 ± 0.030 , $\chi^2 = 18.346$, $p = 1.842 \times 10^{-5}$). Increased DOM-DOM connectedness also correlated to higher cortisol levels in both DOMs and SUBs (Figure 5B; 0.014 ± 0.007 , $\chi^2 = 8.997$, $p = 0.003$). Furthermore, we found a significant interaction between DOM-FEM connectedness (average connections from DOM to FEM) and social status, such that more aggression on average from DOM to FEM predicted higher testosterone among DOM males without a trend among SUB males (Figure 5C; $\chi^2 = 7.705$, $p = 0.006$). Similarly, we found a significant interaction with the SUB-SUB connectedness, such that more connections between SUBs predicted higher testosterone levels in SUBs but not DOMs (Figure 5D; $\chi^2 = 5.778$, $p = 0.0162$).

Finally, we used two different modeling approaches to examine the extent to which community-level regulation of androgens was related to overall network stability. In the

first approach we subtracted for each community the average DOM testosterone level from the average SUB testosterone level and regressed those differences against the stability index. We found a positive correlation such that the difference between DOM and SUB T levels increased with community stability (Figure 6: Kendall's rank correlation, $\tau=0.643$, $p=0.031$). In the second approach we used a LMM with random effects for community membership and stability index and status as fixed effects. In accordance with the result reported above, we found a stability index-by-status interaction effect, such that in DOMs testosterone tended to increase with increasing stability and in SUBs testosterone tended to decrease with increasing stability resulting in differences in testosterone in DOM and SUB animals in stable communities (stability-by-status: $\chi^2 = 9.791$, $p = 0.002$). The effect of community membership on Cortisol levels (see above) was not correlated to the stability index.

DISCUSSION

In the present study we have applied social network analysis to the fast-paced lives of a highly social cichlid fish. Our analysis shows that dyadic and community-level factors are correlated to individual-level behavior and physiology. We found that in general *A. burtoni* form stable social networks with social interactions that are highly correlated across days. DOM males act as hubs for social interactions, receiving and displaying more behavior than other community members. The direct and indirect correlations that individuals have with their social partners ultimately has implications for the stability of the social network as a whole and the likelihood of social change.

Individual-level analyses

On an individual level, we found correlations between circulating testosterone levels and behavior. With respect to aggression we found that, surprisingly, there was no

association between androgens and aggression toward males, but there was a correlation between androgens and aggression (which consisted almost exclusively of fast chases) towards females. This may arise because courtship displays (e.g., quivering and leading) frequently follow ritualized chases directed at females, and thus aggressive behavior in this context may be related to reproduction. Future work will follow the sequence of behavioral displays to test whether courtship-related aggression could be differentiated from non-courtship related aggression. We found no evidence for a relationship between courtship and androgen levels in DOM males, despite previous work that did find this relationship as well as evidence that the androgen receptor directly regulates courtship behaviors (O'Connell and Hofmann 2012).

Dyad-level analyses

On a dyadic level we found evidence of both direct and indirect correlations. We discovered social status-dependent correlations between the behavior that individuals direct towards others and the behavior they receive. DOMs that directed fewer aggressive displays towards females and other DOMs, received more aggressive displays from SUBs, which suggests that SUB males challenge DOMs they perceive as being lower in the dominance hierarchy. Consistent with this notion is our finding that lower aggression towards females is associated with lower androgen levels. In DOM males, interacting more with other DOMs was correlated to higher levels of sexual behavior and lower levels of aggression towards SUB males. This may indicate that DOM males that are higher in the hierarchy interact more with other DOMs, are not as threatened by SUB males and more sexually active. In SUB males receiving aggression from DOMs was correlated to a reciprocal increase in aggression towards DOMs. This effect is driven by intermediate males, which challenge DOM males and in turn are targeted by those DOMs (Desjardins

et al., 2012). In SUB males, receiving aggression from other SUBs was correlated to lower amounts of aggression towards SUBs. This is consistent with a dominance hierarchy among SUB males, where the least aggressive SUBs are targeted the most by other SUBs higher in the hierarchy.

Community-level analyses

The behavior and physiology of group living animals may be intimately tied to the structure of the community in which they exist (Krause & Ruxton 2002), and these effects may extend beyond direct interactions among individuals. We found that both circulating levels of testosterone and cortisol were strongly correlated to community membership and social status. In some communities DOM and SUB males have similar levels of these hormones, while in other communities the two groups are strongly divergent with DOM males having much higher testosterone levels and lower cortisol levels. This community effect is intriguing because it suggests that the social environment in some way regulates the hormone levels of individual community members. This in turn might affect their own behavior and alter the social environment further. We found that several elements of the social environment correlated to hormone levels. The amount of DOM-DOM interactions within the community is correlated to lower testosterone levels and higher cortisol levels in both DOM and SUB males. It is possible that high levels of aggression between DOM males is perceived as stressful by both DOM and SUB males and that higher cortisol levels could cause decreases in testosterone through feedback mechanisms on the hypothalamic-pituitary-gonadal axis. Because SUB males do not participate in this interaction, this effect is possibly mediated by third-party observation of the DOM behavior. The amount of DOM-FEM interactions within the community correlated to higher testosterone levels in DOM males, whereas SUB male T levels were not affected. This is likely explained by the

correlation between aggression towards females and androgens seen at the individual level (see above).

At the behavioral level, increased DOM-FEM interactions correlated with lower aggression in SUBs. Importantly, this effect is independent of direct interactions between DOMs and SUBs and instead suggests a possible indirect effect of viewing DOM male aggression towards females suppressing SUB male aggression. Finally, the amount of SUB-SUB aggression in the community correlated to higher testosterone among SUB males. Interestingly, at the individual level, there was no correlation between an individual SUB's testosterone level and the amount of aggression they showed towards other SUBs, so it is possible that simply viewing many aggressive interactions between SUBs is sufficient to increase testosterone levels in SUB community members, even if they do not necessarily show increased aggressive behavior themselves.

Finally, we calculated the average correlation coefficient across days for each network matrix as a novel metric for social network stability. Remarkably, we found that the community effect on circulating testosterone levels was correlated to social network stability. As stability increased DOM male testosterone levels increased as well, while SUB male testosterone levels decreased: in relatively unstable communities DOM and SUB male testosterone levels were similar, and in stable communities DOM males had higher levels of testosterone than SUBs. Males of SUB status may play a passive or active role in this process; unstable communities may give SUB males an opportunity to increase their social rank, leading to associated behavioral and physiological changes (Maruska et al. 2011; Maruska and Fernald 2011; Huffman et al. 2012). Alternatively, SUBs with increased aggression and high androgens may actively destabilize dominance hierarchies by acting aggressively towards DOM males, particularly in communities where DOM-FEM aggression is low, which could also be indicative of lower testosterone among DOMs.

Such a behavioral tactic may well come with fitness benefits. For example, we have previously shown that such “intermediate” SUB males are four times more likely to ascend to dominance as other SUBs (Desjardins et al., 2012).

Conclusions

We have shown here that the cichlid fish *A. burtoni*, which has emerged as a model system in social neuroscience, is ideally suited to detailed analyses of complex community dynamics. Experiments using social engineering techniques (such as removing or adding individual community members; Flack et al., 2006) or pharmacological manipulations that subtly alter the aggressive or sexual behavior of specific individuals (O’Connell and Hofmann 2012) will help untangle cause and effect relationships in these complex community interactions. Furthermore, this approach can then be extended to measuring direct and indirect social interaction has on the activity of specific nodes of the brain’s social decision-making network (O’Connell and Hofmann 2012) as well as the underlying molecular substrates (Williamson, Franks, and Curley 2016; O’Connell, Ding, and Hofmann 2013). Ultimately, this approach will provide insight into the causal mechanisms by which social plasticity spreads across a community and may enlighten our understanding of our own sociality.

Acknowledgements

We thank Maggie Rigney and Gary ‘Bud’ Swindler for fish care; Agosto Rodriguez for technical assistance; Caitlin Friesen and Rebecca Young for commenting on the manuscript; and members of the Hofmann laboratory for insightful discussions. This work was supported by Carl Gottfried Hartman Graduate Endowment Fellowship, The University of Texas Integrative Biology Recruitment Fellowship, and NSF Graduate Research Fellowship to SMM; a Mary Curie Outgoing Fellowship to PDD; an Integrative

Biology Postdoctoral Fellowship to LAJ, the Alfred P. Sloan Foundation (BR-4900) and NSF grants IOS-0843712, IOS-1354942 to HAH, and IOS-1501704 to SMM and HAH; and by the NSF BEACON Center for Science and Technology (DBI-0939454).

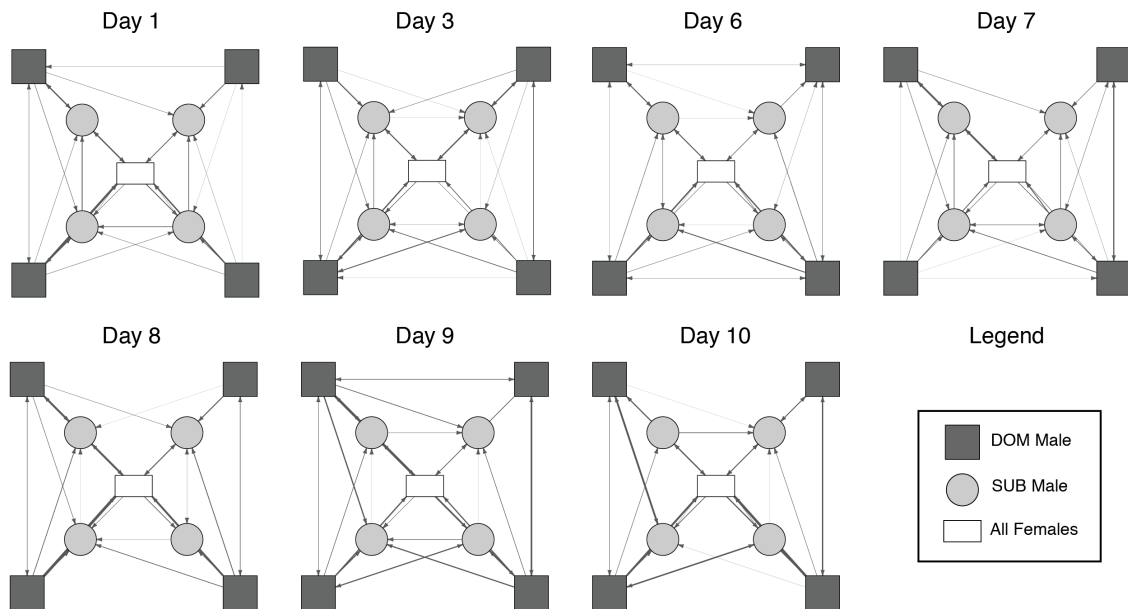


Figure 1.1: Example networks of a single *A. burtoni* community over time. DOM and SUB Individuals are depicted in the same position on each day. DOM males (dark gray squares) are depicted in the corner of the tank that they occupied, while SUB males (light gray circles) are arranged randomly. Females (white rectangles) were not identified individually and are depicted as an aggregate node representing all eight females.

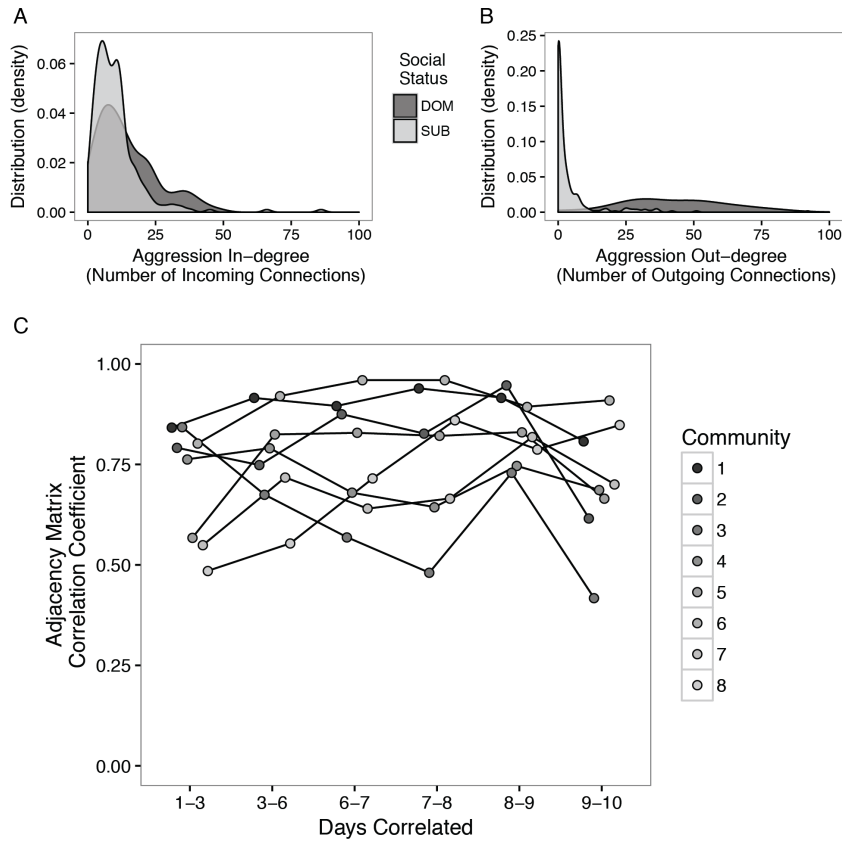


Figure 1.2: DOM males are network hubs and networks are stable over time. A) Density plot of the distribution of in-degree (number of incoming connections) for DOM (dark gray) and SUB (light gray) males. B) Density plot of the distribution of out-degree (number of outgoing connections) in the network as a function of status. C) Correlation coefficients of the matrices representing networks of each community on consecutive days.

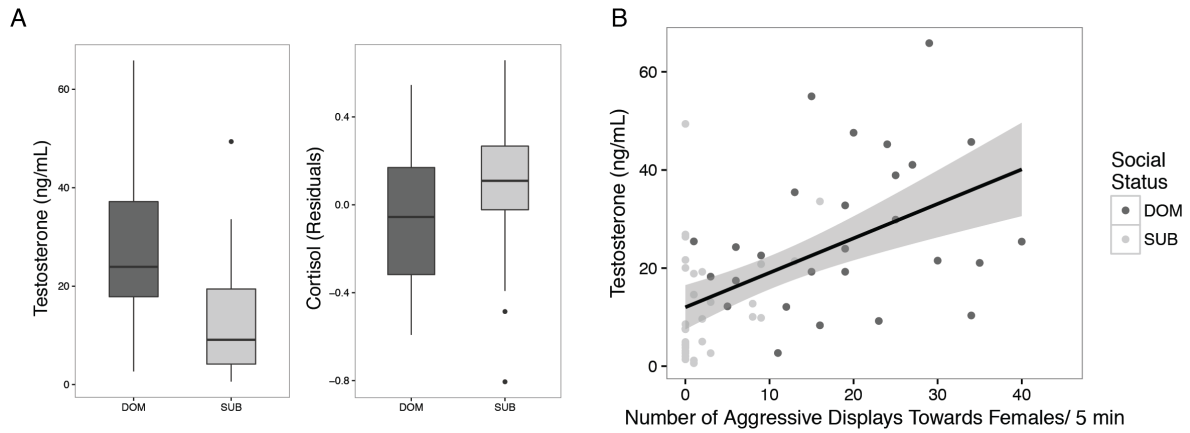


Figure 1.3: A) DOM males (dark gray) have higher testosterone levels and lower cortisol levels compared to SUB males (light gray). B) Testosterone is significantly correlated to aggression directed towards females.

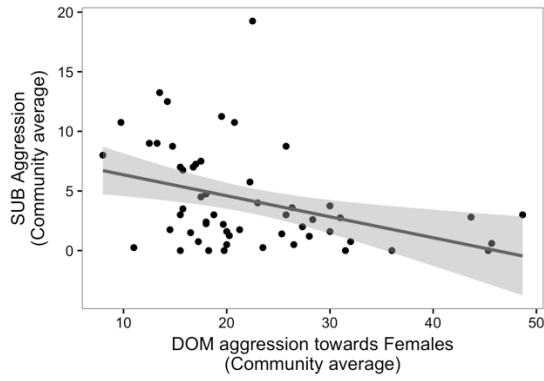


Figure 1.4: The DOM-FEM connectedness (the average amount of aggression directed from DOM males towards females in a community) correlated to lower SUB male aggression, even controlling for direct interactions between DOM and SUB.

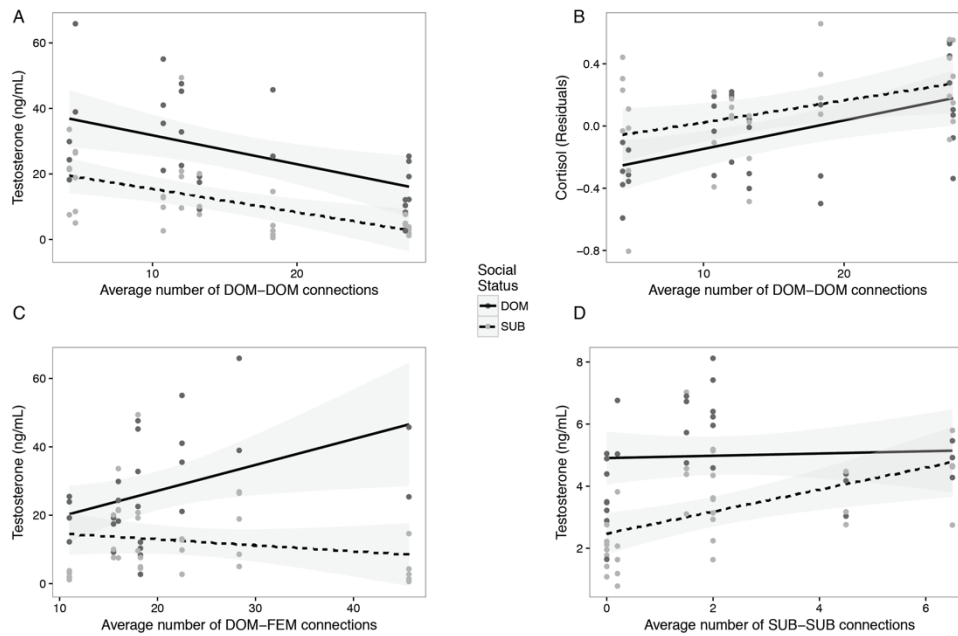


Figure 1.5: The average number of DOM-DOM connections correlates to lower testosterone levels (A) and higher cortisol (B) in both DOM (dark gray) and SUB (light gray) males. C) The average number of DOM-FEM connections in the community correlates to higher levels of testosterone in DOM community members but not SUB. D) The average number of SUB-SUB connections in the community correlates to increases in SUB male testosterone.

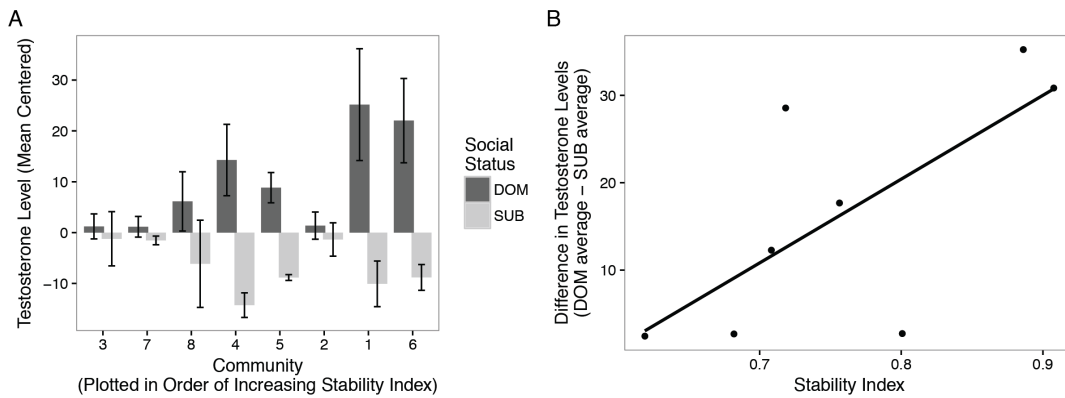


Figure 1.6: The community effect on testosterone correlates to network stability. A) Average and standard error of DOM (dark gray) and SUB (light gray) testosterone levels, centered on the whole community average, plotted for each community. Communities are plotted in order of increasing stability index. B) The difference between the average DOM testosterone levels and the average SUB levels in each community correlates to the stability index.

Incoming behavior	Status	Outgoing behavior	Estimate	Standard Error	Z value	P value
Aggression from DOM	DOM	Aggression to SUB	-0.0264	0.0064	-4.115	3.88 X10⁻⁵
		Aggression to FEM	-0.0032	0.0042	-0.766	0.444
		Courtship	0.0293	0.0052	5.693	1.25 X10⁻⁸
	SUB	Aggression to DOM	0.0421	0.0089	4.754	1.99 X10⁻⁶
		Aggression to SUB	-0.0006	0.0142	-0.039	0.969
		Aggression to FEM	-0.0091	0.0218	-0.418	0.676
		Courtship	0.0266	0.0255	1.042	0.297
	Aggression From SUB	DOM	Aggression to DOM	-0.0784	0.0311	-2.514
Aggression to SUB			0.1344	0.0234	5.751	8.90 X10⁻⁹
Aggression to FEM			-0.0742	0.0214	-3.472	5.16x10⁻⁴
Courtship			0.0061	0.0243	0.25	0.8022
SUB		Aggression to DOM	-0.3166	0.1083	-2.924	3.45x10⁻³
		Aggression to SUB	-0.0566	0.0396	-1.429	0.1531
		Aggression to FEM	-0.0165	0.0567	-0.29	0.7714
		Courtship	0.0765	0.0731	1.047	0.2951

Table 1.1: Receiving aggression from other community members correlates to the behavior that those individuals express. Results of four mixed models comparing the aggression received from DOMs (first two rows) or SUBs (last two rows) depending on the social status of the receiver. Significant effects are displayed in bold.

Chapter 2: The Effects of Social Status on Neural Activity Patterns in Stable and Ascending Males.

ABSTRACT

Social status has wide ranging effects on behavior and physiology. How these effects are mediated by changes to the neural networks controlling social decision making is not well understood. We examined behavior, physiology and brain activity in a highly social cichlid fish *Astatotilapia burtoni*, which has two socially regulated male phenotypes, (DOM) and (SUB). We measured brain activity using a metabolic mapping technique, cytochrome oxidase histochemistry, as well as immediate early gene induction in the same animals across the majority of the forebrain as well as important hypothalamic and midbrain nuclei. In experiment 1 we examine these parameters in stable DOM and SUB males in a naturalistic community, in experiment 2 we allow males to ascend from SUB to DOM status and examine changes after 1 week. We found that social status has effects on brain metabolism on a small number of limbic brain areas but did not affect immediate early gene induction. Comparing the covariance structure of the two measures, we found that they were similar and we identify some possible functional circuits.

INTRODUCTION

Social animals are constantly faced with evaluating complex social cues and the environment and making behavioral decisions. Social decision-making is a process in which individuals integrate social stimuli with contextual information and past experience to make context-appropriate behavioral responses. The mapping of a social stimulus to behavioral response is highly plastic and can be adjusted depending on many factors such as social status, past experience, motivation, stress and hormone levels and other aspects of the social context. This complex process depends on distributed processing of sensory

signals across a highly interconnected set of limbic brain areas in the forebrain and rostral midbrain known as the social decision making network (SDMN; O'Connell and Hofmann 2012).

While particular brain areas within the SDMN are specialized and have been shown to have functional relevance to particular behaviors, the function of a brain area is flexible and activity is not exclusive to any particular category of stimuli (Goodson and Kabelik 2009). One hypothesis about how social contextual information is integrated with sensory signals to achieve behavioral plasticity is the neuromodulatory patterning hypothesis (Newman 1999). In this view it is the pattern of activity across the nodes of the SDMN that correlates to behavior and the activity of any one area can only be interpreted within the overall neural context.

Functional connectivity is defined operationally as correlated activity between distinct brain areas that is assumed to reflect the amount of communication (Gillebert and Mantini 2013; Friston 2011). These correlations can arise in different ways; for example, they could be due to common inputs, direct synaptic connections between the brain areas or through intermediary brain areas (Friston 2011).

The processing of stimuli can depend on the functional network a brain area is embedded in. For example, task performance in stimulus-response tests of human subjects has been shown to be influenced by intrinsic network activity prior to stimulus onset (Hesselmann et al. 2008; Wyart and Tallon-Baudry 2009). A simple example of this can be seen in the comparison of olfactory processing during periods of wakefulness or sleep. Mitral cells in the olfactory cortex of the brain receive input from the sensory olfactory neurons that chemically detect odors. While the sensory input depends solely on odorant type and concentration, the direction and magnitude of the mitral cell response depends on whether or not the animal is anesthetized. While the animal is awake the mitral cell

responses are much more sparse, this is not due to a change in sensory input, but because the other brain areas provide inhibitory input while the animal is awake (Fontanini and Katz 2008). A similar phenomenon in the SDMN could play a large role in behavioral plasticity, as shifts in functional connectivity could allow for context-dependent processing of social information. Functional connectivity within limbic brain areas has been shown to be shifted due to social experience in lizards (Yang and Wilczynski 2007), stimulus salience in frogs (Hoke, Ryan, and Wilczynski 2005) and winning experiences in zebrafish (Teles et al. 2015).

This study measures two different indicators of nervous system activity, cytochrome oxidase (COX) histochemistry and *in situ* hybridization of the immediate early gene *egr-1*. Cytochrome oxidase histochemistry is a measure of metabolic activity in the nervous system as well as a functional stain that can differentiate structure in the neuropil that is not apparent from anatomical stains (Hevner 1998; Wong-Riley et al. 1998; Wong-Riley 1989). Cytochrome oxidase is the final enzyme in the electron transport chain of the mitochondria and is therefore crucial to energy production in cells. Neurons have a high energy demand and rely on oxidative metabolism (Gonzalez-Lima and Garrosa 1991). Long-term increases in neural activity cause increases in energy demand which causes neurons to increase the production of cytochrome oxidase (Wong-Riley 1989). *Egr-1* is an immediate early gene, a transcription factor that responds to changes in neuronal activity and is a powerful marker of stimulus induced neuronal activity (Okuno 2011). While both of these markers respond to changes in neuronal activity they differ markedly in the dynamics of that response. Even with very extreme perturbations (e.g. lesions or tetrodotoxin injections) it takes at least one day to detect the effects of changes in neural activity on cytochrome oxidase levels (Wong-Riley 1989; Gonzalez-Lima and Garrosa 1991; Liang, Ongwijitwat, and Wong-Riley 2006) while changes in *egr-1* mRNA levels

are detectable within an hour or less following stimulus exposure (Hofmann 2010; Okuno 2011).

The African cichlid fish, *Astatotilapia burtoni*, is an ideal model for studying socially regulated behavioral plasticity. *A. burtoni* are polygamous maternal mouth brooding cichlid fish endemic to lake Tanganyika in East Africa, where they live in shallow shore pools and streams (Fernald and Hirata 1977a). They have a lek breeding system and dominant (DOM) males gather in colonies and defend territorial substrate such as tree branches or rocks while subordinate (SUB) males and females school around the edge of the colony (Fernald and Hirata 1977b). Territorial space is limited and defended by DOM males, thus the majority of the population of males (70-90%) are typically SUB (Fernald and Hirata 1977a). DOM males are brightly colored (yellow or blue coloration in the ventro-lateral side) with a prominent black stripe through the eye (“eye-bar”), black coloration on the edges of the fins, a red humeral patch behind the gill and bright orange circles (“egg spots”) on the anal fin. SUB males, in stark contrast, are cryptically colored and vary between light and dark grey in concordance with the color of the substrate. They typically lack a prominent eye-bar, and egg spots are dull in comparison to DOM males. DOM males exhibit a wide range of territorial and sexual behaviors not seen in SUB males. DOM males defend territories by chasing SUB males away and have ritualistic aggressive displays towards neighboring DOM males. In addition, they court females that approach their territory and maintain a breeding area by removing debris and digging a depression in the sand suitable for spawning. SUB males school with females and typically do not display aggressive, sexual or territorial behavior (Fernald and Hirata 1977a). Frequent disruption of territorial substrate, predation, as well as higher growth rate in SUB males lead to frequent changes in male social status when SUB males challenge DOM males for a territory or occupy a vacant territory (Hofmann et al. 1999; Neumeister et al. 2010). In

captivity social status changes may occur as frequently as every 4-6 weeks (Hofmann et al. 1999).

Changes in social status represent a remarkable example of socially regulated phenotypic plasticity and involve a wide range of coordinated physiological changes that begin occurring within minutes after an opportunity to ascend in status. Previous studies have shown that within 15 minutes of an opportunity to ascend in social status males have increases in aggressive and sexual behaviors in addition to increases in androgens and estradiol (Huffman et al. 2012; Maruska and Fernald 2010; Burmeister, Jarvis, and Fernald 2005). Accompanying these changes there is a rapid genomic response in the brain of increased transcription of the immediate early genes, *egr-1* and *c-fos*, across many nodes of the social decision making network, including the preoptic area (POA) and pituitary, indicating increases in neural activity in the brain (Maruska et al. 2013). Within the POA, gonadotropin releasing hormone (GnRH) cells show increases in *egr-1* transcription within minutes of a social opportunity (Burmeister, Jarvis, and Fernald 2005). DOM males have larger GnRH neurons and transitioning animals have been shown to have increases in GnRH soma size within 1 week of transition (White, Nguyen, and Fernald 2002). In addition, there is widespread cell proliferation in the brain that is regulated by social status and ascending males show increases in mitosis within 24 hours of transition (Maruska, Carpenter, and Fernald 2012). The GnRH cells in the POA project directly to the gonadotropin producing cells in the pituitary, stimulating release of the gonadotropins. Increases in gonadotropin mRNA and circulating levels are evident within 30 minutes of transition (Maruska et al. 2011). The gonadotropins target receptors in the testes. Molecular changes to the testes are evident within 6-144 hours of transition (increases in aromatase, estrogen and androgen receptors and increases in steroidogenic acute regulatory protein) while morphological changes including increases in size, mature organization and sperm

production take place over the next 1-2 weeks (Maruska and Fernald 2011; Huffman et al. 2012). This complex, coordinated process can be readily induced in the lab, making *A. burtoni* an ideal model for a study of socially regulated phenotypic plasticity.

In the present study, we conducted two experiments to investigate neural activity patterns in *A. burtoni* and the effects of social status, both in stable social situations and during social transition. In Experiment 1 we compared DOM and SUB males that were stable in their social status over a long period of time. Animals were housed in naturalistic communities and focal animals were observed to be stable in their social status for at least 4 weeks. In Experiment 2, we allowed SUB males to transition to DOM to examine the effects of ascending to DOM status. We designed a novel behavioral paradigm that allows for animals to transition to dominance in a controlled setting. We provide the first extensive survey of cytochrome oxidase activity in a teleost, including the majority of the forebrain and parts of the midbrain and hypothalamus. Our analysis supports many of the regional parcellations proposed by Burmeister et al. (2009), as well as a new parcellation of the granular zone of the dorsal-lateral telencephalon. Additionally, we provide the first comparison between COX and *egr-1* neural activity markers within the same animals and explore similarities and differences in functional connectivity as measured by each. We hypothesized that social status would have a strong effect on functional connectivity based on COX and *egr-1* levels. Based on the neuromodulatory patterning hypothesis we hypothesized that the COX covariance pattern would be predictive of the *egr-1* pattern. By examining hormones, behavior, COX levels and *egr-1* expression simultaneously we conduct an integrated analysis of the effects of social status on neural activity.

METHODS

Animal care

All animals used in this study were adult *A. burtoni* from a laboratory breeding line originally derived from a wild population in Lake Tanganyika, Africa (Fernald and Hirata 1977a). Fish were kept at 27 °C on a 12:12 hr light/dark cycle in 110 L tanks equipped with a recirculating life support system and fed daily with cichlid flake food (OmegaSea Ltd.). In Experiment 1, males were housed in groups of 8 males and 10 females in naturalistic communities, that contained flower pots to serve as territorial substrate. Each community (n = 7) had between 2-4 DOM males and 6-8 SUB males at any given time. DOM (n = 15, mean standard length 69.3 mm) and SUB males (n = 15, mean standard length 58.5 mm) were chosen as focal animals if they were stable in their social status for at least 4 weeks. In the social opportunity experiment, each focal animal (mean standard length 47.4 mm) was housed with 4 males and 6 females in a specially designed enclosure (Figure 1A) that allowed for controlled social ascent to dominant social status (n = 14) or a sham opportunity control (n = 13). All procedures were in compliance with and approved by the University of Texas Institutional Animal Care and Use Committee.

Behavior Studies

Experiment 1: Males were individually tagged with colored beads. After allowing the communities to establish for 1 week, we observed male status 3 times/week for 4-5 weeks. Only males that remained in the same status for the entire observation period were used in the study, if they changed status at any point they were excluded from the study. After focal males were confirmed to be stable in their social status for at least 4 weeks we filmed the communities and scored each focal individual's behavior. Behavior was scored only once, the day the animals were sampled. We used an ethogram based on Fernald and

Hirata (1977a) that includes the following behaviors: chasing (aggression usually directed from a DOM towards a SUB), border conflict (ritualized aggressive displays that occur between DOM males), biting (aggression), and sexual behaviors: leading and quivering (directed towards females). All animals that were housed together were sampled at the same time. Following behavioral observation blood was collected from the dorsal aorta using heparinized 26G butterfly infusion needles (Surflo), blood was kept on ice until the plasma could be separated from the serum by centrifugation and stored at -80 °C. Immediately following blood collection animals were killed by rapid decapitation and their brains were dissected, placed into OCT molds, flash frozen on dry ice, and stored at -80 °C until sectioning.

Experiment 2: Focal males were housed in the enclosure shown in Figure 1A which allows for a controlled transition to DOM social status. Focal males were between a standard length of 40 – 50mm and had access to compartments B, C and D via 16mm diameter holes that allowed them to pass through compartment D. Suppressor males (standard length > 70mm) were restricted to their home compartment (either compartment B or C) because they were too large to pass through the holes in compartment D. The suppressor males serve to socially suppress the focal male, however the design leaves the focal male with a refuge (compartment D) which reduces injuries and allows for the male to be suppressed within the experimental enclosure for long periods of time. Side communities (compartments labeled A) consisted of 1 male, size matched to the focal male, and 3 females and provide visual and olfactory social stimuli for all the animals in the experiment. Prior to the beginning of the experiment focal males were housed with larger males in established communities for at least 2 weeks to ensure that they were SUB social status before going into the experiment. 60 hours prior to the opportunity to transition to DOM social status, males were measured and placed into the experiment. The next day (48

hours prior to the social opportunity) they were allowed to acclimate to the enclosure, no observations were conducted on this day. At each subsequent time point males were videotaped for 10 min for behavioral scoring. Behavior was scored at 9 time points: 24 hours prior to social opportunity (-24 hrs), directly after the social opportunity (0 hrs) and 1, 24, 48, 72, 96, 120 and 144 hours after the removal of the DOM male. On Day 3 (0 hr time point), the suppressor male from compartment C was removed one hour prior to lights-on (Social Opportunity), thus providing an opportunity for the focal male to take over that territory (Burmeister, Jarvis, and Fernald 2005; Huffman et al. 2012; Maruska and Fernald 2010). In the Control treatment, the DOM male was removed and returned immediately afterward. On day 9 of the experiment (144 hr time point) animals were challenged for 1 hour with an equal sized intruder male who was placed into compartment E at the start of the observation. Following this observation blood was collected from the dorsal aorta using heparinized 26G butterfly infusion needles (Surflo), blood was kept on ice until the plasma could be separated from the serum by centrifugation and stored at -80 °C. Immediately following blood collection animals were killed by rapid decapitation and their brains were dissected, placed into OCT molds, flash frozen on dry ice, and stored at -80 °C until sectioning.

Hormone assays

Hormone assays were performed using ELISA (Assay Designs, Enzo life sciences). Plasma was diluted 1:30 and run in duplicate (Kidd, Kidd, and Hofmann 2010). Within each experiment, all samples were run together on the same plate. In the testosterone assay the intraplate coefficient of variation averaged 2.27% in Experiment 1 and 3.02% in Experiment 2. Estradiol was measured only in the Experiment 2. The intraplate coefficient of variation was 4.55%.

Brain Sectioning

All brains were sectioned into four series of alternating 30 μm sections at $-20\text{ }^{\circ}\text{C}$ using a cryostat (2800 Frigocut Reichert-Jung). Sections were thaw mounted on to Superfrost Plus slides (Fisher Scientific) and kept at $-20\text{ }^{\circ}\text{C}$ during sectioning. In both experiments the first series was processed for cytochrome oxidase histochemistry and the second series for Nissl stain to act as a guide for quantification. In Experiment 2 the third and fourth series were used for *egr-1* radioactive *in situ* hybridization.

Cytochrome oxidase histochemistry

Slides were processed for cytochrome oxidase histochemistry using a previously described protocol (Gonzalez-Lima and Jones 1994). The following solutions were used: 1) fixation solution of 0.5% glutaraldehyde (Sigma-Aldrich) in 10% sucrose (Sigma-Aldrich); 2) 0.1 M phosphate buffer (Fisher Scientific; pH 7.6); 3) preincubation solution of 0.05 M Tris buffer (Sigma-Aldrich; pH 7.6), 0.0275% cobalt chloride (Sigma-Aldrich), 10% sucrose, and .5% dimethylsulfoxide (Sigma-Aldrich; DMSO); 4) incubation solution of 0.05% diaminobenzidine (Sigma-Aldrich; DAB), 0.0075% cytochrome c (Sigma-Aldrich), 5% sucrose, 0.002% catalase (Sigma-Aldrich), 0.25% DMSO (v/v), and phosphate buffer. Sections were kept frozen on the slides and solutions were kept at 4 degrees until the start of the procedure so that the sections would warm gradually as they moved through the baths. The sequence of baths was: 1) light fixation in gluteraldehyde solution for 5 min; 2) rinse in phosphate buffer with 10% sucrose, 3 changes for 5 min each; 3) preincubation in cobalt chloride Tris-buffer for 10 min; 4) rinse in phosphate buffer; 5) incubation in DAB solution (oxygenated for 5 min before and throughout the staining) at 37°C in a dark oven for 60 min; 6) post-fixation with 4% buffered formaldehyde in 10% sucrose for 30 min; 7) ethanol baths of 30, 50, 70, 95 (2 changes),

and 100% (2 changes) for 5 min each; 8) xylenes (Millipore), 3 changes for 5 min each; 9) cover-slipped with Permount (Fisher Scientific).

Nissl stain

Alternative sections were stained with cresyl violet to be used as a guide for quantification. Slides were processed through the following series of baths: 1) fixation in chilled 4% paraformaldehyde (Sigma-Aldrich) for 10 min; 2) rinsed in chilled phosphate buffered saline, 3 changes for 5 min each; 3) rinsed in room temperature deionized water; 4) stained with 1% cresyl violet (Sigma-Aldrich) for 3 min; 5) rinsed again in deionized water; 6) ethanol baths of 70% for 30 seconds, 95% for 2 min and 100%, 2 changes for 2 min each; 7) xylenes, 2 changes for 5 min each; 8) cover-slipped with Permount.

Brain Homogenate Standards

Following Gonzalez-Lima and Jones (1994) we prepared cichlid brain homogenate to use as an internal standard in every batch of the cytochrome oxidase stain. 30 adult *A. burtoni* brains from both males and females were dissected, rapidly fresh frozen in plastic tubes and stored at -80 °C until the homogenate was prepared. These animals were gathered over time from surplus stock that had to be euthanized due to injuries in accordance with our animal care protocol. To prepare the homogenate, brains were thawed on ice and crushed into a thick paste using a plastic mortar and pestle in a 2mL centrifuge tube. Each brain was homogenized one after the other in the same tube. Small amounts of water were added as needed (100 µL total) to aid in the homogenization process. To aliquot the homogenate the tapered half of 200 µL pipette tips (Axygen) were cut off so that they made an approximately 5 mm diameter cylinder. The cylinders were filled with brain homogenate using a combination of pipetting and manual packing and frozen on dry ice. These cylinders were kept at -80 °C until the morning each batch was run, at which time

one aliquot was sectioned on the cryostat at $-20\text{ }^{\circ}\text{C}$. 6 series were sectioned from each cylinder, starting with two sections of $10\text{ }\mu\text{M}$ for each series and continuing in $10\text{ }\mu\text{M}$ increments up to $60\text{ }\mu\text{M}$. These standards were used to correct the calibrated optical density measurements for batch effects. Each measurement was referenced to the brain homogenate standard particular to the appropriate batch. Experiment 1 was run across two batches with equal numbers of DOM and SUB males in each batch. Experiment 2 was run in a single separate batch.

Validation studies

We performed validation studies to verify that cytochrome oxidase histochemistry is a suitable technique in teleost brains as previous studies have been conducted mainly in amniotes. For the validation studies, male *A. burtoni* were housed in compartments with three females and allowed to acclimate for two weeks prior to the start of the experiment. We tested the effects of section thickness ($16\text{ }\mu\text{m}$, $30\text{ }\mu\text{m}$, and $60\text{ }\mu\text{m}$) and incubation time (30, 60, 90) min. We determined that cytochrome oxidase histochemistry is a suitable technique for studying teleost fish brains and staining patterns are remarkably similar to those seen in other taxa (COX Brain Atlas, appendix A). We have shown that cichlid brain homogenate can be used to create a reliable and repeatable internal standard (Figure 12). Furthermore, the staining intensity is linear with respect to incubation time (Figure 13) and the staining pattern is robust across brain areas (Figure 14 and 15). We determined that the best conditions for the staining in cichlid fish is $30\text{ }\mu\text{m}$ tissue thickness and 60 min incubation time.

Quantification

Cytochrome oxidase was measured in 31 limbic and sensory brain areas covering the majority of the forebrain as well as parts of the hypothalamus and midbrain (see table

1). Images of each section were taken using an Olympus SZX12 microscope equipped with a 12.5-megapixel camera (Olympus DP70) at 16x magnification. Images were saved as uncompressed files with 16-bit color depth. Illumination and exposure were held constant. Nissl stained adjacent sections were used as a guide to identify regions of interest. Optical density measurements were done using FIJI software (Schindelin et al. 2012). For each region, the brain area was traced in one hemisphere and optical density was measured. This process was continued across the full rostral-caudal extent of each region at an interval of 120 μ M between measurements. Optical density was calibrated using an optical density step tablet (Kodak). All optical density measurements were standardized to the internal brain homogenate standard using a linear model to control for batch effects. The measurements for each brain area were then averaged to give a score for each brain area within each individual.

Egr-1 *in situ* hybridization

Cloning of A. burtoni egr-1 gene fragment

We isolated total RNA from *A. burtoni* brain using TRIzol (Invitrogen) and purified with RNeasy spin columns (Qiagen). We reverse transcribed whole brain cDNA using a mixture of oligo-DT and random hexamer primers using the Superscript III reverse transcriptase kit (Invitrogen). Primers were designed using Primer3 (Rozen and Skaletsky 1998) against the coding sequence of *A. burtoni egr-1* (NCBI reference: NM_001315549.1). A 491 bp fragment of the *egr-1* gene was amplified by PCR (Promega GoTaq Green) using the following primers: Forward: 5'-TCCAGCCTCAGTTCTTCGAT-3', Reverse: 5'-GTCAGCTCATCAGACCGTGA-3'. This fragment was cloned into the pCRII TOPO vector (Qiagen) containing SP6 and T7 polymerase promoters on opposite

sides of the *egr-1* fragment allowing for both sense and antisense transcripts to be generated from the same clone.

Detection of egr-1 mRNA

In situ was performed following a modified version of a previously described protocol (Hoke et al. 2004). Large quantities of the *egr-1* plasmid were prepared using a midiprep kit (Qiagen) and 20µg was linearized by restriction digest with either SpeI-HF (sense; New England BioLabs) or NotI-HF (antisense; New England Biolabs) and purified using spin columns (RNeasy Qiagen). Runoff *in vitro* transcription reactions were used to create S-35 labeled RNA riboprobes using the MAXIscript kit (Ambion). The reaction mixture contained 5 µM S-35 UTP (PerkinElmer), 13.25 µM UTP, 500 µM each of ATP, CTP and GTP, 1 µg of the appropriate linearized DNA and 40 units of either T7 (sense) or SP6 (antisense) polymerase. Reactions were incubated for 4 hrs at 37°C and probes were purified using Micro Bio-Spin P-30 Tris spin columns (Bio-Rad). Probe quality was verified by bleach agarose gel electrophoresis (Aranda, LaJoie, and Jorcyk 2012), agarose gels were dried using a gel drying kit (Promega) and radioactivity was visualized using phosphor screens (Typhoon Phosphoimager GE Healthcare). Probe quantity was determined using a scintillation counter (Beckman Coulter LS6500). Probes were kept at -80 °C overnight.

All slides were processed together in one batch. Slides were thawed and dried at 50 °C for 5 min and fixed for 10 min in 4% paraformaldehyde (diluted from 37% paraformaldehyde ampules; Ted Pella) in 1x PBS (Ambion). Slides were rinsed for 3 min each in 1x PBS and then .1M, pH 8 triethanolamine (TEA; Sigma-Aldrich). Tissue charge was neutralized using 0.25% V/V acetic anhydride (Sigma-Aldrich) in 0.1M pH 8 TEA for 10 min. Slides were rinsed in 2x SSC buffer (Ambion) for 3 min and then dehydrated with

a series of ethanol baths (50, 70, 95 and 2 changes of 100%) for 3 min each. Slides were dried for 15 min at room temperature and a hydrophobic barrier was drawn around the edge of the slide with a PAP pen (Ted Pella) before tissue was rehydrated in a solution containing 4.2×10^6 cpm/ml radiolabeled riboprobe, 0.01 M dithiothreitol (DTT; Sigma-Aldrich) in 1x hybridization solution (Sigma-Aldrich). Slides were covered using HybriSlip hybridization covers (ThermoFisher Scientific) and sealed with clear nail polish. Slides were placed into humidified plastic containers and incubated for 16 hours at 55 °C. After hybridization, slides were placed in 4x SSC and hybridization covers were removed. After covers were removed slides were rinsed in 2x SSC containing 1ul/ml DTT. To digest unbound probe, slides were treated with 20 µg/ml RNase A (Invitrogen) in 500 mM NaCl and 10mM tris buffer (Ambion). Slides were then rinsed in 2x SSC and then washed in 55 °C solutions to remove unbound probe as follows: 1.25 hrs in 2x SSC, 50% formamide (Sigma-Aldrich) and 1 µl/ml DTT followed by two washes in .1x SSC and 1ul/ml DTT for 30 min. Slides were then dehydrated in a series of ethanol baths containing 0.3M ammonium acetate (Fisher Scientific; 50, 70, 95% ethanol) and 2 changes of 100% ethanol for 3 min each. Slides were dried with a vacuum desiccator and stored in a desiccation cabinet at room temperature overnight.

To visualize the hybridized probe, slides were processed for autoradiography. Slides were hung on wires in a light-tight incubator and dipped in 43°C NTB autoradiographic emulsion (Carestream Health). Slides were dried while suspended in the incubator for 1 hr at 50 °C, then placed into light-tight boxes at 4 °C for 5 days. Slides were warmed to room temperature and emulsion was developed using D19 Kodak replacement developer (Electron Microscopy Sciences) diluted 50% with water and Kodak fixer (VWR). Slides were then stained with cresyl violet for 25 min, dehydrated in ethanol (95% and then 2 changes of 100% for 2 min each). Finally, the tissue was cleared using xylenes

(Millipore, 2 changes for 6 min each) and slides were coverslipped with permount (Fisher Scientific). Slides incubated with the antisense probe (Figure 2 C-D) showed strong silver grain staining compared to the sense probe (Figure 2 A-B) which did not stain above background levels and had a more uniform staining pattern indicative of background fog (Chen, Wada, and Jarvis 2012).

Quantification

For each brain area measurement two black and white photographs were taken at a magnification of 40x (Zeiss Axio Scope.A1). One photo was taken under brightfield illumination and one was taken under darkfield. The brightfield image shows Nissl stained cell bodies and silver grains that appear dark black. On the darkfield image cell bodies appear dark and silver grains appear bright. All image processing was done in FIJI (Schindelin et al. 2012) using custom scripts written in the ImageJ macro language. To separate cell bodies and silver grains from the background we processed the brightfield photo with an adaptive thresholding algorithm from the openCV package (Tseng 2016; Bradski 2000). This created a threshold image of cell bodies and silver grains. Silver grains not over cells were filtered from this image by excluding objects that were less than 200 pixels in area. The resulting image is a threshold mask of cell bodies which were then dilated by 3 pixels around the edges to capture silver grains overlapping the edges of cells (Burmeister, Jarvis, and Fernald 2005). The area of the sample covered by cell bodies was calculated using this threshold image, which was then subtracted from the darkfield image to only count silver grains that developed over cell bodies. We used the findFoci algorithm (Herbert et al. 2014) to segment overlapping grains and count the silver grains in the resulting image. We divided the resulting silver grain counts by the area of the photo covered by cells to get a normalized count / cell area. Preliminary testing directly

comparing this method to previously used strategies (Hoke et al. 2004) showed that this method performs equally well (data not shown). Furthermore, this method allows a higher throughput and larger sampling area because images can be taken using air lenses at a lower magnification than the previous method that used oil lenses at 100x magnification. An example photo used for quantification is shown in Figure 2E, and the results of the silver grain counting algorithm is shown in Figure 2F.

Statistical analysis

All analyses were conducted in the R statistical computing environment (R Core Team 2016).

Behavior

Community and transition experiments were analyzed separately using mixed models with The Lme4 R package (Bates et al. 2015). In the community experiment we used a mixed model with a random effect for community to account for the fact that some animals were housed in the same community. For the transition experiment we used a random effect for individual to account for repeated measures across time. In cases where overall ANOVA showed a significant effect, post-hoc testing was done by calculating least-squares means and comparing the Tukey corrected contrasts at each time point.

Growth and GSI

We used ANOVA followed by Tukey post-hoc comparisons. GSI data were log transformed to achieve normality.

Hormone data

Testosterone data was not normally distributed even after transformation so we used the non-parametric Kruskal-Wallis test with Nemenyi *post hoc* testing in the R

package PMCMR (Pohlert 2014). Estrogen data were normal after log transformation so we used and ANOVA on those data.

COX data

Data were square root transformed to improve normality. We used a mixed model with brain area, social status and their interaction as fixed effects and community and individual as random effects. Given a significant interaction effect we then used posthoc testing. We calculated least-squares means and tested the difference between DOM and SUB. P-values were then corrected using the holm correction to control the familywise error rate. Experiment 1 and 2 were analyzed separately.

Egr-1 data

Data were square root transformed to improve normality. We used a mixed model with brain area, social status and their interaction as fixed effects and individual as a random effect.

Principal components analysis

To reduce dimensionality of the dataset and visualize the effect of social status we conducted principal component analysis. We analyzed each dataset separately (Experiment 1 COX, Experiment 2 COX and *egr-1*). We calculated principal components using the base R package (R Core Team 2016). The first four principal components were analyzed for treatment effects using ANVOA.

Covariance Analyses

To compute covariance matrices we first replaced missing values with the mean of that brain area observed within that treatment (Zar 1999, 245–48). Mean substitution of missing values preserves the mean value of each cell, and while this underestimates

variance and over-represents sample size, it is widely accepted that it does not seriously affect analyses as long as the fraction of substituted data points is below 10–15% (Schafer and Graham 2002). Missing data was below 10% for each experiment. We calculated Pearson correlation coefficients for each brain area correlated to every other brain area in both COX and *egr-1* datasets.

We used permutation to assess the similarity of the matrices and effects of treatment. For each permutation strategy we used the same resampling procedure. In each fold of the permutation treatment group labels were randomly swapped, preserving the brain data within an individual. Treatment group labels were sampled without replacement to preserve group sample sizes. In the first strategy we assessed similarity of the correlation matrices by correlating the off-diagonal elements of the correlation matrices for each treatment to each other and compared these correlations to a set of 1000 permutations of the data (figure 16A). To assess the overall strength of correlations across the matrices we compared the sum of the squared correlation coefficients of the off diagonal elements to a set of 1000 permutations of the data (figure 16B). Finally, we assessed the amount of difference between the correlation matrices. For each pair of treatment correlation matrices, we calculated the difference between the off-diagonal elements. We then summed the absolute value of these differences to get a difference score for the matrix pair. The difference score was compared to 1000 random permutations of the treatment groups (figure 16C). These permutations of the treatments showed that the correlation networks were not significantly different among treatment groups, therefore we pooled treatments for each experiment to increase sample size.

We visualized each correlation matrix with a heatmap and clustered brain areas using hierarchical clustering. We used the R package pvclust to generate p-values for each cluster using multiscale bootstrap resampling (Suzuki and Shimodaira 2015). Clusters for

which $p < 0.05$ are highlighted with squares. To examine similarity of the matrices, we used the Mantel test in R package *ade4* to compute the correlation between the correlation matrices (Dray and Dufour 2007). The mantel test iteratively permutes the rows of the correlation matrix and recalculates the correlation between the two matrices each time. The null hypothesis is that that matrices are unrelated, so $p < 0.05$ indicates that the matrices are more similar than expected by chance.

RESULTS

DOM and ascending males show more aggressive and sexual, and fewer submissive behavioral displays. In the community experiment, DOM males showed significantly more aggressive (LMM, $t = -4.77$, $p = 8.03 \times 10^{-5}$) and sexual displays (LMM, $t = -3.071$, $p = 6.50 \times 10^{-3}$) and fewer submissive displays (LMM, $t = 5.733$, $p = 3.76 \times 10^{-6}$) as compared to SUB males (Figure 1 B-D). In experiment 2 ascending males significantly increased aggressive (ANOVA, $\chi^2 = 96.02$, $df = 7$, $p < 2 \times 10^{-16}$) and sexual behavior (ANOVA, $\chi^2 = 17.74$, $df = 7$, $p = 1.32 \times 10^{-2}$) and decreased in submissive behavior (ANOVA, $\chi^2 = 17.77$, $df = 7$, $p < 1.31 \times 10^{-2}$) over time. Changes in aggressive and submissive behavioral displays were significant within 1 hour of the social opportunity while changes in sexual behavior were significant after 48 hours. Statistical results from the comparisons at each time point are summarized in table 2.

There was an effect of treatment on growth rate (Figure 3A, ANOVA: $F = 11.39$, $p = 2.13 \times 10^{-5}$). Stable DOM males ($p = 2.82 \times 10^{-4}$) and ascending males ($p = 6.86 \times 10^{-5}$) had higher growth rates than the control males. Stable SUB males had intermediate growth rates that were not significantly different from the growth rates of any other group. There was an effect of treatment on relative gonad size (Figure 3B, ANOVA: $F = 5.91$, $p = 1.65 \times 10^{-3}$). Stable DOM males ($p = 1.49 \times 10^{-3}$) and ascending males ($p = 2.43 \times 10^{-2}$) had

larger gonads than stable SUB males. Control males had intermediate gonad sizes that were not significantly different from the other groups.

Circulating testosterone levels were affected by the treatments (Figure 3C, Kruskal-wallis, $\chi^2 = 19.95$, $p = 1.74 \times 10^{-4}$). As expected, stable DOM males had higher testosterone levels than stable SUB ($p = 2.30 \times 10^{-4}$) and control groups ($p = 1.41 \times 10^{-2}$) but were not significantly different from the ascending group. The ascending group had intermediate testosterone levels, they were higher than the stable SUB group ($p = 3.01 \times 10^{-2}$) but not significantly different from the control group. Stable SUB and control groups had the lowest T levels and were not significantly different from one another. Circulating estradiol levels were higher in ascending animals compared to the control (Figure 3D, ANOVA, $F = 21.7$, $p = 9.90 \times 10^{-5}$). Estradiol was not measured in the experiment 1.

In experiment 2 animals were presented with an intruder male stimulus. Neither latency to first attack (Figure 4A, Kruskal-wallis, $\chi^2 = 0.038$, $p = 0.845$) or aggressive displays towards the intruder (Figure 4B, Kruskal-wallis, $\chi^2 = 0.283$, $p = 0.595$) differed between the social opportunity treatment and sham control. Body weight of the focal male was a predictor of the amount of aggression displayed to the intruder among ascending males but not among control males (Figure 4C; interaction, $t=2.377$, $p = 0.0281$). Among social opportunity males, total aggression was positively correlated to both estradiol levels (Figure 5D; $F = 8.785$, $p = 0.0129$) and testosterone levels (Figure 5B; $F = 7.61$, $p = 0.0186$). Intruder directed aggression was positively correlated to estradiol levels (Figure 5C; $F = 5.358$, $p = 0.0410$) and showed a positive trend with testosterone levels (Figure 5A; $F = 3.738$, $p = 0.0793$). Aggression did not significantly correlate with hormone levels among the control males.

We measured COX activity in 31 limbic and sensory brain areas covering the majority of the forebrain as well as parts of the hypothalamus and midbrain. We found

strikingly similar patterns of COX activity among all four groups in terms of differences between brain areas (figure 6; LMM brain area: $\chi^2 = 2698.30$, $p < 2.2 \times 10^{-16}$). In cytochrome oxidase staining a new parcellation of the granular zone of the dorsal-lateral telencephalon (dlg) was readily apparent and strongly differentiated with lighter staining from the rest of the dlg ($\chi^2 = 54.39$, $p = 1.56 \times 10^{-9}$). At about the level of the anterior commissure the dlg separates into two parts with the ventromedial part (dlg2) having fewer and less densely packed lamina which are rotated at an approximately 45° angle to the more densely packed lamina of the dorsolateral portion (dlg1; see COX brain atlas 30-150 μM , Appendix). In experiment 1, we found a significant brain area by social status interaction effect, indicating that some brain areas were affected by social status ($\chi^2 = 57.32$, $p = 0.00192$). In posthoc testing we found three brain areas with marginally significantly higher levels of COX in stable DOM males: dc5 ($p = 0.0741$), dm2c ($p = 0.0246$), and vdc ($p = 0.0044$) and one brain area that was significantly lower in stable DOM males: dp ($p = 0.0655$). None of these differences survived multiple hypothesis test correction. In the transition paradigm we found a significant brain area by social status interaction effect, indicating that some brain areas were affected by social status ($\chi^2 = 50.530$, $p = 0.0109$). Despite the significant interaction, none of the brain areas were significantly different between control and ascending males in posthoc testing. Statistical results for all brain areas are summarized in table 3.

In the transition experiment we measured *egr-1* in 25 limbic and sensory brain areas covering the majority of the forebrain as well as parts of the hypothalamus. Midbrain areas were not measured (Figure 7). There were no significant differences between the ascending and control males in the amount of *egr-1* expression (brain area by status: $\chi^2 = 13.670$, $p = 0.9538$).

Principal component analysis of the cytochrome oxidase data showed that there was a significant effect of social status in experiment 1 (Figure 8B, ANOVA $F = 4.094$, $p = 8.82 \times 10^{-3}$) but not in experiment 2 (Figure 8D, $p = 0.07$). The first four principal components described the majority of the variation in the community experiment (56.1%). Despite the overall treatment effect, none of the components showed a significant treatment effect in Posthoc testing. The treatment effect was most strongly driven by PC1 ($p = .315$), PC2 ($p = .163$) and PC4 ($p = .070$). There was no significant treatment effect in the *egr-1* data (Figure 9; ANOVA, $F = 0.604$, $p = 0.615$). PC loadings are summarized in table 4. PC1 loadings between the community COX data and the transition COX were substantially similar ($r^2 = 0.55$, $p = 1.25 \times 10^{-5}$) as were the transition COX and transition *egr-1* loadings ($r^2 = .36$, $p = 3.301 \times 10^{-3}$) indicating similar covariance structure between these datasets.

To investigate functional connectivity, we constructed Pearson correlation matrices of the COX and *egr-1* data, treatments within each experiment were pooled as permutation testing indicated no effects of treatment on correlation structure (see methods). We visualized the matrices using heatmaps and clustered brain areas using hierarchical clustering with bootstrapping to assess statistical confidence in the clusters (figure 10). We found significant clustering in each matrix (bootstrap support $\geq 95\%$) and similarities in covariance structure across experiments. Significant clusters are shown in Figure 10 and listed in table 5. According to the Mantel test, the correlation structure was significantly similar across the three datasets. Correlation structure of the COX levels in the community experiment was similar to the correlation structure of COX levels in the transition experiment (Figure 11A, $r = 0.335$, $p = 1 \times 10^{-4}$) and the *egr-1* levels in the transition experiment (Figure 11C, $r = .331$, $p = 1 \times 10^{-4}$). In the transition experiment, correlation structure in the COX data was significantly similar the structure in *egr-1* data (Figure 11B, $r = .440$, $p = 1 \times 10^{-4}$).

DISCUSSION

In the present study we confirmed that *A. burtoni* males ascending to DOM social status increase aggression within 1 hr of a social opportunity and increase to aggression levels near DOM levels within 1 day of transition (Huffman et al. 2012; Burmeister, Jarvis, and Fernald 2005; Maruska and Fernald 2011). Furthermore we replicate the finding that sexual behavior increases more gradually and that GSI, androgens and estrogens increase to near DOM levels within 1 week of transition (Huffman et al. 2012). Finally we replicate the finding that ascending in status increases the growth rate (Hofmann, Benson, and Fernald 1999).

Our study uses a novel experimental paradigm that allows SUB males a refuge, extending the time that SUB males can be held subordinated in the experimental tank up to 10 days from 1 day in previous designs (Huffman et al. 2012; Burmeister, Jarvis, and Fernald 2005; Maruska and Fernald 2011). This enclosure also allows the presentation of stimulus males exclusively to SUB males. This was not possible with previous designs because a DOM male would be needed to suppress social transition and would minimize any interactions between the focal SUB male and the intruder male (O'Connell et al. 2013; Weitekamp and Hofmann 2017). Interestingly SUB males have a robust aggressive reaction to unknown intruder males. SUB males show the same amount of aggression toward the intruder males and respond with the same latency as transitioning males, although overall aggression is higher in the transitioning males because parts of their aggressive activity is directed toward the side communities as well. Previous studies have shown that DOM males respond strongly to unfamiliar males (Weitekamp and Hofmann 2017) and that SUB males are capable of showing a full range of aggressive displays, especially when they are not being observed by DOM males (Desjardins, Hofmann, and Fernald 2012), however this is the first study to directly test the SUB male response to an

intruder male. Interestingly among the ascending males, testosterone and estradiol levels were predictive of aggression while among the control males aggression was independent from hormone levels which suggests that there may be different hormonal responses depending on social status. In several species of tropical song birds territorial aggression appears to be facilitated by androgens during the breeding season but different hormonal mechanisms are involved during the non-breeding season when their gonads are regressed (Hau, Stoddard, and Soma 2004; Canoine and Gwinner 2002; Hau and Beebe 2011)

We investigated COX patterns across the forebrain of the teleost fish. We found several areas that were higher in stable DOM males including dc5 (dorsal pallium), dm2c (pallial amygdala), vdc (nucleus accumbens) and one area that was higher among Stable SUB males, dp (olfactory cortex). These differences should be considered as provisional and exploratory since they were not strongly supported in posthoc testing. Dc5 is the dorsal division of the central part of DC and is enlarged in the Cichlid lineage. It is putatively homologous to the dorsal pallium, although this is tentative as it may be composed of migrated components from other pallial areas (Mueller et al. 2011; Northcutt 2011). It receives sensory afferents directly from the diencephalon as well from the major sensorimotor integrative centers of the teleost brain, the thalamus and the preglomerular complex (Demski 2013). In addition, it has reciprocal connections to all other major pallial areas (Demski 2013). Given its connections throughout the pallium as well as all sensory areas it is likely to be important for integration and processing of multimodal sensory information. Stimulation of the area in bluegill sunfish males causes nest building behavior, an appetitive sexual behavior likely via a connection to the POA (Demski and Knigge 1971). Lesions of the area disrupt visual associative learning in squirrelfish and goldfish (Rooney and Laming 1986; Laming 1987). Increased levels in DOM males may reflect an increase in sexual behavior or an increased demand in processing multimodal signals.

Dm2c (also called dmdv in tilapia) is the caudal part of dm2 which is a nucleus possibly unique to the cichlid lineage (Burmeister, Munshi, and Fernald 2009). Dm is homologous to the pallial amygdala of other vertebrate lineages. Because dm2 is only known in the cichlid lineage, functional studies are lacking, however it is generally assumed to have a similar function in limbic processing as the rest of the amygdala. Electrical stimulation of Dm3 in bluegill sunfish causes increases in defensive, escape and anxiety related behaviors consistent with the role of the amygdala in other vertebrate lineages (O'Connell and Hofmann 2011; Demski 2013). Increases in dm2c in DOM males could possibly be related to increases in territorial defense and challenges from rival males. Vdc is the caudal part of vd which is thought to be homologous to the nucleus accumbens. It receives dopaminergic input from the putative VTA homolog, the Tpp, and is thought to be involved in motivated behavior and reward based learning similar to its function across vertebrates (O'Connell and Hofmann 2011). Increase in the activity of vdc in DOM males may reflect increases in appetitive sexual and territorial behaviors that are known to be modulated by dopaminergic inputs. Dp is homologous to the olfactory pallium in other vertebrate lineages. It is involved in higher order processing of odorants including integration of olfactory information with other pallial circuits in the amygdala and hippocampus. Higher activity in the dp of SUB males may reflect differences in the salience or processing of odorants depending on social status. Cichlids communicate via chemicals in their urine and the urine of SUB and DOM males causes different transcriptional programs in the dp of male tilapia (Simões et al. 2015).

Our study supports many of the parcellations identified by Burmeister et al (2009). In addition, we identified a new parcellation of dl, dlg2. Dlg2 separates from dlg1 at the level of the lateral forebrain bundle and is clearly distinguished from dlg1 because it has much lower levels of cytochrome oxidase. The lower levels of cytochrome oxidase are

probably indicative of a different organization in the neuropil of this brain area or lower activity (Wong Riley 1994). In addition, it can be seen in the Nissl stained sections that there are fewer lamina and the cell density is lower (Burmeister, Munshi, and Fernald 2009). Finally, differences in sex steroid hormone receptor levels further support this region as being a separate parcellation as *dlg2* has stronger expression of estrogen receptor alpha than *dlg1* (Munchrath and Hofmann 2010).

No mean differences were found in the *egr-1* data. This may be due to the fact that all animals in this experiment were exposed to the same stimulus (an intruder male) and both groups (ascending males vs control) had a similar response. Single label immediate early gene studies are limited because the molecular phenotype and connectivity information of the activated cells are unknown. In a study of rats in comparing cells activated during a rewarding experience (appetitive cocaine dosing) and an adverse experience (foot shock), the vast majority of limbic brain areas had the same number of cells activated in both experiences (Ye et al. 2016). Interestingly, follow up experiments show that while the number of cells activated was similar, the molecular phenotype and connectivity pattern of the subsets of cells recruited in each experience was different. In addition, this difference led to divergent correlation patterns between brain areas depending on the experience (Ye et al. 2016).

We examined correlation patterns in our study as a proxy of functional connectivity. Similar experiments using COX histochemistry and immediate early gene markers have found that correlation patterns can differ based on experience or stimulus salience, even when mean levels are similar. We found similar correlation structures across all of our treatments and datasets including in comparisons between *cox* and *egr-1* data. Using permutation, we found that treatment effects on correlation structure were not detectable beyond the differences expected by random subsampling of the data. Our study may be

underpowered for this kind of analysis since we are estimating all the pairwise correlations for 25 brain areas and have between 13 – 15 individuals in each group. To address this problem, we continued our analyses by pooling experimental treatment groups in order to increase the sample size. Using these pooled datasets, we compared correlation structure in the COX dataset from experiment 1 and experiment 2 and the *egr-1* dataset from experiment 2. We found that all the datasets had a significantly similar correlation structure possibly indicative of functional circuits, based on the results of the mantel test which showed the correlation matrices in the different experiments were more similar to each other than would be expected by chance. For example, we might expect that *vdr* and *vc* would have correlated activity since they are widely believed to be the homolog of the striatal formation in mammals, are known to have a large number of synaptic connections and in some parts of the brain are intercalated at their border. Indeed, we find that *vdr* and *vc* are clustered in two of the three datasets. Other possible functional circuits in our cluster analysis include *dp* (olfactory cortex), *poa*, *dd* (medial pallium), *dm3* (pallial amygdala), and *vsm* (extended amygdala); *dc5* (dorsal pallium) and *dlg2* (hippocampus); *vdr* (striatum) and *vv* (ventral pallidum).

Conclusion

We found that males responded robustly to an opportunity transition in status. Surprisingly both ascending and SUB males strongly responded to an intruder male stimulus, although the SUB response was independent of circulating levels of androgens and estrogens while the DOM response was correlated. Social status affects brain activity in subtle ways. It is probable that we are missing much of the variation caused by status, because of the coarse whole area measurements in this study. Although the groups differed substantially in behavior, both sets of animals are constantly evaluating the environment

and social environment and therefore it is perhaps unsurprising that most brain areas were equally active. The evidence of functional circuits shown here help to bolster some of the homology relationships proposed from hodological, anatomical and molecular marker studies. Future studies can further address the mechanisms of these behavioral differences by double labeling specific cell types to identify more specific circuits that may vary more than whole brain area measurements of brain activity.

ACKNOWLEDGEMENTS

We thank Caleb Ellington for technical assistance; Ross Gillette and David Crews for COX expertise and equipment; Sylvia Garza for technical assistance and fish care; Eva Fischer for commenting on drafts of this manuscript; and members of the Hofmann laboratory for insightful discussions.

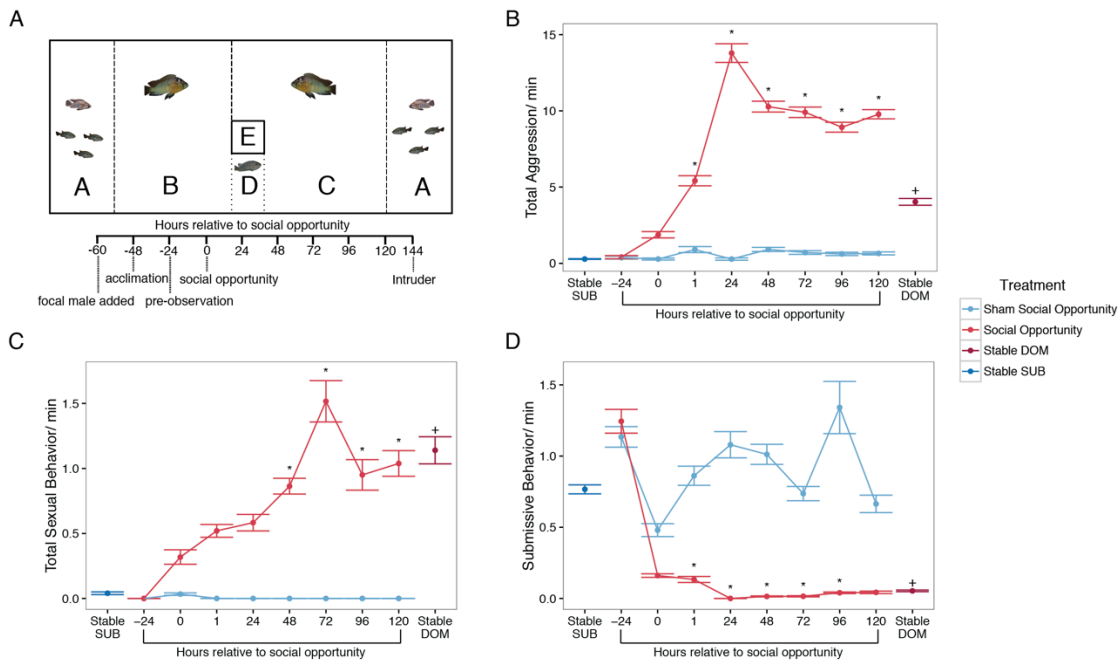


Figure 2.1: A) Experimental paradigm and timeline. Compartments-A side communities of one male and three females which serve as a social stimulus for all animals in the paradigm. Compartment-B suppressor male. Compartment C-Suppressor male that is removed in the social opportunity treatment. Compartment D – refuge for focal male. Compartment E – chamber that allows for the presentation of an intruder male to both transitioning animals or the subordinate controls. Stable DOM males (dark red) have more aggressive (B) and sexual behavior (C) than stable SUB males (dark blue) and less submissive behavior (D). Social opportunity males (light red) rapidly increase levels of aggression (B) and sexual behavior (C) and decrease levels of submissive behavior (D) after the opportunity to ascend in status compared to sham controls (light blue).+ = $p < 0.05$ in the comparison between Stable DOM and SUB, * = $p < 0.05$ in the comparison between ascending males and control within that time point.

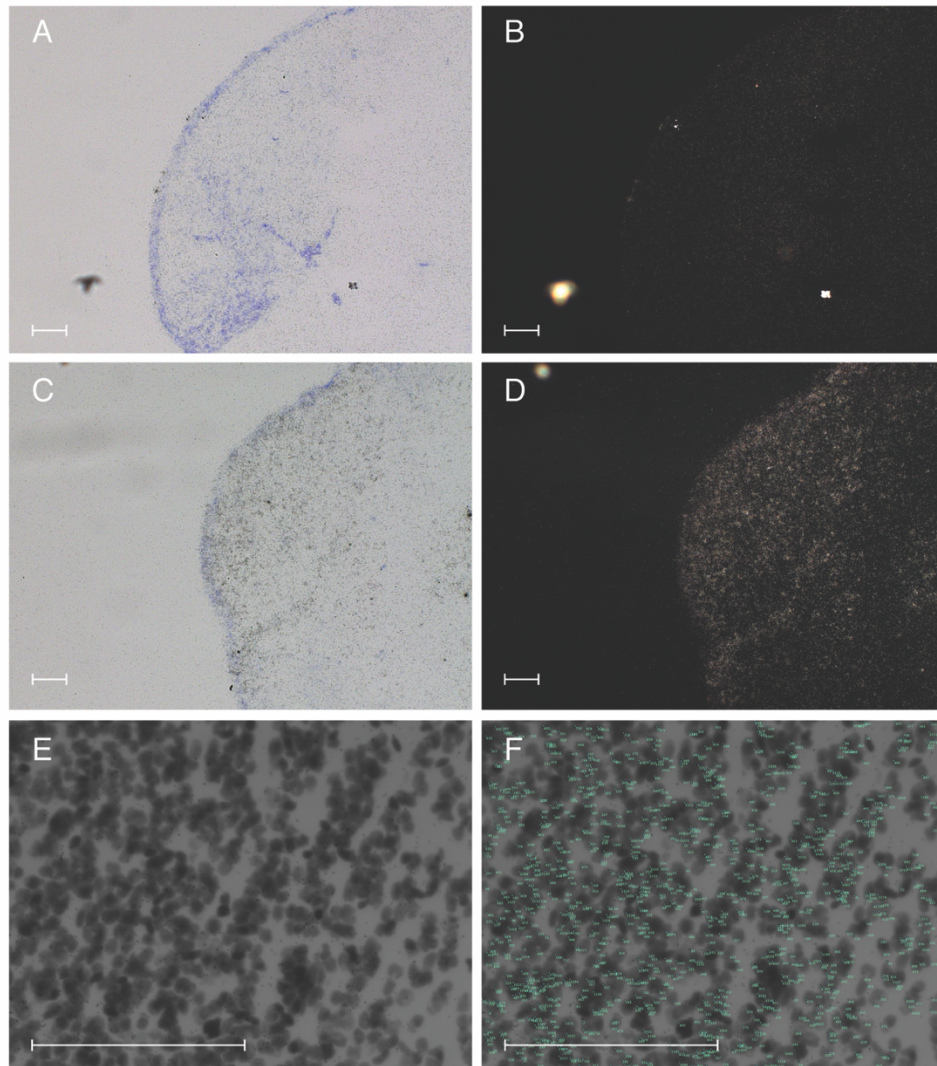


Figure 2.2: Example micrographs of radioactive *in situ*. All photos depict the granular zone of the dorsolateral part of the pallium (dlg1). A) 5x Brightfield and corresponding darkfield (B) micrograph of a slide incubated with the sense control probe. C) 5x Brightfield and corresponding darkfield (D) micrograph of a slide incubated with the antisense probe. E) An example of the 40x magnification used for quantification. F) The result of processing the photo in (E) with our imaging processing and silver grain counting program. Numbered blue dots represent individual silver grains counted by our algorithm. All scale bars = 0.1 mm.

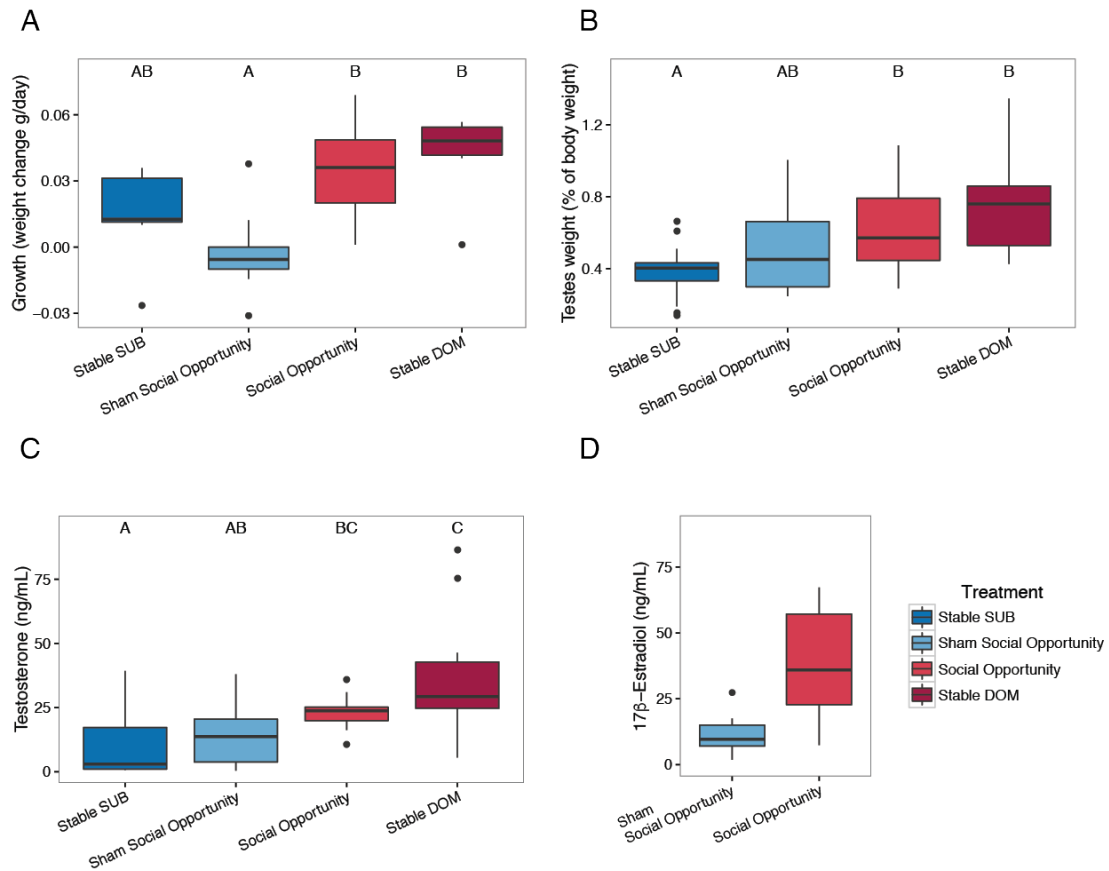


Figure 2.3: Social status influences many physiological parameters, letter codes in A-C represent statistical differences between groups. A) Stable DOM (dark red) and ascending males (light red) had a higher growth rate than control males (light blue). Stable SUB males (dark blue) were intermediate. B) DOM and ascending males had relatively larger gonads than stable SUB males. Control males were intermediate. C) DOM and ascending males had elevated testosterone levels compared to stable SUB males. Control males were lower than stable DOM males but not different from ascending males. D) Ascending males had higher levels of circulating estradiol compared to control.

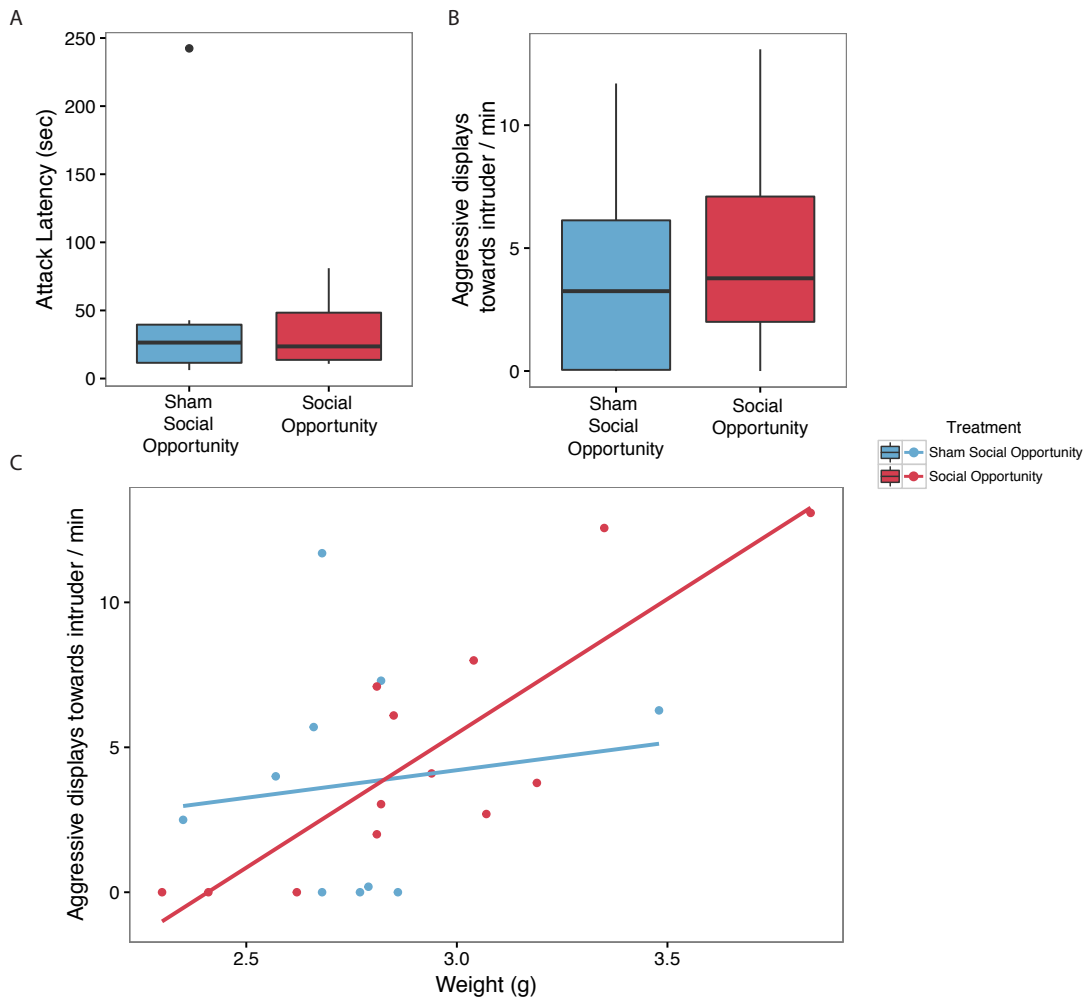


Figure 2.4: Aggression towards the intruder was not significantly different between ascending (light red) and control males (light blue). A) Latency to attack the intruder. B) Number of aggressive displays toward the intruder/ min. C) In ascending males, body weight predicted the amount of aggression displayed to the intruder but was not significant in control males.

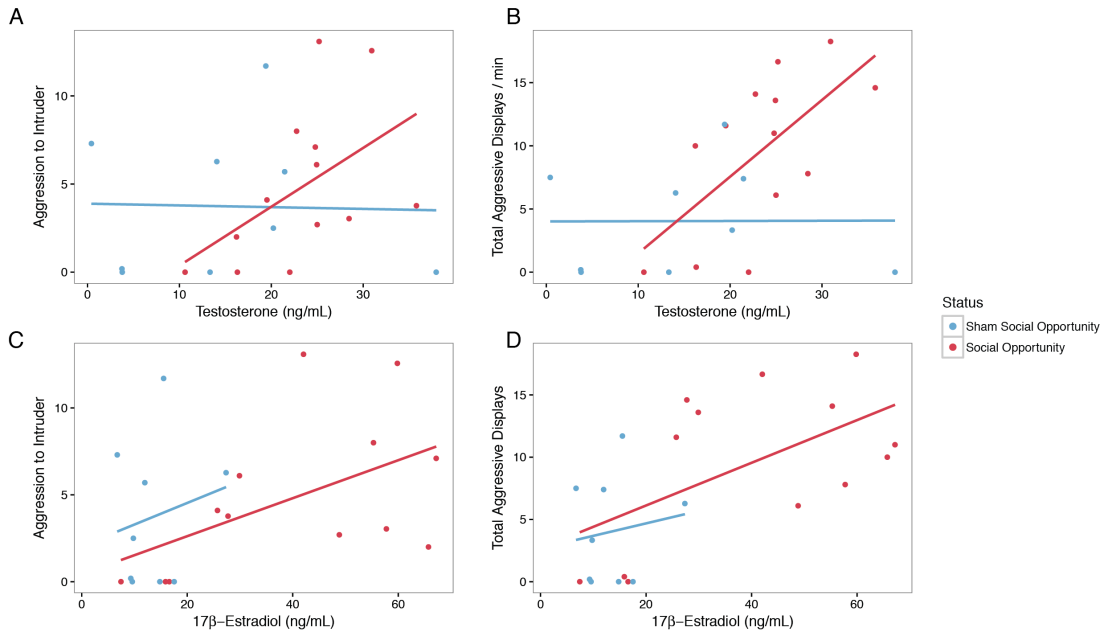


Figure 2.5: A-B) Correlations between testosterone and aggression towards the intruder (A) and total aggression (B) in ascending (light red) and control males (light blue). C-D) Correlations between estradiol and aggression towards the intruder (C) and total aggression (D).

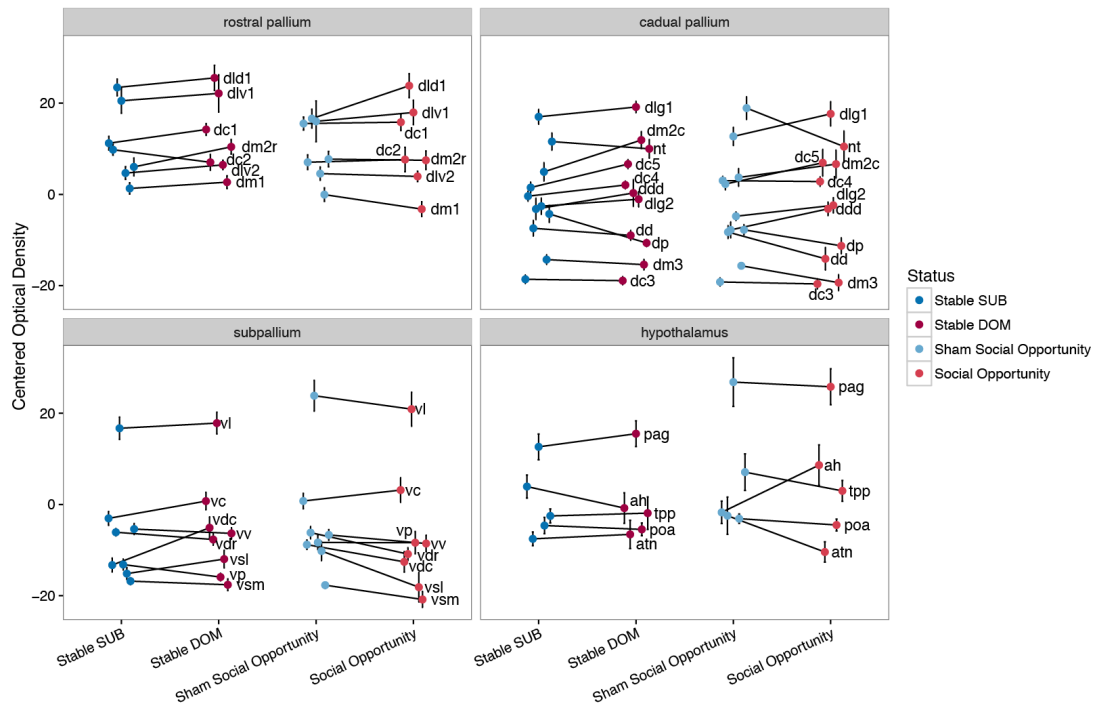


Figure 2.6: Calibrated optical density measurements of COX levels were centered within each individual and are depicted for each brain area measured. Brain areas are split into four panels depending on their origin. Points and error bars represent the group average \pm the standard error for each brain area. Groups within each experiment are connected by a line.

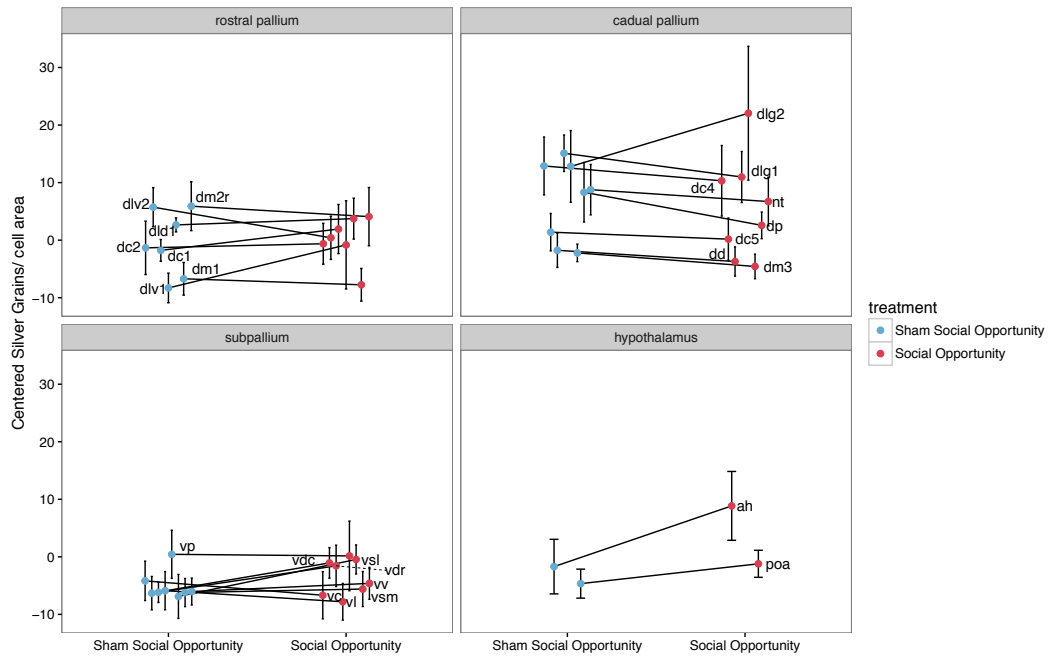


Figure 2.7: Number of *egr-1* silver grains /mm covered by cells were centered within each individual and are depicted for each brain area measured. Brain areas are split into four panels depending on their origin. Points and error bars represent the group average \pm the standard error for each brain area. Groups within each experiment are connected by a line.

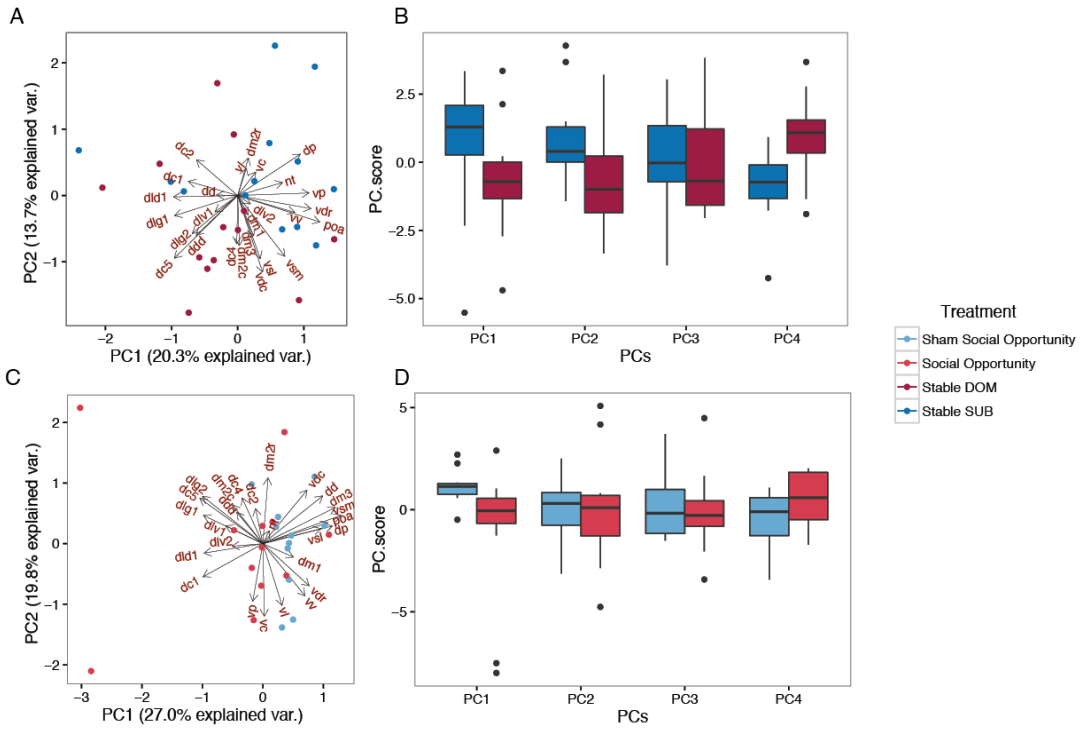


Figure 2.8: Principal component analysis of COX datasets. A) Biplot of experiment 1, PCs 1 and 2 showing the loadings. B) Experiment 1 principal component scores as a function of social status for the first four components. C) Biplot of experiment 2, PCs 1 and 2 showing the loadings. D) Experiment 2 principal component scores as a function of social status for the first four components.

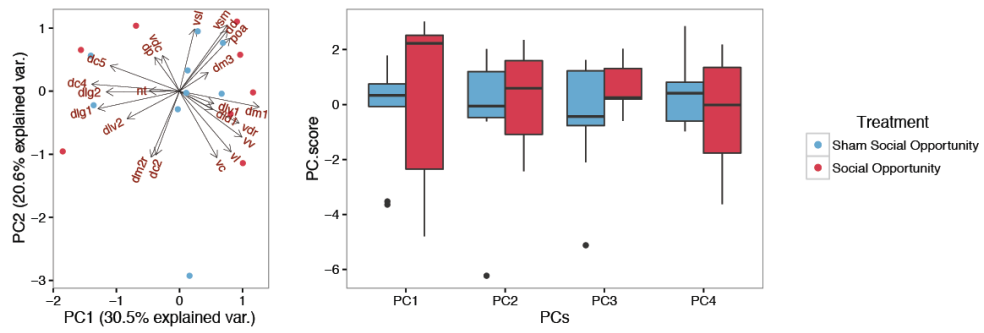


Figure 2.9: Principal component analysis of *egr-1* in experiment 2. A) Biplot of PCs 1 and 2 showing the loadings. B) Principal component scores as a function of social status for the first four components.

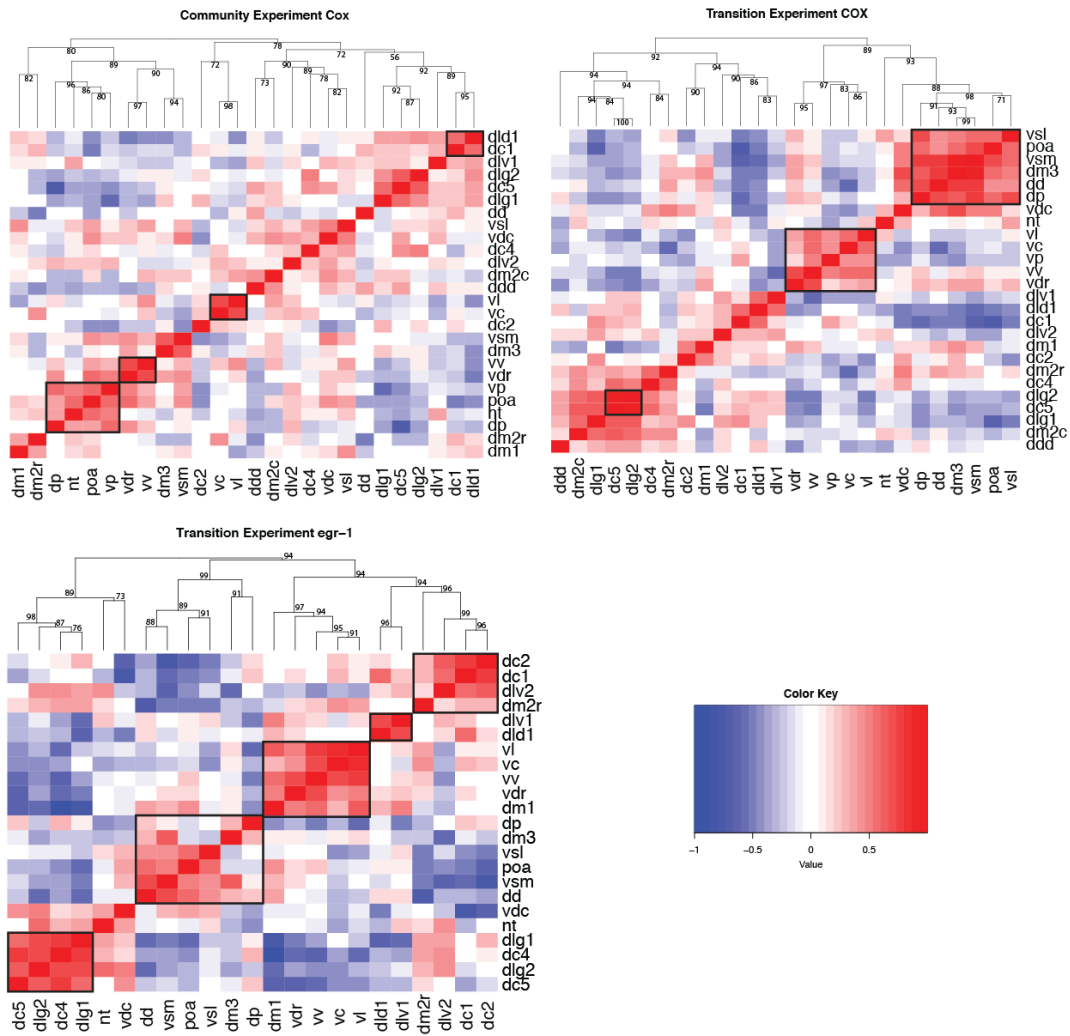


Figure 2.10: Clustered heatmaps of all pairwise correlations between brain areas. Color represents Pearson correlation coefficients. Experiment 1 COX dataset (top left), Experiment 2 COX dataset (top right) and Experiment 2 *egr-1* dataset (bottom left). Bootstrap resampling was used to identify significant clusters which are depicted with black boxes.

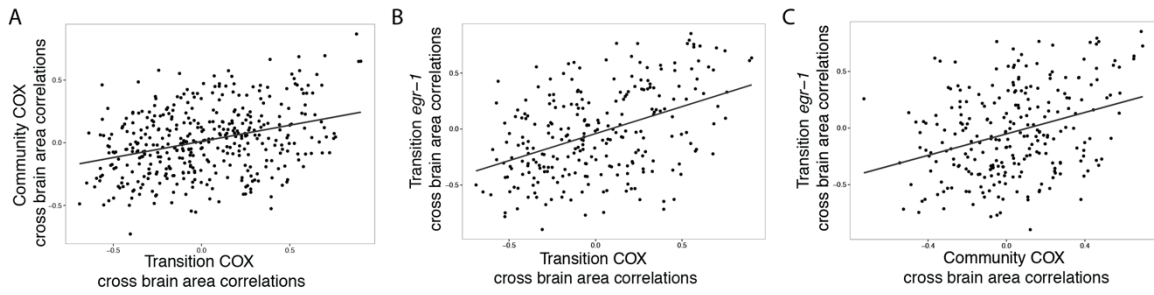


Figure 2.11: Correlations of the covariance matrices comparing across datasets. Each point represents the Pearson correlation coefficient between a pair of brain areas in one dataset, compared to the correlation coefficient of that pair in another dataset. A) Experiment 1 COX compared to Experiment 2 COX. B) Experiment 2 *egr-1*, compared to Experiment 2 COX. C) Experiment 2 *egr-1* compared to experiment 1 COX.

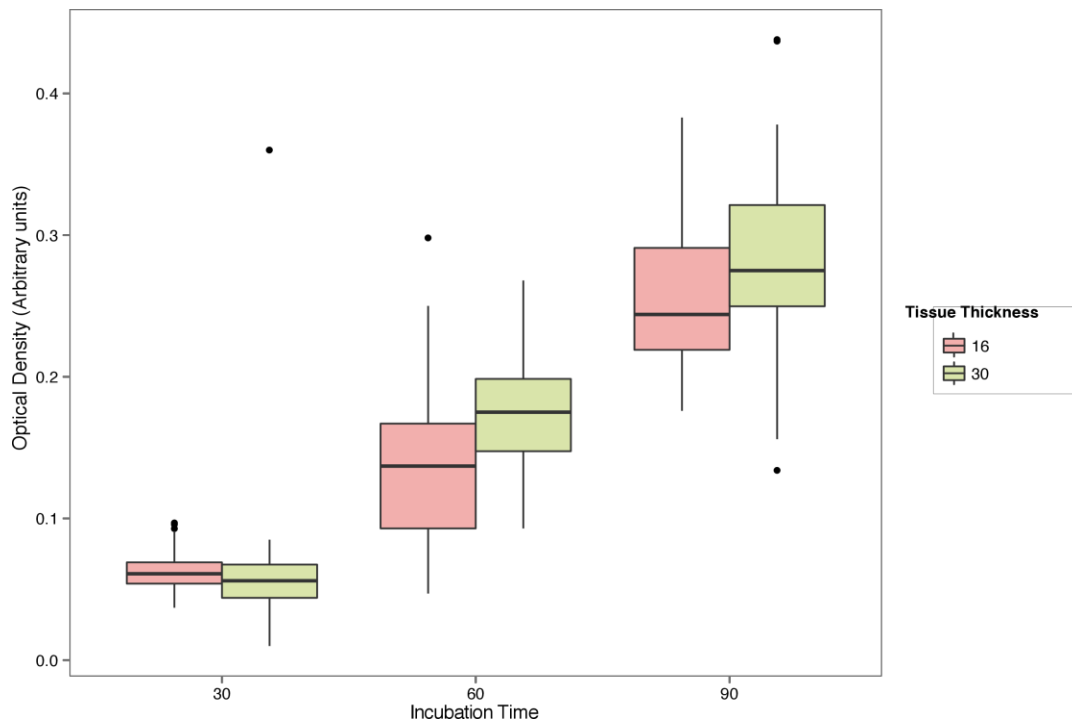


Figure 2.12: Staining density as a function of incubation time across the brain areas measured in this study. Staining density approximately doubled on average with each 30 min increment of incubation time (X axis). Tissue thickness was a less important factor ($16\mu\text{M}$ in red, $30\mu\text{M}$ in green), at least at this level of examination.

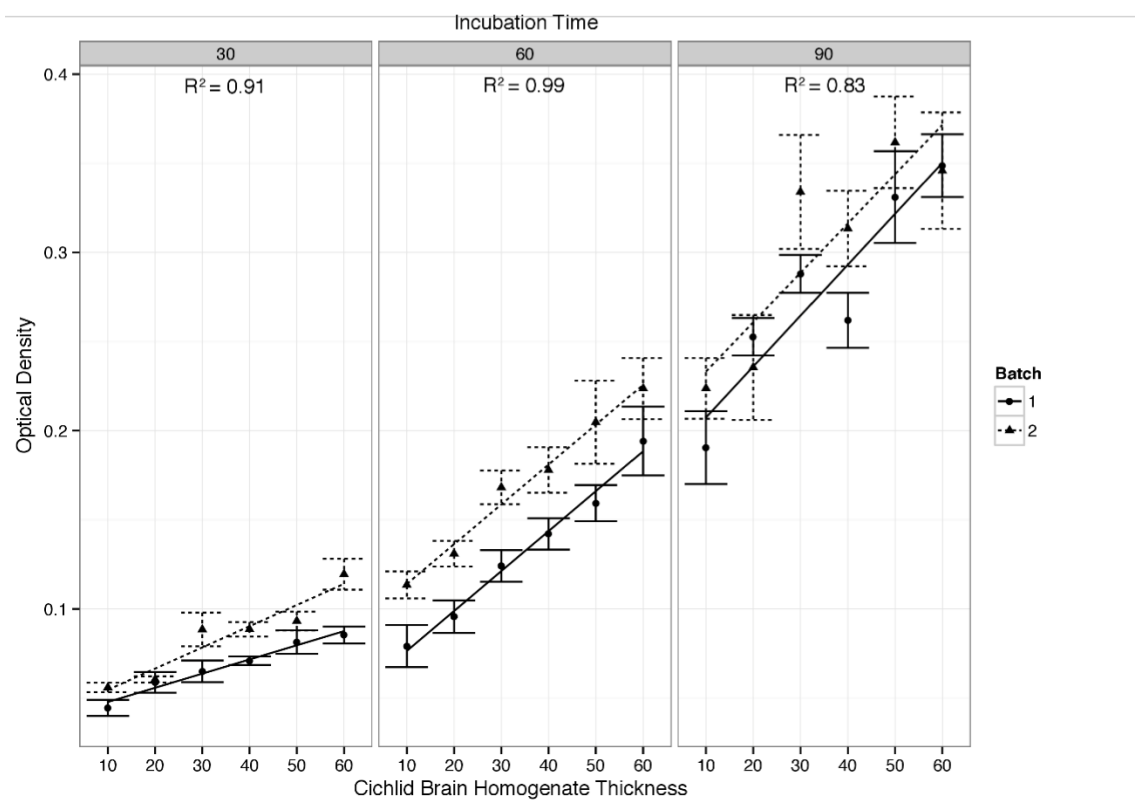


Figure 2.13: Optical density of increasingly thick cichlid brain homogenate. Slides were processed in two batches (line type) and at three incubation times: 30, 60 and 90 min (Panels). R-squared values are calculated from linear models that include both batches with the batch effect as a parameter.

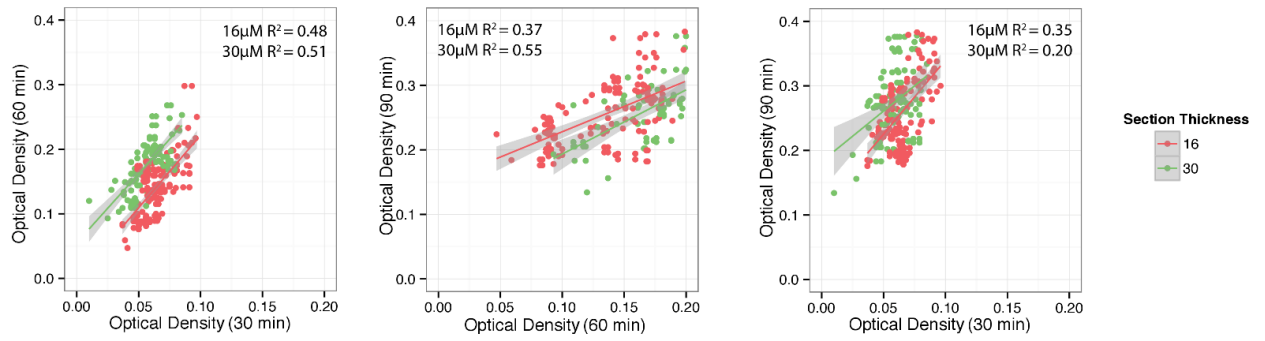


Figure 2.14: Correlations between brain areas measured on adjacent sections. Each panel shows the correlations between two incubation times. Panel 1: 30 - 60 min, Panel 2: 60 - 90 min, Panel 3: 30 - 90 min. 16µM sections are shown in red, 30µM sections are shown in green.

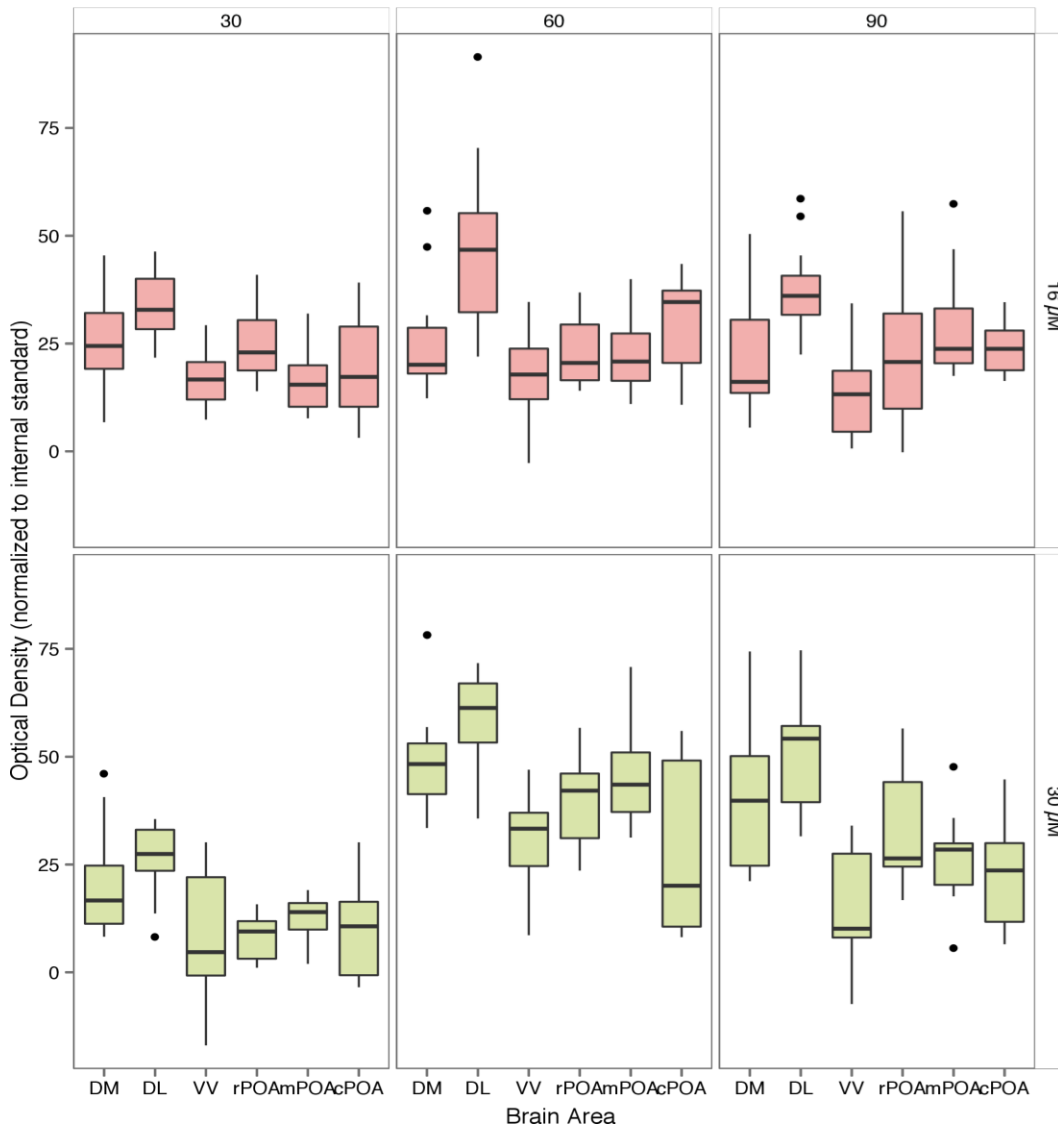


Figure 2.15: Optical density was measured in each brain area and then normalized to the internal tissue homogenate standard for that time point. The panels are arranged by incubation time (columns) and tissue thickness (rows, 16 μM in red, 30 μM in green).

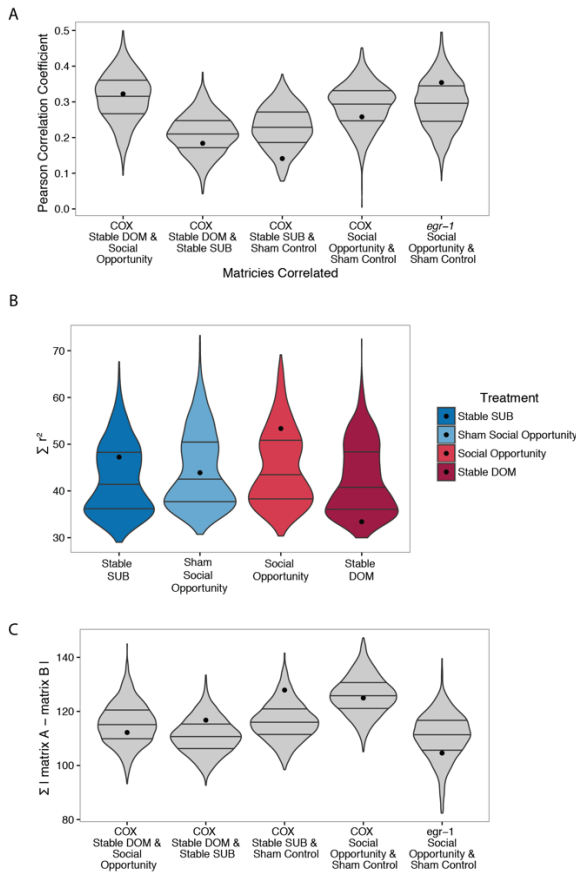


Figure 2.16: Permutation of covariance matrices. A) Permutations comparing similarities (matrix correlations) of the covariance matrix of each group. Violin plots show the distribution of correlation coefficients of the matrices after random permutation of the group labels. Points are the real correlation coefficient between the two matrices. B) For each covariance matrix we calculated the sum of the square of the Pearson correlation coefficients which is a measure of the overall strength of correlations across the matrix and compared that to random sampling (preserving sample size of each group) of the full dataset. Violin plots show the distribution of the sum of r^2 of the randomly permuted data while points show the sum of r^2 of the real data. C) For each pair of correlation matrices we calculated the sum of the absolute value of the differences between each off-diagonal element of the matrices. Violin plots show the distribution of the difference scores of the randomly permuted data while points show the difference score of the real data.

Abbreviation	Full Name	Putative mammalian homolog
Atn	Anterior tuberal nucleus	ventral medial hypothalamus
Ah	Anterior hypothalamus	Anterior hypothalamus
D	Dorsal division of the telencephalon	Pallium
Dc-1,2,3,4,5	Central division of D (5 subdivisions).	Pallium (specific homology unclear)
Dd	Dorsal division of D	Pallium (specific homology unclear)
Ddd	Dorsal subdivision of dd	
Ddv	Ventral subdivision of dd	
Dl	Lateral division of D	Hippocampus
Dld1	Dorsal subdivision of dl	
Dlg1	Dorsal-lateral part of the Granular zone of dl	
Dlg2	Ventral-medial part of the granular zone of dl	
Dlv -1,2	Ventral division of dl (2 subdivisions)	
Dm – 1,2,3	Medial division of D (3 subdivisions)	Pallial amygdala
Dm2c	Caudal part of dm2	
Dm2r	Rostral part of dm2	
Dp	Posterior division of D	Olfactory pallium
Nt	Nucleus taenia	
OB	Olfactory bulb	Olfactory bulb
Pag	Periaqueductal gray	Periaqueductal gray
Poa	Preoptic area	Preoptic area
Tpp	Posterior tuberculum	Ventral tegmental area

Table 2.1: Brain area abbreviations used in this paper and putative mammalian homologous (O’Connell and Hofmann 2011). Continued on the next page.

V	Ventral subdivision of the telencephalon	Subpallium
Vc	Central nucleus of V	Striatum
Vd	Dorsal nucleus of V	Nucleus accumbens
Vdc	Caudal part of vd	
Vdr	Rostral part of vd	
Vl	Lateral nucleus of v	Lateral septum
Vp	Postcommissural nucleus of V	Basal amygdala
Vs	Supracommissural nucleus of V	Bed nucleus of the stria terminalis/ medial amygdala
Vsl	Lateral subdivision of vs	
Vsm	Medial subdivision of vs	
Vv	Ventral nucleus of V	Dorsal part of vv: Pallidum Ventral part of vv: Septum

Table 2.1: Continued.

<i>Contrast</i>	<i>time point</i>	<i>estimate</i>	<i>se</i>	<i>df</i>	<i>t-value</i>	<i>p-value</i>
<i>Aggressive Displays (Control - Social Opportunity)</i>	-24	0.2279507	1.380263	147.43	0.165	0.8691
	0	-1.4862502	1.380421	152.93	-1.077	0.2833
	1	-4.4398638	1.440446	163.06	-3.082	0.0024
	24	-13.253420	1.401355	150.47	-9.458	<.0001
	48	-9.1227797	1.404565	151.32	-6.495	<.0001
	72	-8.8642967	1.401178	150.51	-6.326	<.0001
	96	-8.1375872	1.417802	153.09	-5.74	<.0001
	120	-8.9472103	1.409901	147.34	-6.346	<.0001
<i>Submissive Displays (Control - Social Opportunity)</i>	-24	-0.1163757	0.3005414	176.81	-0.387	0.6991
	0	0.2942069	0.3016918	179.52	0.975	0.3308
	1	0.6791416	0.3170101	183.98	2.142	0.0335
	24	1.0705833	0.305762	178.35	3.501	0.0006
	48	0.9729257	0.306625	178.69	3.173	0.0018
	72	0.7124464	0.3057374	178.41	2.33	0.0209
	96	1.3231375	0.3098479	178.98	4.27	<.0001
	120	0.6043379	0.3069751	176.76	1.969	0.0506
<i>Sexual Displays (Control - Social Opportunity)</i>	-24	0.0383136	0.341596	139.42	0.112	0.9109
	0	-0.2606916	0.3412523	145.25	-0.764	0.4462
	1	-0.4734701	0.3553321	156.29	-1.332	0.1846
	24	-0.6711057	0.3466017	142.63	-1.936	0.0548
	48	-0.8247675	0.3473341	143.55	-2.375	0.0189
	72	-1.4542747	0.3465562	142.66	-4.196	<.0001
	96	-0.9285954	0.3504662	145.58	-2.65	0.0089
	120	-1.0063222	0.3489376	139.32	-2.884	0.0046

Table 2.2: Full statistical results of least-square means comparing behavior of ascending and control males at each time point.

<i>Brain Area</i>	<i>Paradigm</i>	<i>Estimate</i>	<i>SE</i>	<i>df</i>	<i>T</i>	<i>P value</i>	<i>Holm P value</i>
<i>ah</i>	communit	-0.289	0.216	120.735	-1.335	0.184	1
<i>atn</i>	y	0.043	0.22	129.049	0.197	0.844	1
<i>dc1</i>		0.22	0.199	89.575	1.101	0.274	1
<i>dc2</i>		-0.118	0.199	89.575	-0.591	0.556	1
<i>dc3</i>		0.031	0.199	89.575	0.156	0.876	1
<i>dc4</i>		0.192	0.199	89.575	0.964	0.338	1
<i>dc5</i>		0.36	0.199	89.575	1.807	0.074	1
<i>dd</i>		-0.051	0.199	89.575	-0.257	0.798	1
<i>ddd</i>		0.263	0.199	89.575	1.32	0.19	1
<i>dld1</i>		0.153	0.199	89.575	0.765	0.446	1
<i>dlg1</i>		0.169	0.199	89.575	0.847	0.399	1
<i>dlg2</i>		0.149	0.199	89.575	0.746	0.458	1
<i>dlv1</i>		0.107	0.199	89.575	0.538	0.592	1
<i>dlv2</i>		0.153	0.199	89.575	0.766	0.445	1
<i>dm1</i>		0.127	0.199	89.575	0.635	0.527	1
<i>dm2c</i>		0.456	0.199	89.575	2.286	0.025	0.738
<i>dm2r</i>		0.302	0.199	89.575	1.514	0.133	1
<i>dm3</i>		-0.024	0.199	89.575	-0.12	0.905	1
<i>dp</i>		-0.372	0.199	89.575	-1.865	0.065	1
<i>nt</i>		-0.06	0.199	89.575	-0.299	0.765	1
<i>pag</i>		0.214	0.21	108.506	1.018	0.311	1
<i>poa</i>		-0.02	0.199	89.575	-0.101	0.92	1
<i>tpp</i>		0.032	0.216	120.989	0.15	0.881	1
<i>vc</i>		0.275	0.199	89.575	1.378	0.172	1
<i>vdc</i>		0.583	0.199	89.575	2.921	0.004	0.137
<i>vdr</i>		-0.067	0.199	89.575	-0.335	0.738	1
<i>vl</i>		0.095	0.199	89.575	0.476	0.635	1

Table 2.3: Posthoc testing of the least-square means of COX levels of each brain area compared between ascending and control males.

<i>vp</i>		-0.155	0.199	89.575	-0.777	0.439	1
<i>vsl</i>		0.282	0.199	89.575	1.416	0.16	1
<i>vsm</i>		-0.004	0.199	89.575	-0.02	0.984	1
<i>vv</i>		-0.021	0.199	89.575	-0.103	0.918	1
<i>ah</i>	transition	-0.906	0.625	17.444	-1.45	0.165	1
<i>atn</i>		0.518	0.625	17.444	0.828	0.419	1
<i>dc1</i>		-0.169	0.574	11.103	-0.295	0.773	1
<i>dc2</i>		-0.21	0.574	11.103	-0.367	0.721	1
<i>dc3</i>		-0.071	0.625	17.444	-0.113	0.911	1
<i>dc4</i>		-0.167	0.574	11.103	-0.29	0.777	1
<i>dc5</i>		-0.471	0.574	11.103	-0.82	0.429	1
<i>dd</i>		0.282	0.574	11.103	0.491	0.633	1
<i>ddd</i>		-0.579	0.576	11.281	-1.005	0.336	1
<i>dld1</i>		-0.621	0.574	11.103	-1.082	0.302	1
<i>dlg1</i>		-0.473	0.574	11.103	-0.824	0.427	1
<i>dlg2</i>		-0.373	0.574	11.103	-0.65	0.529	1
<i>dlv1</i>		-0.33	0.576	11.281	-0.572	0.578	1
<i>dlv2</i>		-0.159	0.574	11.103	-0.276	0.787	1
<i>dm1</i>		0.012	0.574	11.103	0.021	0.984	1
<i>dm2c</i>		-0.343	0.574	11.103	-0.598	0.562	1
<i>dm2r</i>		-0.176	0.574	11.103	-0.307	0.764	1
<i>dm3</i>		0.006	0.574	11.103	0.01	0.992	1
<i>dp</i>		0.047	0.574	11.103	0.082	0.936	1
<i>nt</i>		0.428	0.574	11.103	0.745	0.472	1
<i>pag</i>		-0.123	0.63	17.994	-0.195	0.847	1
<i>poa</i>		-0.162	0.574	11.103	-0.282	0.783	1
<i>tpp</i>		0.131	0.625	17.444	0.209	0.837	1
<i>vc</i>		-0.38	0.574	11.103	-0.663	0.521	1
<i>vdc</i>		0.12	0.574	11.103	0.21	0.838	1
<i>vdr</i>		0.16	0.574	11.103	0.279	0.785	1
<i>vl</i>		0.03	0.574	11.103	0.053	0.959	1
<i>vp</i>		-0.098	0.574	11.103	-0.17	0.868	1
<i>vsl</i>		0.431	0.574	11.103	0.751	0.468	1
<i>vsm</i>		-0.033	0.574	11.103	-0.058	0.955	1
<i>vv</i>		-0.074	0.574	11.103	-0.129	0.899	1

Table 2.3: Continued.

	<i>PC1</i>			<i>PC2</i>			<i>PC3</i>			<i>PC4</i>		
	Community COX	Transition COX	Transition <i>egr-1</i>	Community COX	Transition COX	Transition <i>egr-1</i>	Community COX	Transition COX	Transition <i>egr-1</i>	Community COX	Transition COX	Transition <i>egr-1</i>
<i>dld1</i>	-0.28	-0.25	0.14	-0.01	-0.05	-0.12	-0.32	0.31	-0.29	0.03	0.19	0.28
<i>dc5</i>	-0.28	-0.26	-0.28	-0.33	0.22	0.15	0	-0.21	0.05	0.08	0	-0.11
<i>dlg1</i>	-0.28	-0.25	-0.33	-0.11	0.14	-0.07	0	0	0.13	0.04	-0.28	-0.13
<i>dc1</i>	-0.22	-0.25	NA	0.08	-0.16	NA	-0.18	0.14	NA	0.06	-0.14	NA
<i>dlg2</i>	-0.2	-0.25	-0.3	-0.2	0.23	0.03	0.01	-0.13	0.25	0.07	0.04	0.06
<i>ddd</i>	-0.18	-0.11	NA	-0.21	0.15	NA	0.13	-0.07	NA	-0.07	0.18	NA
<i>dc2</i>	-0.18	-0.03	-0.1	0.19	0.17	-0.32	0.14	0.39	-0.26	0.09	-0.24	0.14
<i>dvl1</i>	-0.1	-0.16	0.16	-0.09	0.09	-0.08	-0.35	0.28	0	-0.06	0.11	0.44
<i>dd</i>	-0.09	0.25	0.22	0	0.23	0.29	0.06	0.09	-0.16	-0.31	-0.02	0.07
<i>dc4</i>	0	-0.09	-0.35	-0.26	0.22	0.05	-0.04	-0.28	-0.01	0.25	-0.14	-0.01
<i>dm2c</i>	0.01	-0.13	NA	-0.27	0.19	NA	0.23	-0.29	NA	0.26	-0.29	NA
<i>vc</i>	0.04	0.01	0.15	0.15	-0.35	-0.35	0.13	-0.16	0.05	0.5	-0.03	-0.24
<i>dm1</i>	0.05	0.13	0.34	-0.1	-0.07	-0.06	-0.27	0.43	0.07	0.11	-0.27	0.12
<i>dm2r</i>	0.05	0.02	-0.14	0.2	0.32	-0.32	-0.26	-0.16	0.14	0.31	-0.19	-0.1
<i>dvl2</i>	0.06	-0.13	-0.2	-0.04	-0.01	-0.14	-0.15	0.1	-0.12	0.3	-0.34	0.43
<i>dm3</i>	0.07	0.3	0.11	-0.21	0.18	0.1	0.24	0.16	-0.2	-0.23	-0.1	-0.4
<i>vl</i>	0.08	0.08	0.19	0.12	-0.3	-0.31	0.36	-0.21	0.19	0.3	-0.2	-0.21
<i>vsl</i>	0.1	0.24	0.1	-0.34	0.07	0.32	-0.18	-0.16	0.12	0.13	0.11	0.2
<i>vdc</i>	0.11	0.18	-0.06	-0.41	0.26	0.2	-0.1	0.02	0.49	0.12	-0.24	-0.03
<i>nt</i>	0.2	0.03	-0.12	0.07	0.06	0	-0.37	-0.11	0.31	-0.01	-0.25	0.29
<i>vsm</i>	0.21	0.33	0.2	-0.32	0.14	0.33	0.04	0.01	0.05	-0.25	0.02	-0.15
<i>vv</i>	0.25	0.18	0.24	-0.09	-0.25	-0.23	0.21	-0.12	0.25	0.12	-0.25	-0.09
<i>dp</i>	0.28	0.29	-0.12	0.22	0.09	0.17	-0.06	-0.01	-0.4	-0.1	0.11	-0.2
<i>vp</i>	0.31	-0.04	NA	0.01	-0.28	NA	-0.16	-0.19	NA	-0.11	0	NA
<i>vdr</i>	0.32	0.19	0.23	-0.07	-0.2	-0.16	0.1	0	0.13	0	-0.32	-0.01
<i>poa</i>	0.36	0.27	0.23	-0.14	0.1	0.25	-0.13	-0.11	0.18	0.08	0.26	0.11

Table 2.4: Loadings of the first four principal components in each dataset. PCs with a magnitude $\geq .25$ are shown in bold.

<i>Experiment</i>	<i>Cluster 1</i>	<i>Cluster 2</i>	<i>Cluster 3</i>	<i>Cluster 4</i>	<i>Cluster 5</i>
<i>Stable - COX</i>	dp, nt, poa, vp	vdr, vv	vc, vl	dc1, dld1	NA
<i>Transition – COX</i>	dp, dd, dm3, vsm, poa, vsl	vdr, vv, vp, vc, vl, nt	dc5, dlg2	NA	NA
<i>Transition – egr-1</i>	dp, dd, dm3, vsm, poa, vsl	vdr, vv, vc, vl, dm1	dc5, dlg2, dc4, dlg1	dld1, dlv1	dm2r, dlv2, dc1, dc2

Table 2.5: Significant clusters of correlated brain areas identified by multiscale bootstrapping of the correlation matrix. Clusters were ordered to highlight similarities across datasets.

Chapter 3: Influences of an androgen receptor antagonist and aromatase inhibitor on social transition, physiology and brain activity.

ABSTRACT

Steroid hormones help to integrate an individual's internal status and experiences with social stimuli to generate context appropriate behavioral responses. The question of how these hormones alter brain function in a coordinated manner to facilitate behavioral plasticity remains unanswered. The African cichlid fish has socially regulated male phenotypes that differ substantially in behavior, circulating hormone levels and brain gene expression. Here we examine the effects of inhibiting estrogen and androgen signaling on the behavior of males transitioning from a subordinate phenotype (SUB) to a dominant phenotype (DOM). We found surprisingly little impact of inhibiting the nuclear androgen signaling pathway on behavior or physiology. Inhibiting estrogen signaling caused males to become hyperaggressive and substantially altered circulating levels of estrogen and testosterone. This hyperaggressive phenotype was associated with decreased brain activity as measured by cytochrome oxidase histochemistry and immediate early gene expression in the lateral septum, an area associated with male aggression across vertebrates.

INTRODUCTION

A major outstanding question in neuroscience is how the brain generates behavioral plasticity. Animals must integrate internal signals and experiences with external information to make adaptive behavioral decisions. Steroid hormones are intricately linked to the expression of context appropriate social behaviors across all vertebrate species. These hormones have been widely studied in the context of sexual differentiation, where steroid hormones are critical during development to establish the neural circuitry necessary for sex typical behavior, but also during adulthood where changes in hormone levels increase or decrease the likelihood of a particular behavioral response (Arnold 2009).

While hormones do not cause particular behaviors to occur in the absence of the appropriate social stimulus, they do make these responses more or less likely to occur (Beach 1983).

Therefore, the same social stimulus could cause different responses in individuals depending on their hormone levels. These hormones change according internal and environmental signals, such as changes in social status, health, breeding condition, season, experience or parental status (Maruska and Fernald 2010; Wingfield et al. 1990; Hirschenhauser and Oliveira 2006; Kempnaers, Peters, and Foerster 2008; Goodson and Kabelik 2009). In this way hormones help to integrate an individual's internal physiological state and experiences with social stimuli to generate context appropriate responses. Steroid hormones can act through nuclear receptors, which are translocated to the nucleus, altering the transcription of specific genes over the course of hours and often leading to long term changes in gene expression (Wahli and Martinez 1991). They can also act through non-transcriptional mechanisms by interacting with various membrane associated receptors, exerting rapid (within minutes) effects on neuronal excitability and behavior (Remage-Healey and Bass 2006; Wang, Liu, and Cao 2014; Foradori, Weiser, and Handa 2008; Michels and Hoppe 2008). These receptors are expressed throughout the social decision making network in the brain, which is a set of limbic brain areas linked to social behavior across vertebrates (O'Connell and Hofmann 2012).

Androgens and estrogens have been linked to sex and social status across vertebrates. Circulating androgen levels have been linked male typical behavior and social dominance across vertebrates and respond to social stimuli such as aggressive interactions (Wingfield et al. 1990; Katharina Hirschenhauser and Oliveira 2006; Goodson, Evans, and Soma 2005). The estrogen system affects a wide array of social behaviors and there is a growing appreciation for the role that estrogens play in male aggressive and reproductive behavior (Trainor, Kyomen, and Marler 2006; Trainor, Greiwe, and Nelson 2006; Ervin et

al. 2015; Schlinger and Callard 1989; Lauren A. O'Connell and Hofmann 2012; Zumpe, Bonsall, and Michael 1993; Balthazart et al. 2004). Some of the effects of estrogens on male behavior are due to the local production of estrogen in the central nervous system via aromatization of testosterone to estradiol (Forlano, Schlinger, and Bass 2006). The aromatase enzyme is expressed in the brain and gonads across vertebrates. Aromatase expression in the brains of teleost fish is particularly high compared to other mammals (estimated to be 100-1000 times higher) and is expressed throughout the forebrain and hypothalamus as well as many other areas (Forlano, Schlinger, and Bass 2006).

Sex steroid hormones can have profound effects on brain activity, the activation of brain areas in response to stimuli and the functional connectivity between brain areas. Functional connectivity is defined operationally as correlated activity between distinct brain areas that is assumed to reflect the amount of synaptic connectivity and the extent of co-activation (Gillebert and Mantini 2013; Friston 2011). These correlations can arise in different ways; for example, they could be due to common inputs, direct synaptic connections between the brain areas, or through intermediary brain areas (Friston 2011). Brain activity can be measured using a metabolic mapping technique called cytochrome oxidase histochemistry (Wong-Riley 1989). Cytochrome oxidase is the final electron acceptor in the mitochondria and is crucial for energy production in the cell (Wong-Riley et al. 1998). Levels of cytochrome oxidase are tightly correlated to metabolic activity in the cell and can be used to quantitatively map differences in brain activity between behavioral phenotypes or morphs (Gonzalez-Lima and Garrosa 1991). Studies of the leopard gecko, *Eublepharis macularius*, have shown that incubation temperature, which influences the gonadal sex and the endocrine environment of the developing embryos, causes changes in behavior as well as differences in cytochrome oxidase in the adult brain (Sakata and Crews 2004a; Sakata and Crews 2004b; Crews 2003). Furthermore incubation

temperature affects functional connectivity between brain areas and covaries with high and low aggression phenotypes (Sakata et al. 2000).

Another commonly used marker of neural activity is immediate early genes (IEGs). IEGs are transcription factors that responds to changes in neuronal activity and are a powerful marker of stimulus induced neuronal activity (Okuno 2011). While both of these markers respond to changes in neuronal activity they differ markedly in the dynamics of that response. Even with very extreme perturbations (e.g. lesions or tetrodotoxin injections) it takes at least one day to detect the effects of changes in neural activity on cytochrome oxidase levels (Wong-Riley 1989; Gonzalez-Lima and Garrosa 1991; Liang, Ongwijitwat, and Wong-Riley 2006) while changes in IEG mRNA levels are detectable within an hour or less following stimulus exposure (Hofmann 2010; Okuno 2011). Sex steroid hormones can alter the IEG response to social stimuli. In female white throated sparrows, *Zonotrichia leucophrys*, male song elicits a strong response in the gene *egr-1*, an IEG, across many nodes of the SDMN. However, in females that are not in breeding condition or not given exogenous estradiol, male song does not elicit a response greater than that from random tones or noise (Maney et al. 2008). In zebrafish, *Danio rerio*, winning experiences cause an androgen response and have been shown to shift functional connectivity of the brain as measured by correlations of IEGs (Teles and Oliveira 2016; Teles et al. 2015).

While the role of steroid hormones in the development and expression of behavior has been widely studied, it is less well known how they mediate the transition from one behavioral phenotype to another. *Astatotilapia burtoni*, an African cichlid fish, is an ideal model to investigate how steroid hormones mediate behavioral transitions. *A. burtoni* males exhibit two plastic behavioral phenotypes, dominant (DOM) and subordinate (SUB). DOM males aggressively defend territories, are brightly colored and exhibit a range of aggressive and sexual behaviors. SUB males are dull in coloration similar to females, reproductively

suppressed and much less aggressive. DOM males have higher levels of both major androgens (testosterone and 11-ketotestosterone) and estradiol than subordinate males (Parikh, Clement, and Fernald 2006; Maruska and Fernald 2010; Huffman et al. 2012). The expression levels of androgen and estrogen receptors depend on social status (Burmeister, Kailasanath, and Fernald 2007; Maruska et al. 2013). The expression of androgen receptor (AR), estrogen receptor alpha (ER α) and estrogen receptor beta (ER β) have been mapped in the brain of both SUB and DOM males and while the levels of these receptors vary depending on brain area and social status, presence or absence did not depend on social status (Munchrath and Hofmann 2010). Treatment with a non-aromatizable androgen caused increases in sexual behavior in DOM and males, while an antagonist caused decreases but neither affected aggression. Treatment with an estrogen receptor agonist increased aggression in both DOM and SUB males while the antagonist had the opposite effect on DOM males (O'Connell and Hofmann 2012). This suggests that the relationship between androgens and aggression in this species is mediated via aromatization to estradiol. Consistent with this, inhibiting aromatase with fadrozole treatment causes a decrease in aggression in DOM males despite substantially increasing circulating levels of testosterone (Huffman, O'Connell, and Hofmann 2013).

Given an opportunity to acquire a territory, SUB males will undergo a remarkable phenotypic transition to DOM status. Within moments of an opportunity to transition, SUB males increase aggressive and sexual behavior (Maruska and Fernald 2010; Huffman et al. 2012; Maruska and Fernald 2013). Within 30 minutes of an opportunity to transition (the earliest point measured), levels of androgens, estradiol and cortisol are all elevated as are estrogen and androgen receptors in several areas of the social decision making network (Maruska et al. 2013). This suggests that sex steroid hormones play a crucial role in the transition to dominant social status, however it is not clear to which extent the behavioral

changes are influenced by the rising levels of estradiol and androgens or what effect that may have on brain activity.

In the current study we manipulate the androgen and estrogen system using an androgen receptor antagonist, flutamide and the aromatase inhibitor fadrozole during social ascent from SUB to DOM social status. We hypothesized that inhibiting androgen signaling would interfere with the transition given its strong association with DOM status and inhibiting estradiol signaling would cause a decrease in aggression consistent with its effect on DOM males. We mapped cytochrome oxidase and *egr-1* responses across the majority of the forebrain. We find surprisingly few effects of blocking androgen signaling on behavior, physiology or brain activity. Inhibiting aromatase caused transitioning males to become hyperaggressive and caused differences in circulating levels of testosterone and estradiol.

METHODS

Animal care

All animals used in this study were adult *A. burtoni* from a laboratory breeding line originally derived from a wild population in Lake Tanganyika, Africa (Fernald and Hirata 1977a). Fish were kept at 27 °C on a 12:12 hr light/dark cycle in 110 L tanks equipped with a recirculating life support system and fed daily with cichlid flake food (OmegaSea ltd.). Each focal animal (mean standard length 49.1 mm) was housed with 4 males and 6 females in a specially designed enclosure (Figure 1A) that allowed for controlled social ascent to dominant social status. All procedures were in compliance with and approved by the University of Texas Institutional Animal Care and Use Committee.

Pharmacology

Flutamide

To avoid added stress from daily injections, flutamide (FLUT; Sigma Aldrich) was given using coconut oil implants (Leatherland 1985). In preliminary testing we found that these implants were tolerated much better in our study species than silastic tubes. The melting point of the oil can be calibrated by mixing organic and hydrogenated oils, which have an increased melting point. We found that 100% hydrogenated oil implants did not resorb at all (and therefore potentially not releasing much drug), while 100% organic oil implants resorbed too quickly thereby potentially causing an overdose. We found that at the 27°C temperature of our aquarium, 40% hydrogenated coconut oil created a semi-solid implant. Preliminary testing showed that a 75 μ L implant was very well tolerated and slowly resorbed after about 9 days. We targeted a dose of 1 μ g/gram body weight (g.b.w.)/day based on previous dosages of androgen antagonists in this species (O'Connell and Hofmann 2012). Our experiment lasted 9 days and therefore each implant contained 9 μ g/g.b.w. We made a 50 μ g/ μ L FLUT stock solution dissolved in ethanol. Each 75 μ L implant was mixed individually based on the body weight of the focal animal and contained 75 μ L total volume consisting of 40% hydrogenated coconut oil and either FLUT solution or Vehicle (100% ethanol) control. Just prior to entering the experiment males were weighed and then kept in a holding tank while implants were prepared. Implants were then heated to 40°C to liquefy the oil and injected IP using an insulin syringe. We observed that animals fully recovered from this procedure within an hour or less. To test our method, we did a preliminary study on stable DOM males. We placed a divider into 30L aquaria and allowed DOM males to establish a territory for one week on either side of the divider with 3 females in each compartment. One male in each tank was assigned to receive either FLUT (n = 4) or a control (n = 4) implant. We recorded behavior for two days prior to injecting

the implant and for 6 days after. We observed that the FLUT group had a significant decrease in aggression compared to controls (figure 14: POST – PRE aggression, $p = 0.027$).

Fadrozole

We attempted to use the coconut oil implants with fadrozole (FAD; Sigma) as well, however we found that it would not dissolve in the oil. We therefore utilized daily IP injections instead to achieve a long-term blockade of aromatase activity. We used a dose of 10 $\mu\text{g/g}$ b.w. based on a previous study in this species (Huffman et al. 2012). We prepared a 10 $\mu\text{g}/\mu\text{L}$ FAD stock solution dissolved in ethanol. FAD stock or an equivalent volume of vehicle (100% ethanol) control were mixed with phosphate buffered saline to a final concentration of 10 $\mu\text{g/g}$.b.w. and injected IP in a final volume of 75 μL . Fish received injections every evening at 7pm to avoid injection effects on behavior which were recorded the following morning. They received the first dose just prior to entering the experiment and each evening after that for a total of 9 doses.

Behavior Studies

Focal males were housed in the enclosure shown in Figure 1A which allows for a controlled transition to DOM social status. Focal males were between a standard length of 40 – 50mm and had access to compartments B, C and D via 16mm diameter holes that allowed them to pass through compartment D. Suppressor males (standard length > 70mm) were restricted to their home compartment (either compartment B or C) because they were too large to pass through the holes in compartment D. The suppressor males serve to socially suppress the focal male, however the design leaves the focal male with a refuge (compartment D) which reduces injuries and allows for the male to be suppressed within the experimental enclosure for long periods of time. Side communities (compartments

labeled A) consisted of 1 male, size matched to the focal male, and 3 females and provide visual and olfactory social stimuli for all the animals in the experiment. Prior to the beginning of the experiment focal males were housed with larger males in established communities for at least 2 weeks to ensure that they were SUB social status before going into the experiment. 60 hours prior to the opportunity to transition to DOM social status, males were measured and placed into the experiment. In the flutamide experiment, the coconut oil implant was injected just prior to the animals being placed in the experiment and they were not subsequently handled. In the fadrozole experiment, animals received their first injection 60 hours prior to the opportunity to transition. Subsequent injections occurred every 24hrs at 7pm. The next day (48 hours prior to the social opportunity) they were allowed to acclimate to the enclosure, no observations were conducted on this day. At each subsequent time point males were videotaped for 10 min for behavioral scoring at 9:30am. Behavior was scored at 9 time points: 24 hours prior to social opportunity (-24 hrs), directly after the social opportunity (0 hrs) and 1, 24, 48, 72, 96, 120 and 144 hours after the removal of the DOM male. On Day 3 (0 hr time point), the suppressor male from compartment C was removed one hour prior to lights-on, thus providing an opportunity for the focal male to take over that territory (Burmeister, Jarvis, and Fernald 2005; Huffman et al. 2012; Maruska and Fernald 2010). On day 9 of the experiment (144 hr time point) animals were challenged for 1 hour with an equal sized intruder male who was placed into compartment E at the start of the observation. Following this observation blood was collected from the dorsal aorta using heparinized 26G butterfly infusion needles (Surflo), blood was kept on ice until the plasma could be separated from the serum by centrifugation and stored at -80 °C. Immediately following blood collection animals were killed by rapid decapitation and their brains were dissected, placed into OCT molds, flash frozen on dry ice, and stored at -80 °C until sectioning. Both the FAD and FLUT experiment were run in

a set of 4 cohorts containing both 6-7 males treated with either fadrozole (FAD N = 14), fadrozole vehicle control (FAD CON, N = 11), flutamide (FLUT N = 14), flutamide vehicle control (FLUT N = 11). In both experiments each cohort consisted of a mixture of control and treated animals.

Behavioral scoring

Videotape of all 9 time points was scored using chronoViz software (Fouse et al. 2011). We used an ethogram based on Fernald and Hirata (1977a) that includes the following behaviors: Chasing (aggression usually directed from a DOM towards a SUB), Border Conflict (ritualized aggressive displays that occur between DOM males), Biting (aggression), and sexual behaviors: leading and quivering (directed towards females).

Hormone assays

Hormone assays were performed using ELISA (Assay Designs, Enzo life sciences). Plasma was diluted 1:30 and run in duplicate (Kidd, Kidd, and Hofmann 2010). All samples were run on the same plate. The intraplate coefficient of variation averaged 2.27% and 4.13% in the testosterone and estradiol assays respectively.

Brain Sectioning

All brains were sectioned into four series of alternating 30 μ m sections at -20 °C using a cryostat (2800 Frigocut Reichert-Jung). Sections were thaw mounted on to Superfrost Plus slides (Fisher Scientific) and kept at -20 °C during sectioning. The first series was processed for cytochrome oxidase histochemistry and the second series for Nissl stain to act as a guide for quantification. The third and fourth series were used for *egr-1* radioactive *in situ* hybridization.

Cytochrome oxidase histochemistry

Slides were processed for cytochrome oxidase histochemistry using a previously described protocol (Gonzalez-Lima and Jones 1994). The following solutions were used: 1) fixation solution of 0.5% glutaraldehyde (Sigma-Aldrich) in 10% sucrose (Sigma-Aldrich); 2) 0.1 M phosphate buffer (Fisher Scientific; pH 7.6); 3) preincubation solution of 0.05 M Tris buffer (Sigma-Aldrich; pH 7.6), 0.0275% cobalt chloride (Sigma-Aldrich), 10% sucrose, and .5% dimethylsulfoxide (Sigma-Aldrich; DMSO); 4) incubation solution of 0.05% diaminobenzidine (Sigma-Aldrich; DAB), 0.0075% cytochrome c (Sigma-Aldrich), 5% sucrose, 0.002% catalase (Sigma-Aldrich), 0.25% DMSO (v/v), and phosphate buffer. Sections were kept frozen on the slides and solutions were kept at 4 degrees until the start of the procedure so that the sections would warm gradually as they moved through the baths. The sequence of baths was: 1) light fixation in gluteraldehyde solution for 5 min; 2) rinse in phosphate buffer with 10% sucrose, 3 changes for 5 min each; 3) preincubation in cobalt chloride Tris-buffer for 10 min; 4) rinse in phosphate buffer; 5) incubation in DAB solution (oxygenated for 5 min before and throughout the staining) at 37°C in a dark oven for 60 min; 6) post-fixation with 4% buffered formaldehyde in 10% sucrose for 30 min; 7) ethanol baths of 30, 50, 70, 95 (2 changes), and 100% (2 changes) for 5 min each; 8) xylenes (Millipore), 3 changes for 5 min each; 9) cover-slipped with Permount (Fisher Scientific).

Nissl stain

Alternative sections were stained with cresyl violet to be used as a guide for quantification. Slides were processed through the following series of baths: 1) fixation in chilled 4% paraformaldehyde (Sigma-Aldrich) for 10 min; 2) rinsed in chilled phosphate buffered saline, 3 changes for 5 min each; 3) rinsed in room temperature deionized water; 4) stained with 1% cresyl violet (Sigma-Aldrich) for 3 min; 5) rinsed again in deionized

water; 6) ethanol baths of 70% for 30 seconds, 95% for 2 min and 100%, 2 changes for 2 min each; 7) xylenes, 2 changes for 5 min each; 8) cover-slipped with Permount.

Brain Homogenate Standards

Following Gonzalez-Lima and Jones (1994) we prepared cichlid brain homogenate to use as an internal standard in every batch of the cytochrome oxidase stain. 30 Adult *A. burtoni* brains from both males and females were dissected, rapidly fresh frozen in plastic tubes and stored at -80 °C until the homogenate was prepared. These animals were gathered over time from surplus stock that had to be euthanized due to injuries in accordance with our animal care protocol. To prepare the homogenate, brains were thawed on ice and crushed into a thick paste using a plastic mortar and pestle in a 2mL centrifuge tube. Each brain was homogenized one after the other in the same tube. Small amounts of water were added as needed (100 µL total) to aid in the homogenization process. To aliquot the homogenate the tapered half of 200 µL pipette tips (Axygen) were cut off so that they made an approximately 5 mm diameter cylinder. The cylinders were filled with brain homogenate using a combination of pipetting and manual packing and frozen on dry ice. These cylinders were kept at -80 °C until the morning each batch was run, at which time one aliquot was sectioned on the cryostat at -20 °C. 6 series were sectioned from each cylinder, starting with two sections of 10 µM for each series and continuing in 10 µM increments up to 60 µM. These standards were used to correct the calibrated optical density measurements for batch effects. Each measurement was referenced to the brain homogenate standard particular to the appropriate batch. The flutamide and fadrozole experiments were run in separate batches including all treated and controls for each experiment in each batch.

COX Quantification

Cytochrome oxidase was measured in 31 limbic and sensory brain areas covering the majority of the forebrain as well as parts of the hypothalamus and midbrain (see table 1 for abbreviations). Images of each section were taken using an Olympus SZX12 microscope equipped with a 12.5-megapixel camera (Olympus DP70) at 16x magnification. Images were saved as uncompressed, single channel files with 16-bit color depth. Illumination and exposure were held constant. Nissl stained adjacent sections were used as a guide to identify regions of interest. Optical density measurements were done using FIJI software (Schindelin et al. 2012). For each region, the brain area was traced in one hemisphere and optical density was measured. This process was continued across the full rostral-caudal extent of each region at an interval of 120 μM between measurements. The flutamide experiment included 1,901 measurements on 22 individuals and the fadrozole experiment included 2,028 measurements on 24 individuals. Optical density was calibrated using an optical density step tablet (Kodak). All optical density measurements were standardized to the internal brain homogenate standard using a linear model to control for batch effects. These standardized measurements were then centered by subtracting the mean of all measurements in an individual. The measurements for each brain area were then averaged to give a score for each brain area within each individual.

Egr-1 in situ hybridization

Cloning of A. burtoni egr-1 gene fragment

We isolated total RNA from *A. burtoni* brain using TRIzol (Invitrogen) and purified with RNeasy spin columns (Qiagen). We reverse transcribed whole brain cDNA using a mixture of oligo-DT and random hexamer primers using the Superscript III reverse transcriptase kit (Invitrogen). Primers were designed using Primer3 (Rozen and Skaletsky

1998) against the coding sequence of *A. burtoni egr-1* (NCBI reference: NM_001315549.1). A 491 bp fragment of the *egr-1* gene was amplified by PCR (Promega GoTaq Green) using the following primers: Forward: 5'-TCCAGCCTCAGTTCTTCGAT-3', Reverse: 5'-GTCAGCTCATCAGACCGTGA-3'. This fragment was cloned into the pCRII TOPO vector (Qiagen) containing SP6 and T7 polymerase promoters on opposite sides of the *egr-1* fragment allowing for both sense and antisense transcripts to be generated from the same clone.

Detection of egr-1 mRNA

In situ was performed following a modified version of a previously described protocol (Hoke et al. 2004). Large quantities of the *egr-1* plasmid were prepared using a midiprep kit (Qiagen) and 20µg was linearized by restriction digest with either SpeI-HF (sense; New England BioLabs) or NotI-HF (antisense; New England Biolabs) and purified using spin columns (RNeasy Qiagen). Runoff *in vitro* transcription reactions were used to create S-35 labeled RNA riboprobes using the MAXIscript kit (Ambion). The reaction mixture contained 5 µM S-35 UTP (PerkinElmer), 13.25 µM UTP, 500 µM each of ATP, CTP and GTP, 1 µg of the appropriate linearized DNA and 40 units of either T7 (sense) or SP6 (antisense) polymerase. Reactions were incubated for 4 hrs at 37°C and probes were purified using Micro Bio-Spin P-30 Tris spin columns (Bio-Rad). Probe quality was verified by bleach agarose gel electrophoresis (Aranda, LaJoie, and Jorcyk 2012), agarose gels were dried using a gel drying kit (Promega) and radioactivity was visualized using phosphor screens (Typhoon Phosphoimager GE Healthcare). Probe quantity was determined using a scintillation counter (Beckman Coulter LS6500). Probes were kept at -80 °C overnight.

All slides were processed together in one batch. Slides were thawed and dried at 50 °C for 5 min and fixed for 10 min in 4% paraformaldehyde (diluted from 37% paraformaldehyde ampules; Ted Pella) in 1x PBS (Ambion). Slides were rinsed for 3 min each in 1x PBS and then .1M, pH 8 triethanolamine (TEA; Sigma-Aldrich). Tissue charge was neutralized using 0.25% V/V acetic anhydride (Sigma-Aldrich) in 0.1M pH 8 TEA for 10 min. Slides were rinsed in 2x SSC buffer (Ambion) for 3 min and then dehydrated with a series of ethanol baths (50, 70, 95 and 2 changes of 100%) for 3 min each. Slides were dried for 15 min at room temperature and a hydrophobic barrier was drawn around the edge of the slide with a PAP pen (Ted Pella) before tissue was rehydrated in a solution containing 4.2×10^6 cpm/ml radiolabeled riboprobe, 0.01 M dithiothreitol (DTT; Sigma-Aldrich) in 1x hybridization solution (Sigma-Aldrich). Slides were covered using HybriSlip hybridization covers (ThermoFisher Scientific) and sealed with clear nail polish. Slides were placed into humidified plastic containers and incubated for 16 hours at 55 °C. After hybridization, slides were placed in 4x SSC and hybridization covers were removed. After covers were removed slides were rinsed in 2x SSC containing 1ul/ml DTT. To digest unbound probe, slides were treated with 20 µg/ml RNase A (Invitrogen) in 500 mM NaCl and 10mM tris buffer (Ambion). Slides were then rinsed in 2x SSC and then washed in 55 °C solutions to remove unbound probe as follows: 1.25 hrs in 2x SSC, 50% formamide (Sigma-Aldrich) and 1 µL/ml DTT followed by two washes in .1x SSC and 1ul/ml DTT for 30 min. Slides were then dehydrated in a series of ethanol baths containing 0.3M ammonium acetate (Fisher Scientific; 50, 70, 95% ethanol) and 2 changes of 100% ethanol for 3 min each. Slides were dried with a vacuum desiccator and stored in a desiccation cabinet at room temperature overnight.

To visualize the hybridized probe, slides were processed for autoradiography. Slides were hung on wires in a light-tight incubator and dipped in 43°C NTB

autoradiographic emulsion (Carestream Health). Slides were dried while suspended in the incubator for 1 hr at 50 °C, then placed into light-tight boxes at 4 °C for 5 days. Slides were warmed to room temperature and emulsion was developed using D19 Kodak replacement developer (Electron Microscopy Sciences) diluted 50% with water and Kodak fixer (VWR). Slides were then stained with cresyl violet for 25 min, dehydrated in ethanol (95% and then 2 changes of 100% for 2 min each). Finally, the tissue was cleared using xylenes (Millipore, 2 changes for 6 min each) and slides were coverslipped with permount (Fisher Scientific).

Egr-1 Quantification

For each brain area measurement two black and white photographs were taken at a magnification of 40x (Zeiss Axio Scope.A1). One photo was taken under brightfield illumination and one was taken under darkfield. The brightfield image shows Nissl stained cell bodies and silver grains that appear dark black. On the darkfield image cell bodies appear dark and silver grains appear bright. All image processing was done in FIJI (Schindelin et al. 2012) using custom scripts written in the ImageJ macro language. To separate cell bodies and silver grains from the background we processed the brightfield photo with an adaptive thresholding algorithm from the openCV package (Tseng 2016; Bradski 2000). This created a threshold image of cell bodies and silver grains. Silver grains not over cells were filtered from this image by excluding objects that were less than 200 pixels in area. The resulting image is a threshold mask of cell bodies which were then dilated by 3 pixels around the edges to capture silver grains overlapping the edges of cells (Burmeister, Jarvis, and Fernald 2005). The area of the sample covered by cell bodies was calculated using this threshold image, which was then subtracted from the darkfield image to only count silver grains that developed over cell bodies. We used the findFoci algorithm

(Herbert et al. 2014) to segment overlapping grains and count the silver grains in the resulting image. We divided the resulting silver grain counts by the area of the photo covered by cells to get a normalized count / cell area. Preliminary testing directly comparing this method to previously used strategies (Hoke et al. 2004) showed that this method performs equally well (data not shown). Furthermore, this method allows a higher throughput and larger sampling area because images can be taken using air lenses at a lower magnification than the previous method that used oil lenses at 100x magnification.

Statistical analysis

All analyses were conducted in the R statistical computing environment (R Core Team 2016).

Behavior

Behavior data were analyzed using mixed models with The Lme4 R package (Bates et al. 2015). We included time point, treatment and their interaction as fixed effects and a random effect for individual to account for repeated measures across time. We ran an initial model including only the separate control groups. Controls were not different from one another, either in the main effects or in exploratory post-hoc testing and were analyzed as a single group. In cases where overall ANOVA showed a significant effect, post-hoc testing was done by calculating least-squares means and comparing the Tukey corrected contrasts at each time point.

Growth and Gonad size

Gonadosomatic index (GSI) was calculated by dividing the weight of the gonad by body weight and multiplying by 100. GSI data were log transformed to achieve normality and analyzed with ANOVA. Growth data were not normal and were analyzed with a non-

parametric Kruskal-Wallis test with Nemenyi *post hoc* testing in the R package PMCMR (Pohlert 2014).

Hormone data

Testosterone data were normally distributed and estradiol was log transformed to achieve normality. Data were analyzed with ANOVA followed by Tukey contrast post-hoc testing. We tested whether aggressive behavior toward the intruder and total aggression correlated to testosterone and estradiol levels. We used regular linear models with the behavior from the last time point. Square root transformed aggression levels were used as the response variable with treatment, hormone levels and their interactions as main effects.

COX and *egr-1* mean differences

Data were square-root transformed. We used mixed models with a random effect for cohort. We used separate linear models for each brain area and corrected the p-values with the Holm correction to control the familywise error rate.

Correlations between COX, *egr-1* and behavior

For each behavior we tested the correlation against each of the 26 (*egr-1*) or 31 (COX) brain areas. We used models that included behavior (chasing, lateral display, border conflict, fleeing, sexual displays, intruder aggression, or total aggression) as the response variable and the COX or *egr-1* level of each brain area as the predictor. We first ran these models with the interaction between treatment and COX or *egr-1* as a factor. Since none of the interaction effects survived multiple hypothesis correction, we reran the models without the treatment effect included. We then corrected the p-values with the Holm correction to control the familywise error rate for the family of 26-31 tests.

Principal components analysis

In order to reduce dimensionality and to visualize any treatment effects we used principal component analysis. We analyzed each dataset separately (FLUT COX, FLUT *egr-1*, FAD COX, FAD *egr-1*). We calculated principal components using the base R package (R Core Team 2016). The first four principal components were analyzed for treatment effects using ANVOA.

Analysis of receptor densities

We classified receptor levels as either absent or cytosolic, low, medium or heavy based on photomicrographs and written descriptions of *in situ* and antibody staining by Munchrath and Hofmann (2010). For each brain area described we calculated effect size of treatment in our COX and *egr-1* data using Cohen's D. Cohen's D was calculated as $\frac{x_1 - x_2}{s}$ where x_1 is the mean of the treated group, x_2 is the mean of the control group and s is the pooled variance in the R package *effsize* (Torchiano 2016). We then tested if effect sizes covaried with receptor density categories for either AR, ER α or ER β with ANOVA.

Covariance Analyses

To compute covariance matrices we first replaced missing values with the mean of that brain area observed within that treatment (Zar 1999, 245–48). Mean substitution of missing values preserves the mean value of each cell, and while this underestimates variance and over-represents sample size, it is widely accepted that it does not seriously affect analyses as long as the fraction of substituted data points is below 10–15% (Schafer and Graham 2002). Missing data was below 10% for each experiment. We calculated Pearson correlation coefficients for each brain area correlated to every other brain area in both COX and *egr-1* datasets.

We used permutation to assess the similarity of the matrices and effects of treatment. For each permutation strategy we used the same resampling procedure. In each fold of the permutation treatment group labels were randomly swapped, preserving the brain data within an individual. Treatment group labels were sampled without replacement to preserve group sample sizes. In the first strategy we assessed similarity of the correlation matrices by correlating the off-diagonal elements of the correlation matrices for each treatment to each other and compared these correlations to a set of 1000 permutations of the data (figure 15A, 16A). To assess the overall strength of correlations across the matrices we compared the sum of the squared correlation coefficients of the off diagonal elements to a set of 1000 permutations of the data (figure 15B, 16B). Finally, we assessed the amount of difference between the correlation matrices. For each pair of treatment correlation matrices, we calculated the difference between the off-diagonal elements. We then summed the absolute value of these differences to get a difference score for the matrix pair. The difference score was compared to 1000 random permutations of the treatment groups (figure 15C, 16C). These permutations of the treatments showed that the correlation networks were not significantly different among treatment groups, therefore we pooled treatments for each experiment to increase sample size.

We visualized each correlation matrix with a heatmap and clustered brain areas using hierarchical clustering. We used the R package pvclust to generate p-values for each cluster using multiscale bootstrap resampling (Suzuki and Shimodaira 2015). Clusters for which $p < 0.05$ are highlighted with squares. To examine similarity of the matrices, we used the Mantel test in R package ade4 to compute the correlation between the correlation matrices (Dray and Dufour 2007). The mantel test iteratively permutes the rows of the correlation matrix and recalculates the correlation between the two matrices each time. The

null hypothesis is that that matrices are unrelated, so $p < 0.05$ indicates that the matrices are more similar than expected by chance.

RESULTS

Animals in the fadrozole experiment (FAD and FAD CON) and flutamide experiment (FLUT and FLUT CON) all showed a robust response to social opportunity, increasing in aggressive and sexual behavior and decreasing in submissive behavior over time (Figure 1 B-D, ANOVA statistics summarized in table 2). We then tested planned contrasts between treatment and control at each time point. We found that FAD treated animals were significantly more aggressive than controls, starting after 24 hours (Figure 1B, Least-square means contrasts summarized in table 3). Furthermore, we found that both flutamide and fadrozole treated animals showed fewer submissive behaviors on the day prior to social transition, an effect that disappeared after the opportunity to transition (Figure 1D, Least-square means contrasts summarized in table 3).

There was a difference between the fadrozole and flutamide experiments in growth rate (Figure 2A: Kruskal-Wallis, $\chi^2 = 22.537$, $df = 3$, $p = 5.042 \times 10^{-5}$). In the flutamide experiment, both FLUT and FLUT CON gained weight consistent with the increased growth associated with transition seen in Chapter 2. In the fadrozole experiment both groups tended to lose weight. However, there was not a difference in relative gonad size among the groups (Figure 2B: ANOVA, $F = 1.642$, $df = 3$, $P = 0.199$).

There were treatment effects on circulating levels of both testosterone (Figure 2C: ANOVA, $F = 19.56$, $p = 6.70 \times 10^{-8}$) and estradiol (Figure 2D: ANOVA, $F = 14.16$, $p = 2.15 \times 10^{-6}$). Specifically, Fadrozole treatment increased circulating testosterone levels compared to all other groups ($p < 1 \times 10^{-5}$ in all contrasts) and decreased circulating estradiol levels compared to all other groups ($p < 1 \times 10^{-3}$ in all contrasts). Flutamide treatment did not

significantly affect hormone levels compared to control. Flutamide treated animals had increased variance in estradiol levels because a subset had elevated levels however the difference in variance was not significant (Levene's tests, $F = 0.1834$, $p = 0.673$).

Animals were presented with an intruder male stimulus on the last day. Neither fadrozole or flutamide treatment significantly affected the amount of aggression shown towards the intruder (Figure 3A: FAD ANOVA, $p = 0.656$, FLUT ANOVA, $p = .300$) or the latency to first display (Figure 3B: FAD Kruskal Wallis, $p = 0.8382$, FLUT ANOVA, $p = .222$). Testosterone levels (Figure 4A: $F = 4.817$, $p = 0.035$) were a significant predictor of aggression towards the intruder in the first five minutes after intruder presentation, while estradiol levels were not (Figure 4B: $F = 1.811$, $p = 0.188$). Both testosterone (Figure 4C: $F = 8.290$, $p = 0.008$) and estradiol levels (Figure 4D: $F = 7.404$, $p = 0.003$) were a significant predictor of total aggressive displays in the last five minutes of the intruder presentation. Interactions between hormones and drug treatment were included in these models, but were not significant.

We measured COX activity in 31 limbic and sensory areas across the forebrain and parts of the midbrain and hypothalamus (Table 4, Figure 5). In the fadrozole experiment we found marginally significant increases in treated animals in the atn ($p = 0.087$) and dm3 ($p = 0.064$) and marginally significant decreases in the areas dlv1 ($p = 0.069$) and vl ($p = 0.088$), however none of these differences were significant after multiple hypothesis test corrections. In the flutamide experiment we did not find any significant treatment effects. Full statistical results are given in table 4.

We measured *egr-1* levels in a subset of 26 of these brain areas (Figure 6). In the fadrozole experiment we found marginally significant decreases in the treated group in the areas dd ($p = 0.094$) and vl (Figure 7: $p = 0.0818$). However, these differences were not significant after multiple test correction. In the flutamide experiment we found marginally

significant decreases in ah ($p = 0.081$), dd ($p = 0.036$), poa ($p = 0.069$) and vsl (Figure 8: $p = 0.020$), however these differences were not significant after multiple test correction. Full statistical results are given in table 5.

We then tested for correlations between behavior, hormones and both COX and *egr-1* levels. We did not find strong evidence of interaction effects so treatment effects were left out of the final models, so treatment and control groups were analyzed together to look for significant correlations between brain activity measures and behavior. The FAD and FLUT datasets were analyzed separately. We found two correlations in the *egr-1* data that survived multiple test corrections. In the fadrozole dataset there was a negative correlation between the total amount of aggression and *egr-1* levels in vl (Lateral septum, Figure 9A: $t = -10.041$, Holm corrected $P = 3.980 \times 10^{-5}$). In the flutamide dataset there was a correlation between the amount of aggression towards the intruder and *egr-1* levels in dlv2 (hippocampus, Figure 9B: $t = -3.883$, Holm corrected $P = 0.034$). We did not find any significant correlations between hormones or behavior and COX levels.

We next conducted an analysis to see if treatment effects covaried with receptor densities of the androgen and estrogen receptors: ER α , ER β , and AR. For each brain area we calculated Cohen's D as a measure of effect size, with positive values indicating higher activity on average in the treated group. We compared the distribution of effect sizes to receptor densities which we categorized as either absent or cytosolic, low, medium, or heavy based on (O'Connell et al. 2010, Table 6). In the fadrozole dataset we found that none of the receptor densities covaried with either *egr-1* or COX effect sizes. In the flutamide dataset we found significant variation with *egr-1* effect sizes and AR density (Figure 10A: Permutation ANOVA $p = 0.020$). Brain areas that lacked AR or were in the medium category tended to have increased amounts of *egr-1* with flutamide treatment on average, while those in the low and heavy category tended to decrease on average. We also

found significant variation with COX effect sizes and ER β receptor densities (Figure 10B: Permutation ANOVA $p = 0.017$). Brain areas lacking ER β tended to have decreased levels of COX after flutamide treatment, while areas with low, medium or heavy densities tended to have neutral or slightly positive effect sizes. The effect sizes did not covary with the densities of the other receptors.

PCA analysis showed no treatment effects in either the COX (Figure 11) or *egr-1* datasets (Figure 12) indicating that the covariance structure in these data were not affected by treatment. We tested this further by permuting treatment labels and calculating the similarity of the resulting correlation matrices. We found that the correlation matrices of the treated animals were as similar to each other as expected by random chance and we therefore collapsed treated and control animals into one pool for covariance analyses (figure 15).

Bootstrap hierarchical clustering of the correlation matrices showed several robust clusters in each dataset (Figure 13). There were some similarities in which brain areas clustered together as well as unique clusters in each dataset (clusters are listed in Table 7). Brain areas that are clustered in multiple datasets may have relevance to functional connectivity. We also used Mantel tests to test the hypothesis that the correlation matrices were more similar to each other than expected by chance. All 6 pairwise comparisons of the 4 datasets showed significant similarities ($p < 0.01$ in all comparisons, full statistics summarized in table 8).

DISCUSSION

In the present study, we applied an antiandrogen or aromatase inhibitor during social ascent and examined the effects on behavior, physiology, and brain activity.

Inhibiting the aromatization of testosterone into estradiol with fadrozole resulted in increased aggression, along with the expected increase of circulating testosterone and decrease in estradiol. Inhibiting the nuclear androgen receptor pathway did not result in any clear behavioral or hormonal effects, although treatment effects on both COX and *egr-1* co-varied with known receptor densities of the androgen and estrogen receptors in the flutamide experiment.

Neither an antiandrogen or aromatase inhibitor block social transition:

While several studies have been done measuring sex steroid hormones and social transition in *A. burtoni* (reviewed in Maruska 2015), this is the first to manipulate these hormones during social ascension and examine the effects on behavior, hormones, and the brain. We found that neither flutamide nor fadrozole blocked animals from transitioning from SUB to DOM social status and that they both increased aggressive and sexual behavior and decreased fleeing behavior after the opportunity to transition.

The antiandrogen treatment did not affect behavior or physiology:

Flutamide, an antiandrogen, did not affect behavior or physiology during social ascent. This is interesting in light of the fact that testosterone is one of the first hormones to increase after the opportunity to transition, showing significant increases within 30 min of an opportunity to transition (Maruska and Fernald 2010; Huffman et al. 2012; Maruska and Fernald 2013). One study of *A. burtoni* found a correlation between androgens and aggressive behavior during transition (Huffman et al. 2012), while another did not (Maruska and Fernald 2010). In the present study we find support for androgens mediating both aggression towards the intruder as well as total aggression towards the intruder and the other males in the paradigm. There was no significant interaction effect, indicating these correlations were not affected by flutamide treatment, possibly because

the correlation could be driven by aromatization to estradiol. In a study using a different antiandrogen, cyproterone acetate, treatment did not affect aggression in either stable DOM or SUB males (O'Connell and Hofmann 2012). Given the nearly immediate increase of aggressive behaviors and the relatively slower increase in circulating testosterone levels, it has been hypothesized that androgens are not required for the rapid behavioral change during transition (Maruska 2015). This is supported by the fact that flutamide administered throughout the transition did not affect the increase of aggressive behavior. One possibility is that androgens acting via non-genomic mechanisms are important for the transition but are not affected by flutamide. There are a variety of ways that androgens can influence intracellular signaling and neuronal excitability that are independent of AR and thus would not be blocked by flutamide treatment (Foradori, Weiser, and Handa 2008; Michels and Hoppe 2008). Flutamide also did not affect the increase in sexual behavior associated with transition. In a study of ascending males, sexual behavior was significantly correlated to testosterone levels on the first day of transition, however this correlation was not significant after the first day (Huffman et al. 2012). Cyproterone acetate strongly decreased sexual behavior in DOM males (O'Connell and Hofmann 2012), a result that is seemingly at odds with the finding in this study. There are several important differences to consider. O'Connell and Hofmann (2012) was a full contact design in a community setting and therefore there was more opportunity for sexual behavior and interactions with females compared to this study where females were behind a plastic partition. Furthermore, the within-subject design of that study may have had more power to detect changes in sexual behavior which varies substantially among males, than the between-subjects design of this study. Furthermore, there are differences between these drugs. Flutamide is considered to be a pure antiandrogen while cyproterone acetate is also a potent progesterone agonist and may have activity on glucocorticoid receptors as well (Poyet and Labrie 1985). Finally,

there may be different effects on transitioning animals compared to stable DOM males. Therefore, we cannot rule out a role of androgens in sexual behavior, however no effect was detected in this study, and flutamide did not block increases in sexual behavior during social ascent. Finally, flutamide did not affect androgen levels. This was not unexpected as cyproterone acetate also did not affect androgen levels in either stable DOM or SUB males (O'Connell and Hofmann 2012). In humans and rats, flutamide causes increases in circulating testosterone levels as well as increases in gonadotropins, presumably by blocking androgen receptor mediated feedback on the HPG axis (Hellman et al. 1977; Viguier-Martinez et al. 1983). However, in studies of fish and birds, flutamide did not affect circulating testosterone levels despite having effects on behavior in some cases (Jensen et al. 2004; Beletsky, Orians, and Wingfield 1990; Vulllioud, Bshary, and Ros 2013; Hegner and Wingfield 1987). The effect sizes of the flutamide treatment covaried with the AR receptor density in the *egr-1* dataset and the ER β receptor densities in the COX dataset. In the *egr-1* dataset negative effect sizes (meaning FLUT treated males were lower on average in *egr-1* levels) were mainly in areas lacking androgen receptor or with medium levels. The pattern does not lend itself to a simple interpretation because it is non-linear. In the COX dataset, effect sizes covaried with ER β densities, such that effect sizes tended to be more positive with increasing receptor density. This indicates that blocking the androgen receptor affected brain areas differently depending on levels of ER β .

Inhibiting aromatase causes transitioning males to become hyperaggressive and dramatically affected hormone levels

Treatment with fadrozole, an aromatase inhibitor, caused transitioning males to become hyper aggressive and also caused increased testosterone levels and decreased estrogen levels. On average FAD treatment increased testosterone levels by 70.5% over the average of the other groups and decreased estradiol levels by 78.1%. This effect was

expected based on a previous study of DOM *A. burtoni* males given fadrozole, which reported very similar effects on both testosterone and estrogen levels (Huffman, O'Connell, and Hofmann 2013). Similar effects have also been reported in studies of Salmon and the fathead minnow (Afonso et al. 1999; Ankley et al. 2002). This effect indicates that we successfully blocked aromatase function and that testosterone was converted to estradiol at a much lower rate in treated animals. While the effects on hormones reported here are consistent with the effects reported previously for established DOM males (Huffman, O'Connell, and Hofmann 2013), the effects on behavior are not. In established DOM males FAD treatment caused a significant decrease in aggressive behavior, rather than the increase reported here in ascending males. There are several possible explanations for this discrepancy. While the dose used was the same, one possibility is that differences in the dosing schedule between these studies may account for the different effects. In the present study, animals were dosed each night and observed the following morning, 14.5 hours later. In Huffman et al. (2013) the animals were observed 45 min after a morning injection. There are several reasons why this explanation is doubtful. The Huffman et al. study also included a dose-response study with a similar dosing schedule to ours and they did not observe the increases in aggression reported here. Also the similar effects on circulating androgen and estrogen levels indicate that the drug was equally active under both dosing schedules. Another possibility to explain the different effects on behavior could be the increase in testosterone levels. If the hypothetical dose response curve relating aggression and androgen levels follows an "inverted U" shape, increasing DOM male testosterone would be expected to decrease aggression while increasing testosterone in ascending males would increase aggression because they start at a lower androgen level. Again this explanation is doubtful due to the fact that directly increasing androgen levels with a non-aromatizable androgen, DHEA, does not affect aggression in DOM or SUB males (O'Connell and

Hofmann 2012). Studies directly comparing the effects of FAD on DOM, SUB and ascending males are needed to resolve this, however the most likely explanation is that differences in the brain of DOM and ascending males causes these opposing effects.

Across vertebrates, estradiol has been shown to be related to aggression in complex ways, in some species it increases aggression while in others it decreases it (Trainor, Kyomen, and Marler 2006). The most common effect across vertebrates is that estradiol increases aggression (Trainor, Kyomen, and Marler 2006). The best studied system is the house mouse, *Mus musculus*. In this species, treatment of castrated males with estradiol increased aggression compared to treatment with androgens or vehicle (Simon and Whalen 1986). Genetically engineered mice with the aromatase gene removed lose all aggression. This phenotype can be rescued by treatment with exogenous estradiol, but only if it is given continuously during development and throughout testing (Toda et al. 2001). Similar relationships have been shown in a variety of species of birds. For example in pied flycatchers, *Ficedula hypoleuca*, brain aromatase levels positively correlate with aggression (Silverin, Baillien, and Balthazart 2004). In Japanese quail, *Coturnix japonica*, brain aromatase levels correlate positively with aggression and treatment with FAD decreases aggression (Schlinger and Callard 1989). In *A. burtoni*, several lines evidence support a positive relationship between estradiol and aggression at least in stable DOM males, similar to most other vertebrates that have been studied. DOM males have increased circulating levels of estradiol and higher levels of aromatase in the brain (Huffman, O'Connell, and Hofmann 2013). Furthermore, in this study we found a correlation between circulating estrogen levels and total aggression. Finally, treatment with an estrogen receptor agonist increases aggression in stable DOM and SUB males, while the antagonist decreases aggression in DOM males. There are other species, however, that do not follow this pattern. In the California mouse, *Peromyscus californicus*, increased levels of

aromatase in the bed nucleus of the stria terminalis correlated with lower aggression and treatment with FAD caused males to become more aggressive. In groups of the bluebanded goby fish, *Lythrypnus dalli*, removal of the male group member causes a rapid increase in aggression and gonadal sex change in the DOM female, who subsequently becomes the male group member. This increase in aggression is correlated to a decrease in brain aromatase activity (Black et al. 2005). This begs the question as to why estrogen is positively correlated to aggression in some species but negatively in others. Species differences in the expression of estrogen receptor subtypes, aromatase, other sex steroid receptors or other neuromodulators may explain this. Studies of estrogen receptor subtype knockout mice suggest that they may have different effects on aggression, however these animals have many organizational and developmental differences that make interpretation difficult, similar to the difficulties in comparing across species (Trainor, Kyomen, and Marler 2006). In *A. burtoni* DOM and SUB males have differences in the amounts of aromatase (Huffman et al. 2012) and the sex steroid receptors in the brain (Maruska et al. 2013), which could prime the brain to respond differently to FAD treatment depending on social status. In ascending males, mRNA transcripts of the sex steroid receptors begin to change within an hour of social opportunity (Maruska et al. 2013). To our knowledge, *A. burtoni* is the only species reported where FAD treatment can cause strong increases or decreases in aggression depending on social status and thus represents a flexible and powerful system to investigate the factors that may be causing these differences across species.

Antiandrogen treatment did not affect cytochrome oxidase levels throughout fore- and midbrain

We measured cytochrome oxidase to see if the drug treatments affected brain metabolism. In the flutamide treatment we did not find any differences between the treated

animals and control, consistent with a lack of a behavioral or hormonal effect in this treatment.

Inhibiting aromatase affected cytochrome oxidase in select fore- and midbrain areas

In the fadrozole experiment we found marginally significant increases in treated animals in the atn (putative ventral medial hypothalamus) and dm3 (pallial amygdala) and marginally significant decreases in the areas dlvl (hippocampus) and vl (lateral septum). These differences should be considered as exploratory and provisional because they were not strongly supported in the full model. These differences could be caused by the inhibition of aromatase and subsequent lowering of estrogen signaling or the increase in testosterone or both. It is possible that increases in the activity of the ventromedial hypothalamus (VMH) or the pallial amygdala could be related to increased aggression in FAD treated males. In studies of male mice the ventrolateral aspect of the VMH has been identified as a critical locus for aggressive motivation and aggression seeking behavior in males (Falkner et al. 2014; Falkner et al. 2016). The amygdala regulates many aspects of social behavior, in particular avoidance of adverse stimuli, defensive behavior and vigilance and could therefore be related to territorial defense (Davis and Whalen 2001). Interestingly the two areas that decreased, dlvl (hippocampus) and vl (lateral septum) are two of the only areas examined that completely lack ER α expression (Munchrath and Hofmann 2010). Having only ER β may mean that different transcriptional programs are being modulated by estrogen in these brain areas which could cause them to decrease activity after FAD treatment. We did not find any direct correlations with COX levels and behavior, which is likely due to the slow response time of COX as a measurement. It is difficult to assess whether any of these potential treatment differences had an impact on the increased aggression of FAD males however decreases in the activity of the lateral

septum and hippocampus are consistent with the correlations we did find with our *egr-1* measurements, namely that both of these were negatively related to aggression, so lower activity may promote aggressive behavior.

Antiandrogen treatment affected egr-1 activity in several areas

We measured *egr-1* to determine if neural activity as represented by a faster responding IEG would be affected by our treatments. In the flutamide experiment we found marginally significant decreases in ah (anterior hypothalamus), dd (medial pallium), poa (preoptic area) and vsl (extended amygdala). The POA has been studied extensively in the *A. burtoni* in relation to social status, and GnRH cells within the POA are known to enlarge after the opportunity to transition (Maruska and Fernald 2013). Across vertebrates and in teleosts the POA is known to regulate male aggression, sexual behavior and parental care as well as regulating the HPG axis (O'Connell and Hofmann 2011). The anterior hypothalamus also plays a role in aggression and sexual behavior in males, at least in mammals, however it has not been studied extensively in teleost fish (O'Connell and Hofmann 2011). Vs, the putative extended amygdala homolog, again may play a role in aggression and sexual behavior in males, as stimulation in bluegill sunfish increases these behaviors (O'Connell and Hofmann 2011). In *A. burtoni*, social opportunity causes increases in androgen and estrogen receptors in this area. The homology of dd is unclear and this is complicated by the fact that the area called dd in cichlids (Burmeister, Munshi, and Fernald 2009) is most likely homologous to the posterior part of dl in other teleost lineages, with the area called dc2 in cichlids being homologous to the dd of other teleosts (Elliott et al. 2017). If that is correct, then the cichlid dd (dlp) may be homologous to the medial pallium in other vertebrates. Finally, although we did not see any treatment effects on dlv2 (hippocampus), we did find a negative correlation between aggression towards the

intruder and activity in dlv2 in the flutamide dataset. This is similar to a negative correlation found in a previous study of resident-intruder aggression in *A. burtoni* (Weitekamp and Hofmann 2017) and suggests that the hippocampal homolog may regulate aggression in this species. The hippocampus is involved in memory consolidation and retrieval as well as social cognition more generally (Rubin et al. 2014).

Hyperaggression in fadrozole treated animals may be related to reduced activity of the lateral septum

In the fadrozole experiment we found marginally significant decreases in the treated group in the areas dd (medial pallium) and vl (lateral septum). As discussed above the homology and function of dd is not clear, however it clearly warrants further study given the results we found here. VL is part of the putative lateral septum homolog. Lateral septum is related to male aggression across vertebrates, where it acts to suppress aggression. A phenomenon known as “septal rage” has been observed in several species of mammals, where lesions to the lateral septum cause excessive aggression (Albert and Chew 1980; Potegal, Blau, and Glusman 1981; McDonald et al. 2012). One common symptom of tumors involving the septal formation in humans is an abrupt change in personality marked by irritability (Zeman and King 1958). Chemically inhibiting activity of the lateral septum in mice causes hyperaggression towards males and even the expression of aggression towards females, which control animals typically do not attack (Wong et al. 2016). Conversely, activating the septum using optogenetic manipulation or electrical stimulation reduces aggression (Wong et al. 2016). In male song sparrows, *Melospiza melodia*, levels of *egr-1* in lateral septum negatively correlate with aggression in simulated territory intrusion studies (Goodson, Evans, and Soma 2005). Furthermore the lateral septum appears to be the primary area where FAD acts to modulate aggression in mice (Trainor, Greiwe, and Nelson 2006). Levels of ER α in the lateral septum correlate with aggression

and FAD reduced brain activity as reflected by lower levels of the IEG *c-fos*. Consistent with this we found a negative correlation with the amount of *egr-1* activity in the vl (lateral septum) and aggression in the fadrozole dataset. Therefore, it is possible that the hyper aggression phenotype of the FAD animals is driven by lower activity in vl, which was lower in FAD treated animals in both the cytochrome oxidase dataset as well as the *egr-1* dataset.

Covariance analysis suggests possible functional circuits for future studies

Finally, we analyzed covariance patterns of our 4 datasets to look for similarities and differences in functional connectivity. While this study is underpowered for this analysis, we can make several observations. We were not able to detect any treatment effects on the covariance pattern, so we pooled treated and controls within each dataset. According to our Mantel tests comparing each pair of covariance matrices, we found that they were substantially similar across datasets, indicating possible functional circuits. In our clustering analysis several brain areas were clustered together consistently across datasets, suggesting they may be functionally connected. For example, dp (olfactory cortex) and vp (basal amygdala); poa and vsm (medial amygdala); dm2r (pallial amygdala), vdr (nucleus accumbens) and vv (pallidum); dc4 (dorsal pallium), dc5 (dorsal pallium) and dlgl (hippocampus).

Conclusion

Here we have manipulated the androgen and estrogen system during social ascent in *A. burtoni* for the first time. Surprisingly androgens seem to play a minor role in the transition process as we did not observe any effects on behavior or physiology with antiandrogen treatment. fadrozole treatment caused males to become hyperaggressive, a phenotype which may be related to reduced activity in the lateral septum. The modulation

of aggression by estrogens in *A. burtoni* depends on social status making them an ideal model for future studies on the mechanisms involved with this phenomenon across vertebrates.

ACKNOWLEDGEMENTS

We thank Juliette Rubin for technical assistance; Sylvia Garza for fish care; and members of the Hofmann laboratory for insightful discussions.

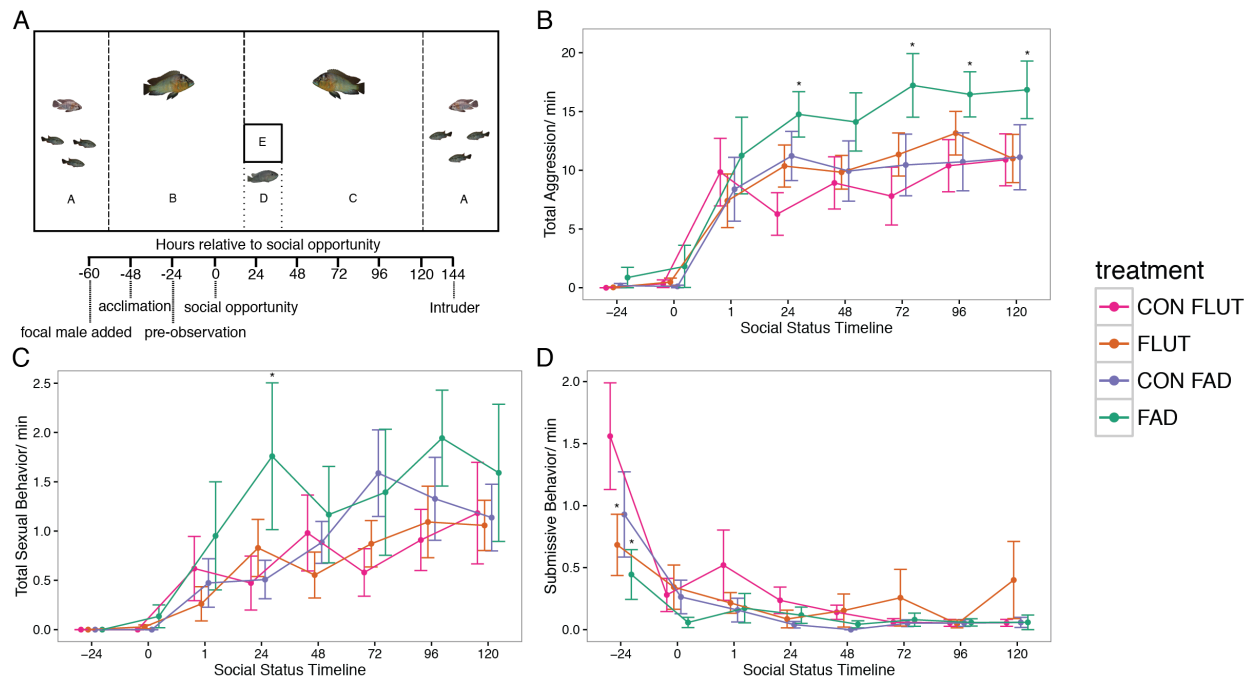


Figure 3.1: A) Experimental paradigm and timeline. Compartments-A: side communities of one male and three females which serve as a social stimulus for all animals in the paradigm. Compartment-B: suppressor male. Compartment-C: Suppressor male that is removed at time point 0. Compartment-D: refuge for focal male. Compartment-E: chamber that allows for the presentation of an intruder male. B-D) Mean and standard error of each group of aggressive (B), sexual (C) and submissive behavior (D) across the time points. * = $p < 0.05$ in the comparison between treatment and control. Flutamide control = pink, flutamide = orange, fadrozole control = blue, fadrozole = green.

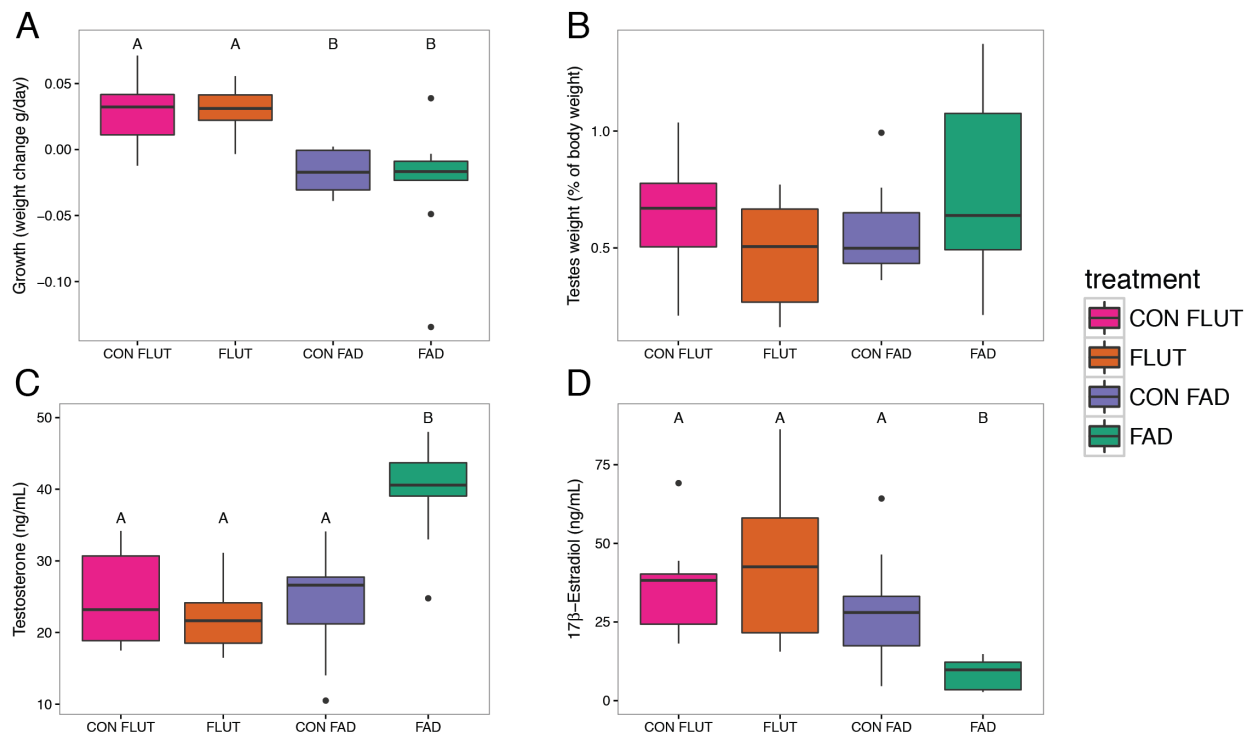


Figure 3.2: A) Growth rate differed between experiments but not treatment. B) Relative gonad size was not different among groups. C) FAD males had elevated testosterone levels. D) FAD males had decreased estradiol levels. Letter codes indicate significant differences between groups. Flutamide control = pink, flutamide = orange, fadrozole control = blue, fadrozole = green.

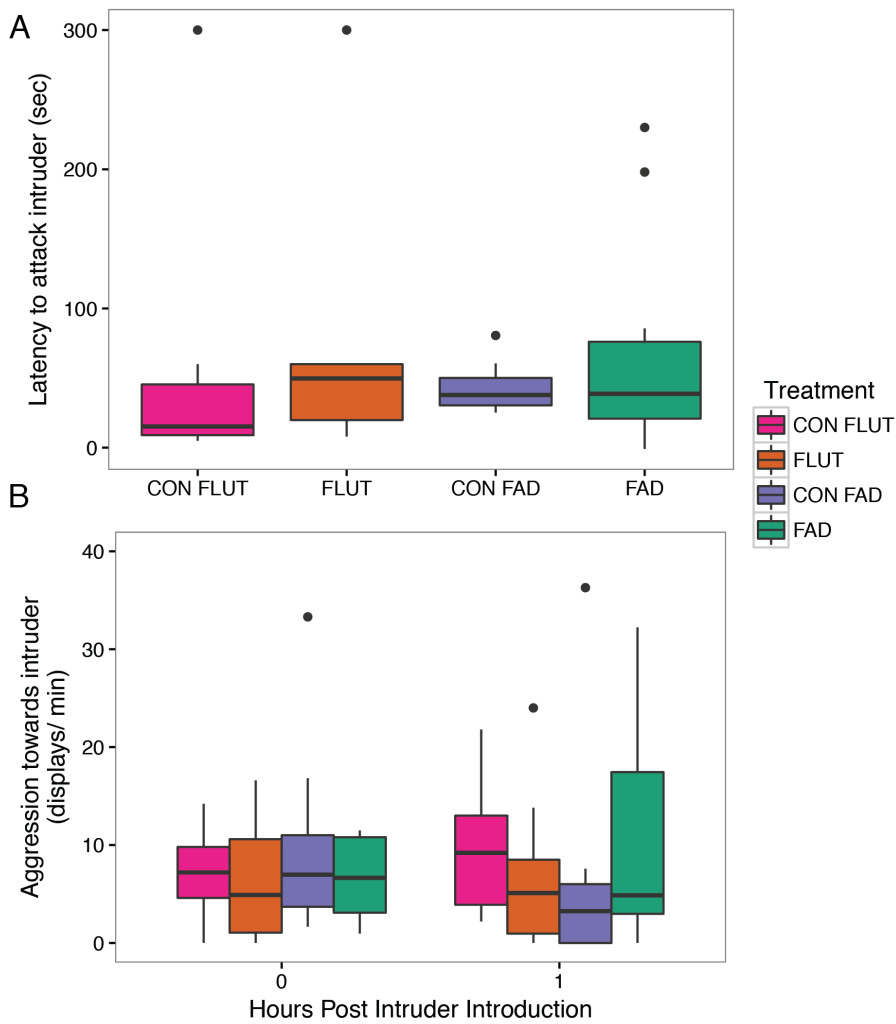


Figure 3.3: Treatment did not affect intruder directed aggression. A) Latency to attack the intruder. B) Number of aggressive displays directed toward intruder. Flutamide control = pink, flutamide = orange, fadrozole control = blue, fadrozole = green.

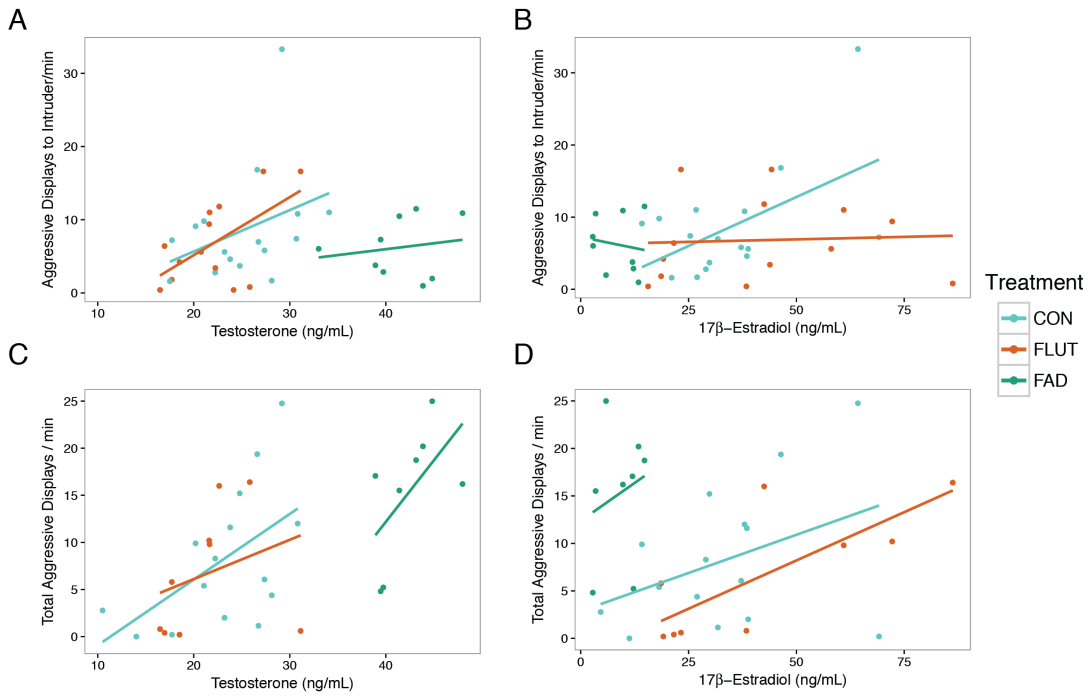


Figure 3.4: A-B) Correlations between aggression towards the intruder and testosterone (A) and estradiol (B). C-D) Correlations between total aggressive displays and testosterone (C) and estradiol (D). Combined controls = blue, flutamide = orange, fadrozole = green.

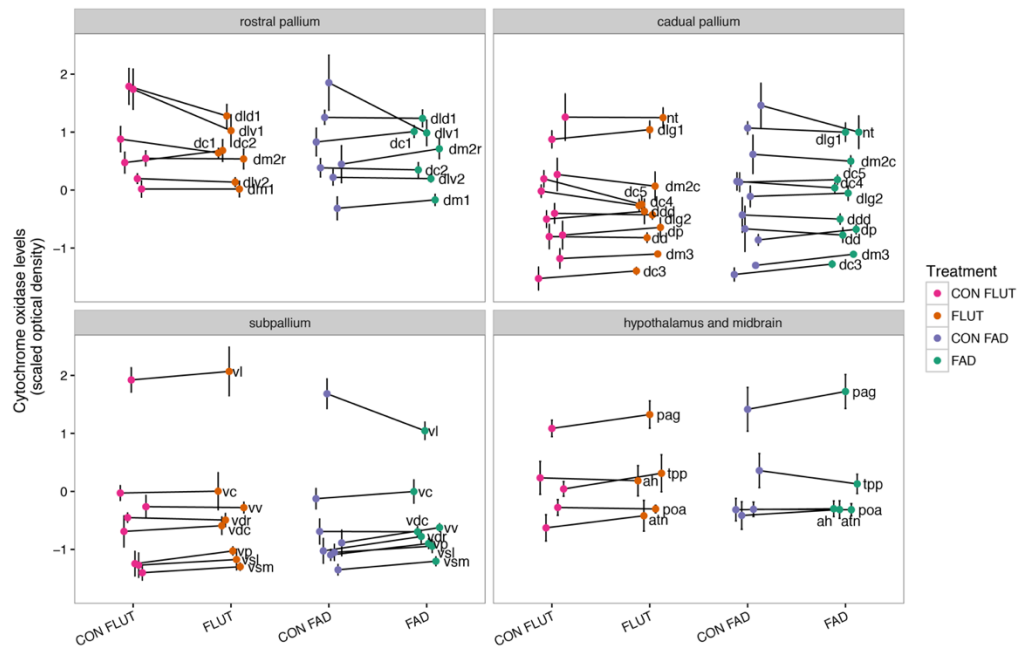


Figure 3.5: Calibrated optical density measurements of COX levels were centered within each individual and are depicted for each brain area measured. For the purposes of the plot we scaled the scores within each experiment using z-scores. Brain areas are split into four panels depending on their origin. Points and error bars represent the group average \pm the standard error for each brain area. Groups within each experiment are connected by a line.

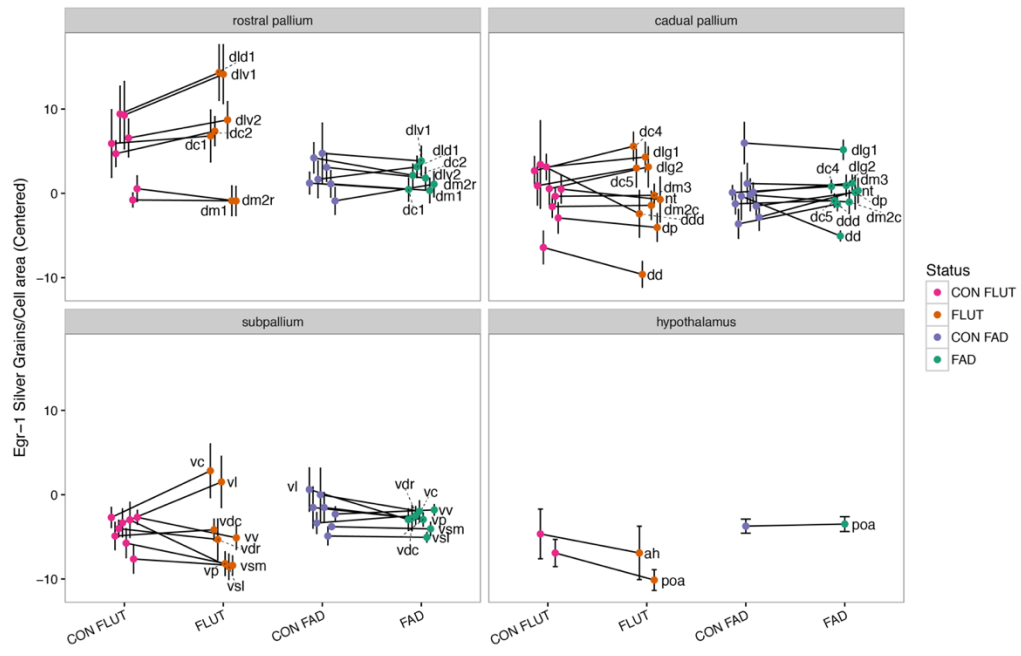


Figure 3.6: Number of *egr-1* silver grains /mm covered by cells were centered within each individual and are depicted for each brain area measured. Brain areas are split into four panels depending on their origin. Points and error bars represent the group average \pm the standard error for each brain area. Groups within each experiment are connected by a line.

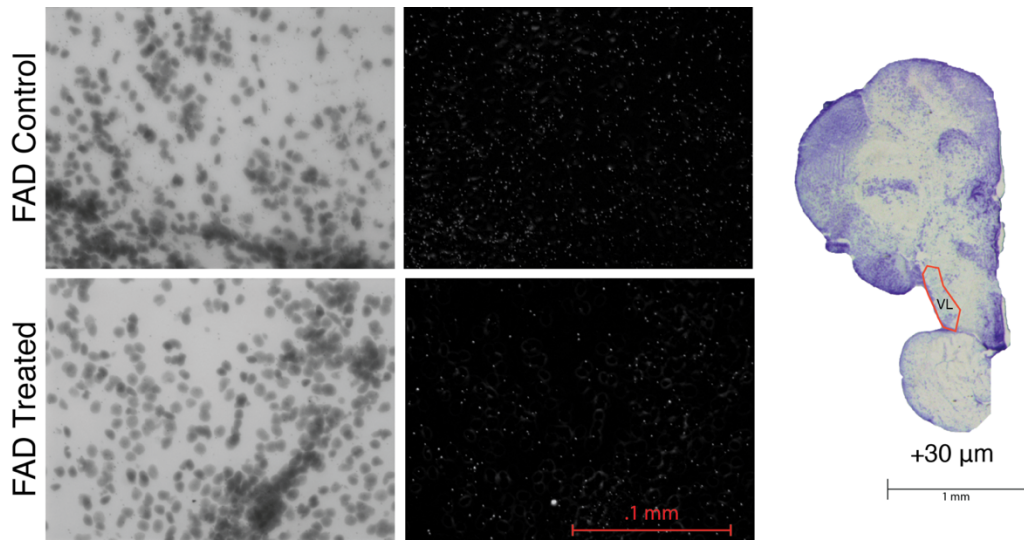


Figure 3.7: Example micrographs of the VL in a control animal (top row) and FAD treated animal (bottom row). Micrographs are presented with the brightfield on the left and the corresponding darkfield photo on the right.

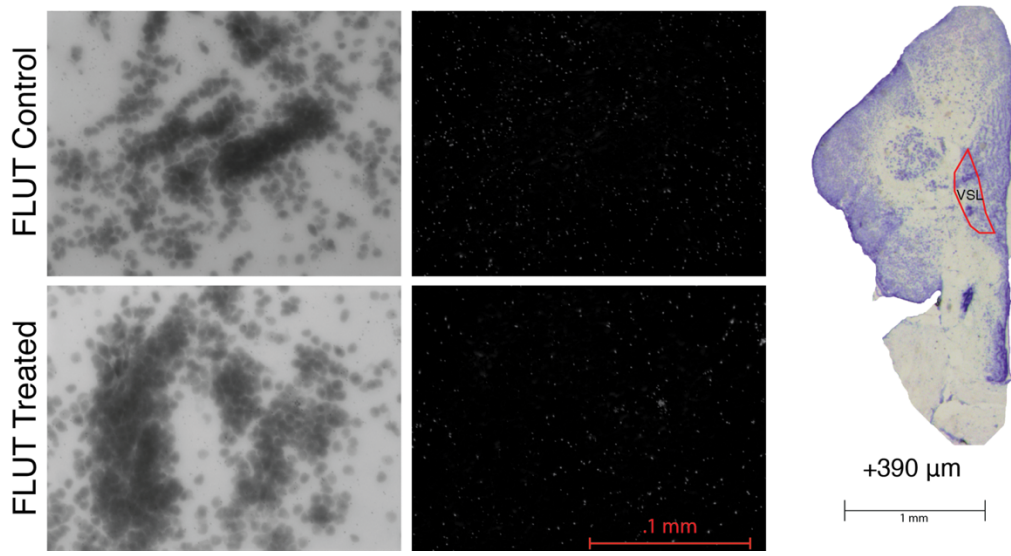


Figure 3.8: Example micrographs of the VSL in a control animal (top row) and FLUT treated animal (bottom row). Micrographs are presented with the brightfield on the left and the corresponding darkfield photo on the right.

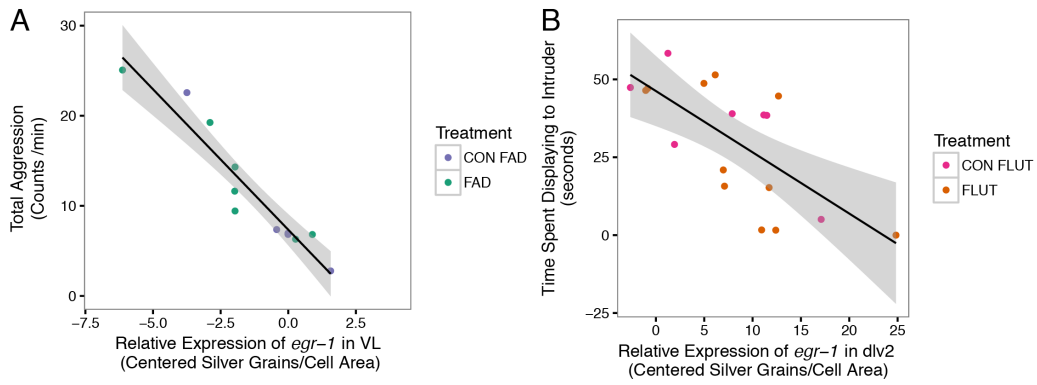


Figure 3.9: A) Correlation between *egr-1* levels in VL and total aggression in the fadrozole dataset. B) Correlation between *egr-1* levels and aggression to the intruder (measured as the time spent displaying) in the flutamide dataset.

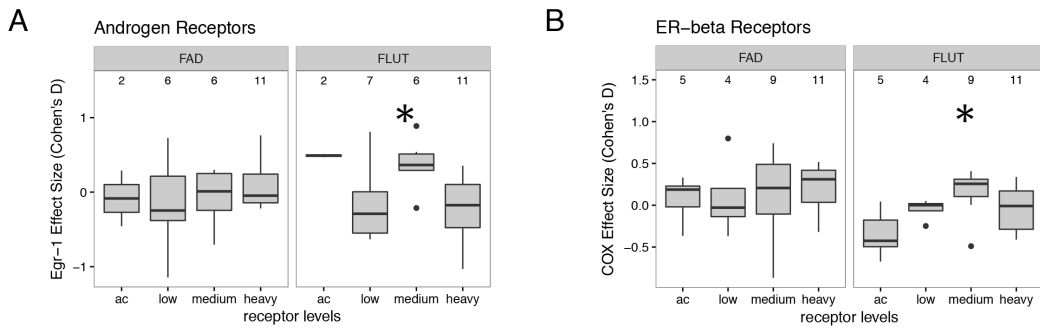


Figure 3.10: A) *Egr-1* effect sizes covaried with androgen receptors in the flutamide dataset, but not in the fadrozole dataset. B) COX effect sizes covaried with estrogen receptor beta levels in the flutamide dataset but not in the fadrozole dataset.

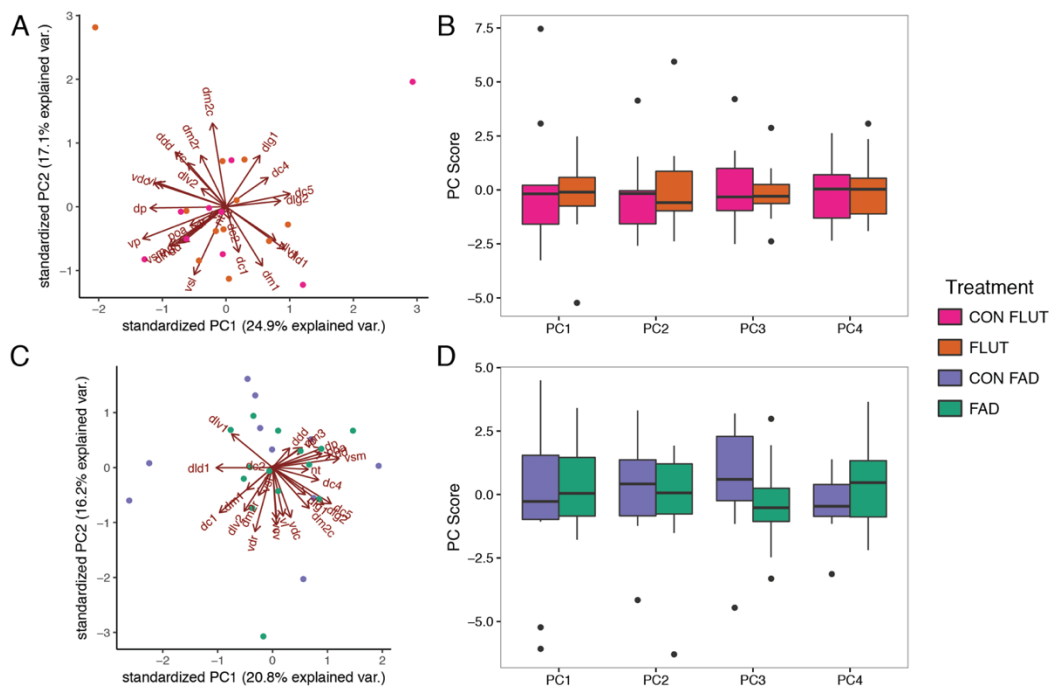


Figure 3.11: Principal component analysis of COX datasets. A) Biplot of the flutamide experiment, PCs 1 and 2 showing the loadings. B) Flutamide principal component scores as a function of treatment for the first four components. C) Biplot of fadrozole experiment, PCs 1 and 2 showing the loadings. D) Fadrozole principal component scores as a function of treatment for the first four components.

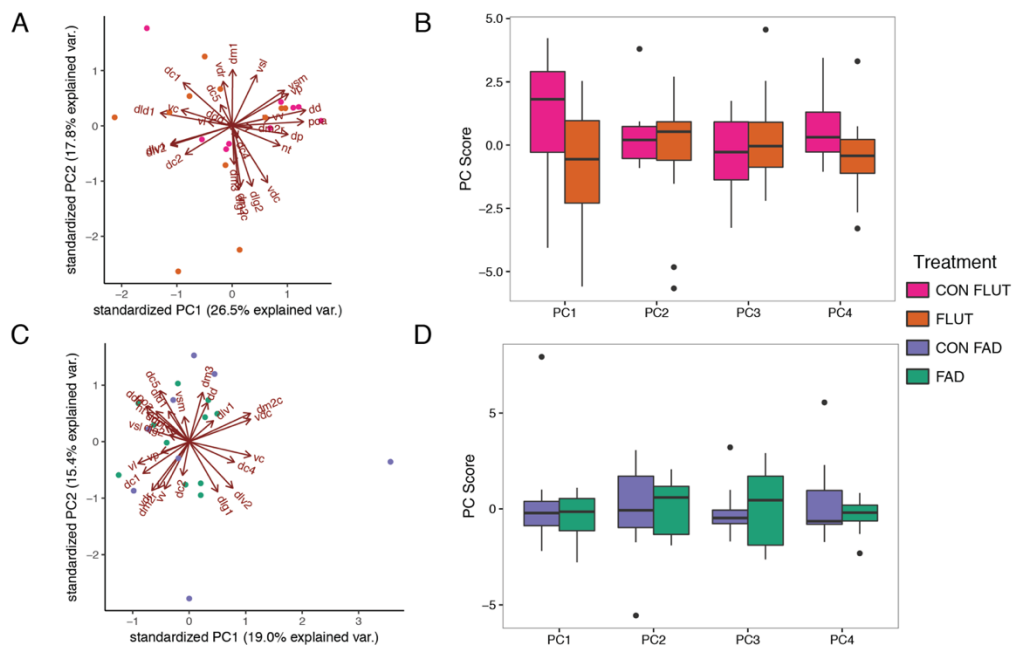


Figure 3.12: Principal component analysis of *egr-1* datasets. A) Biplot of the flutamide experiment, PCs 1 and 2 showing the loadings. B) Flutamide principal component scores as a function of treatment for the first four components. C) Biplot of fadrozole experiment, PCs 1 and 2 showing the loadings. D) Fadrozole principal component scores as a function of treatment for the first four components.

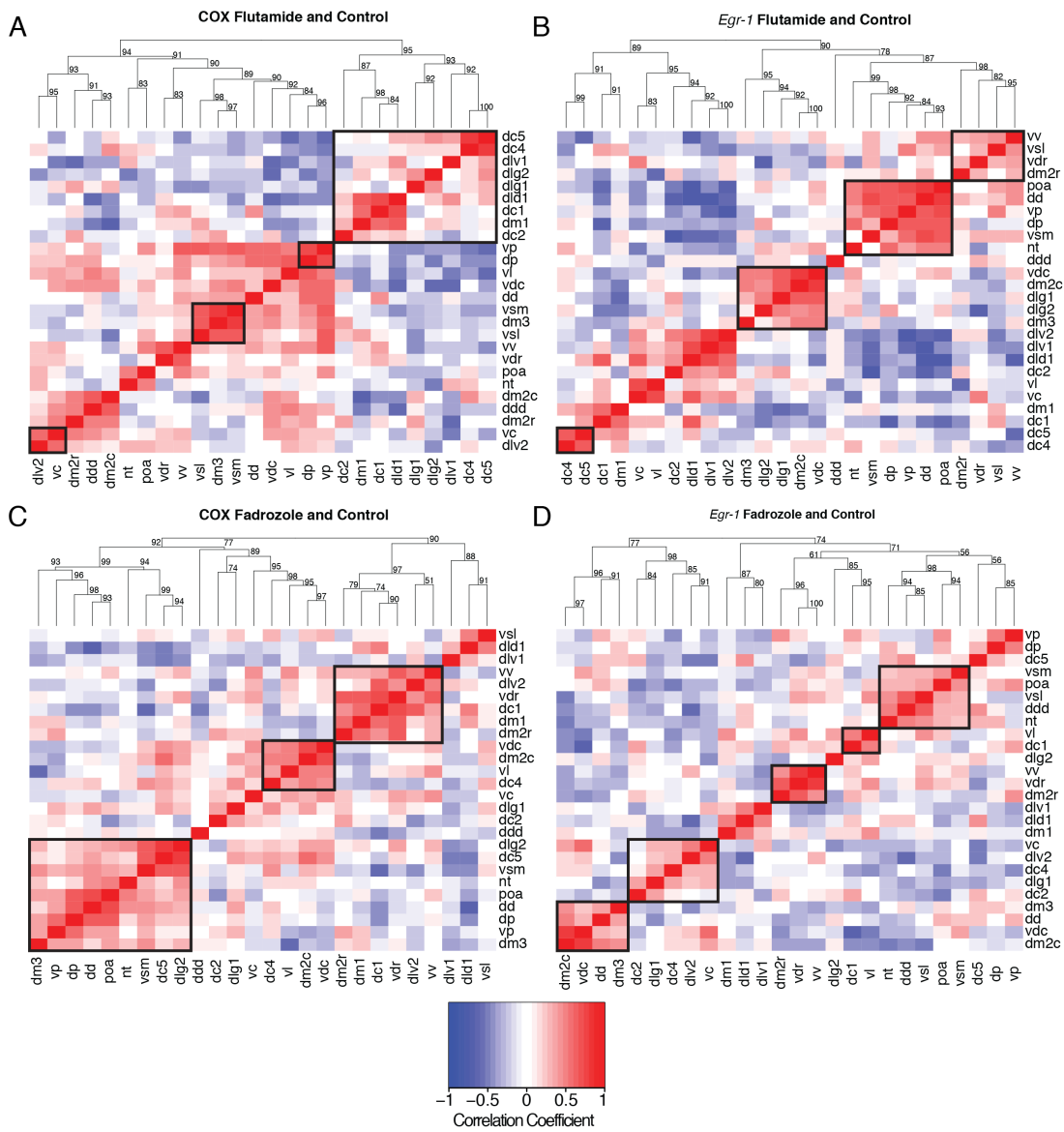


Figure 3.13: Clustered heatmaps of all pairwise correlations between brain areas. Color represents Pearson correlation coefficients. A) Flutamide COX dataset, B) Flutamide *egr-1* dataset. C) Fadzole COX dataset, D) Fadzole *egr-1* dataset. Bootstrap resampling was used to identify significant clusters which are depicted with black boxes.

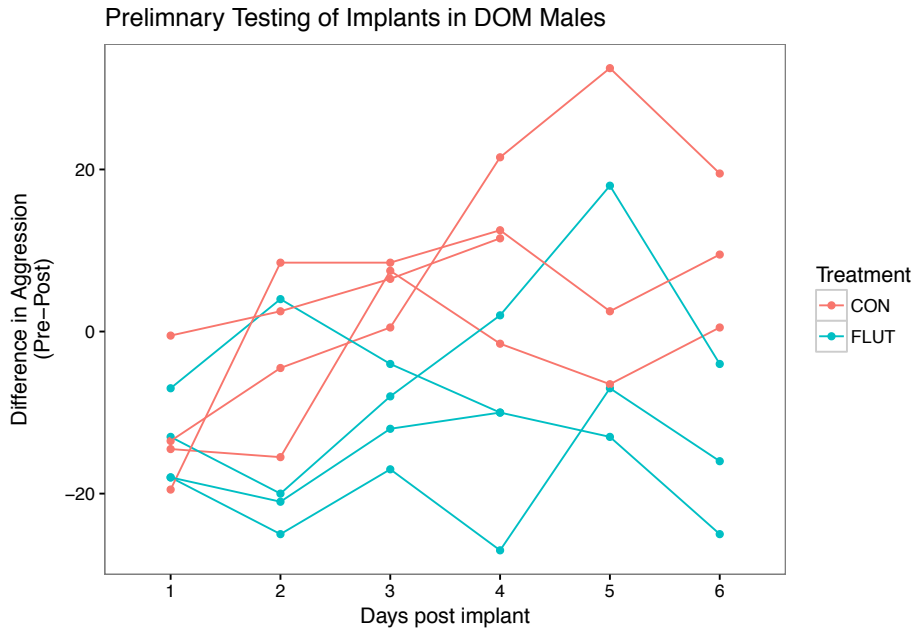


Figure 3.14: Preliminary testing of coconut oil implant technology. Aggression levels prior to receiving the implant was subtracted from the aggression on each day post implant.

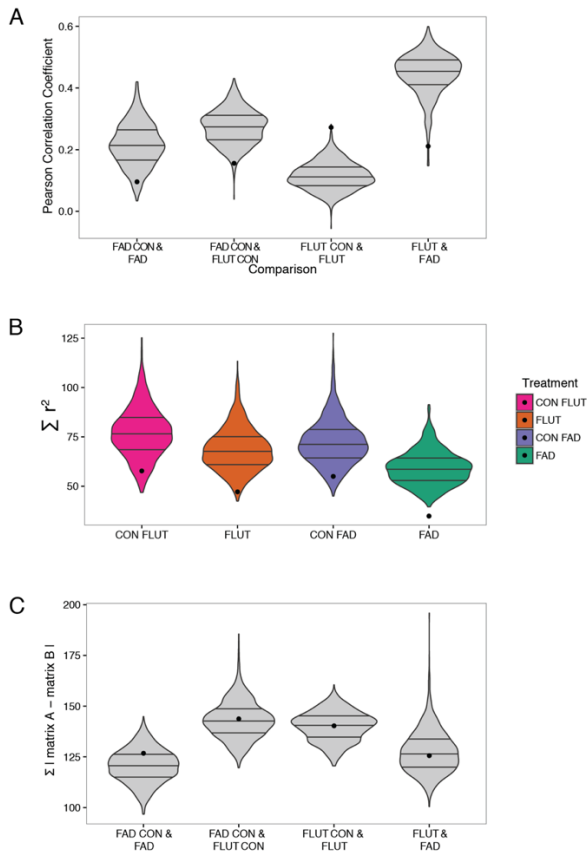


Figure 3.15: Permutation of COX covariance matrices. A) Permutations comparing similarities (matrix correlations) of the covariance matrix of each group. Violin plots show the distribution of correlation coefficients of the matrices after random permutation of the group labels. Points are the real correlation coefficient between the two matrices. B) For each covariance matrix we calculated the sum of the square of the Pearson correlation coefficients which is a measure of the overall strength of correlations across the matrix and compared that to random sampling (preserving sample size of each group) of the full dataset. Violin plots show the distribution of the sum of r^2 of the randomly permuted data while points show the sum of r^2 of the real data. C) For each pair of correlation matrices we calculated the sum of the absolute value of the differences between each off-diagonal element of the matrices. Violin plots show the distribution of the difference scores of the randomly permuted data while points show the difference score of the real data.

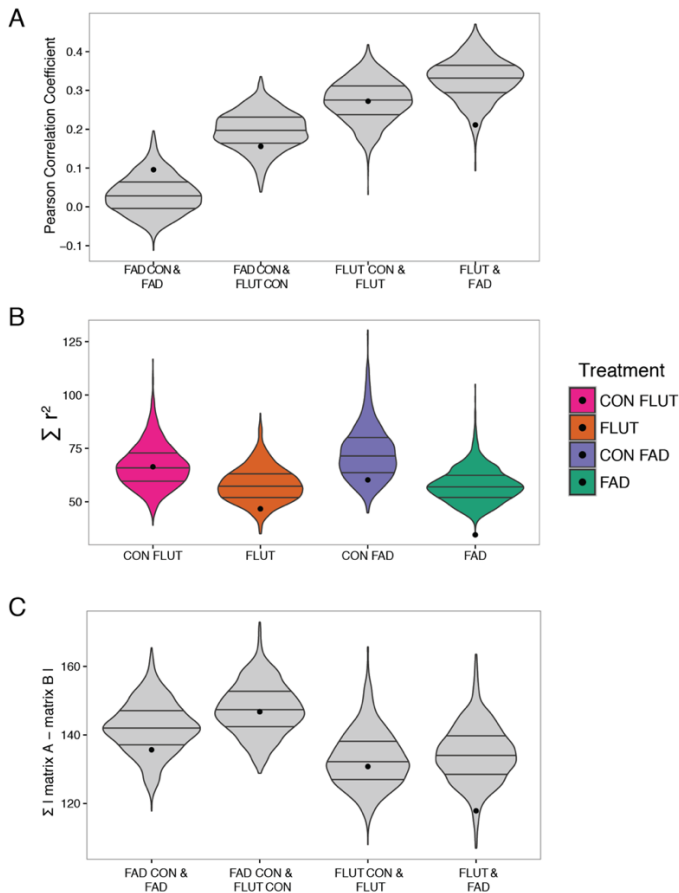


Figure 3.16: Permutation of *egr-1* covariance matrices. A) Permutations comparing similarities (matrix correlations) of the covariance matrix of each group. Violin plots show the distribution of correlation coefficients of the matrices after random permutation of the group labels. Points are the real correlation coefficient between the two matrices. B) For each covariance matrix we calculated the sum of the square of the Pearson correlation coefficients which is a measure of the overall strength of correlations across the matrix and compared that to random sampling (preserving sample size of each group) of the full dataset. Violin plots show the distribution of the sum of r^2 of the randomly permuted data while points show the sum of r^2 of the real data. C) For each pair of correlation matrices we calculated the sum of the absolute value of the differences between each off-diagonal element of the matrices. Violin plots show the distribution of the difference scores of the randomly permuted data while points show the difference score of the real data.

<i>Abbreviation</i>	<i>Full Name</i>	<i>Putative mammalian homolog</i>
<i>Atn</i>	Anterior tuberal nucleus	ventral medial hypothalamus
<i>Ah</i>	Anterior hypothalamus	Anterior hypothalamus
<i>D</i>	Dorsal division of the telencephalon	Pallium
<i>Dc-1,2,3,4,5</i>	Central division of D (5 subdivisions).	Pallium (specific homology unclear)
<i>Dd</i>	Dorsal division of D	Pallium (specific homology unclear)
<i>Ddd</i>	Dorsal subdivision of dd	
<i>Ddv</i>	Ventral subdivision of dd	
<i>dl</i>	Lateral division of D	Hippocampus
<i>Dld1</i>	Dorsal subdivision of dl	
<i>Dlg1</i>	Dorsal-lateral part of the Granular zone of dl	
<i>Dlg2</i>	Ventral-medial part of the granular zone of dl	
<i>Dlv -1,2</i>	Ventral division of dl (2 subdivisions)	
<i>Dm - 1,2,3</i>	Medial division of D (3 subdivisions)	Pallial amygdala
<i>Dm2c</i>	Caudal part of dm2	
<i>Dm2r</i>	Rostral part of dm2	
<i>Dp</i>	Posterior division of D	Olfactory pallium
<i>Nt</i>	Nucleus taenia	
<i>OB</i>	Olfactory bulb	Olfactory bulb
<i>Pag</i>	Periaqueductal gray	Periaqueductal gray
<i>Poa</i>	Preoptic area	Preoptic area
<i>Tpp</i>	Posterior tuberculum	Ventral tegmental area
<i>V</i>	Ventral subdivision of the telencephalon	Subpallium
<i>Vc</i>	Central nucleus of V	Striatum
<i>Vd</i>	Dorsal nucleus of V	Nucleus accumbens

Table 3.1: Abbreviations of brain areas used in this paper and putative mammalian homologies (O'Connell and Hofmann 2011). Continued on the next page.

<i>Vdc</i>	<i>Caudal part of vd</i>	
<i>Vdr</i>	Rostral part of vd	
<i>Vl</i>	Lateral nucleus of v	Lateral septum
<i>Vp</i>	Postcommissural nucleus of V	Basal amygdala
<i>Vs</i>	Supracommissural nucleus of V	Extended amygdala: (Bed nucleus of the stria terminalis/ medial amygdala)
<i>Vsl</i>	Lateral subdivision of vs	
<i>Vsm</i>	Medial subdivision of vs	
<i>Vv</i>	Ventral nucleus of V	Dorsal part of vv: Pallidum Ventral part of vv: Septum

Table 3.1: Continued.

Experiment	Behavior	term	χ^2	Degrees of Freedom	P- Value
Fadrozole	Aggression	Day	105.2517	7	<2e-16
		treatment	0.1417	1	0.7066
		Day:treatment	12.1038	7	0.0972
	Sexual	Day	29.8676	7	0.0001004
		treatment	0	1	0.9951701
		Day:treatment	7.7667	7	0.3536155
	Submissive	Day	109.792	7	< 2.2e-16
		treatment	19.519	1	0.000009963
		Day:treatment	16.954	7	0.0177
Flutamide	Aggression	Day	112.4708	7	<2e-16
		treatment	0.0236	1	0.8779
		Day:treatment	4.2528	7	0.7502
	Sexual	Day	52.8348	7	3.996E-09
		treatment	0	1	0.9969
		Day:treatment	4.7975	7	0.6847
	Submissive	Day	80.3538	7	1.167E-14
		treatment	7.1969	1	0.007303
		Day:treatment	13.9977	7	0.051223

Table 3.2: Results of ANOVA of behavior data.

Contrast	Time point	Estimate	se	df	t-value	p-value
Aggression CON-FAD	-24	-0.9939	2.6402	102.21	-0.376	0.7074
	0	-1.4467	2.6402	102.21	-0.548	0.5849
	1	-2.8005	2.6893	107.57	-1.041	0.3
	24	-6.3212	2.6267	100.73	-2.407	0.0179
	48	-4.772	2.7014	108.99	-1.766	0.0801
	72	-8.5542	2.6893	107.57	-3.181	0.0019
	96	-5.905	2.6145	99.39	-2.259	0.0261
	120	-6.0998	2.6267	100.73	-2.322	0.0222
Aggression CON-FLUT	-24	0.3611	2.3506	129.28	0.154	0.8781
	0	-0.1167	2.2797	118.93	-0.051	0.9593
	1	1.7609	2.2982	121.66	0.766	0.445
	24	-1.9199	2.265	116.81	-0.848	0.3984
	48	-0.5352	2.3125	123.75	-0.231	0.8174
	72	-1.9982	2.265	116.81	-0.882	0.3795
	96	-2.1423	2.2852	119.76	-0.937	0.3504
	120	-0.2513	2.265	116.81	-0.111	0.9119
Sexual CON-FAD	-24	-0.0028	0.468	154.12	-0.006	0.9952
	0	-0.0802	0.468	154.12	-0.171	0.8642
	1	-0.517	0.479	160.35	-1.079	0.282
	24	-1.2844	0.4649	152.33	-2.762	0.0064
	48	-0.2229	0.4817	162.1	-0.463	0.6441
	72	-0.3822	0.479	160.35	-0.798	0.4261
	96	-0.8248	0.4622	150.66	-1.785	0.0764
	120	-0.4513	0.4649	152.33	-0.971	0.3333

Table 3.3: Posthoc testing of least-squares means of the behavior data. Continued on the next page.

Sexual CON-FLUT	-24	0.0013	0.335	174.54	0.004	0.9969
	0	0.0285	0.323	162.58	0.088	0.9297
	1	0.2742	0.3261	165.86	0.841	0.4018
	24	-0.3547	0.3205	160.06	-1.107	0.27
	48	0.383	0.3286	168.28	1.166	0.2454
	72	0.2339	0.3205	160.06	0.73	0.4666
	96	0.0554	0.3239	163.61	0.171	0.8643
	120	0.0816	0.3205	160.06	0.254	0.7994
Submissive CON-FAD	-24	0.8023	0.1816	224.82	4.417	0.0001
	0	0.2141	0.1816	224.82	1.179	0.2398
	1	0.1529	0.1869	225.21	0.818	0.4142
	24	0.0245	0.1802	224.7	0.136	0.8922
	48	0.0267	0.1883	225.37	0.142	0.8873
	72	-0.0284	0.1869	225.21	-0.152	0.8794
	96	-0.0039	0.1788	224.57	-0.022	0.9827
	120	-0.0005	0.1802	224.7	-0.003	0.9978
Submissive CON-FLUT	-24	0.5783	0.2156	222.74	2.682	0.0079
	0	-0.0708	0.2067	214.09	-0.343	0.7322
	1	0.1253	0.2091	216.6	0.599	0.5497
	24	0.0522	0.2049	212.18	0.255	0.7992
	48	-0.0752	0.2109	218.37	-0.357	0.7216
	72	-0.2012	0.2049	212.18	-0.982	0.3273
	96	-0.0626	0.2074	214.91	-0.302	0.763
	120	-0.3374	0.2049	212.18	-1.647	0.1011

Table 3.3: Continued.

Experiment	Brain Area	Estimate	Std. Error	degrees freedom	T-value	P-value	Holm Adjusted P	Sample Size Control	Sample Size Treated
Fadrozole	ah	0.26	0.3	15	0.866	0.4	1	8	9
	atn	0.561	0.306	14.475	1.831	0.088	1	8	11
	dc1	0.123	0.248	22	0.497	0.624	1	10	14
	dc2	0.101	0.204	22	0.494	0.626	1	10	14
	dc3	0.366	0.268	20	1.366	0.187	1	9	13
	dc4	0.006	0.18	18.776	0.032	0.975	1	9	14
	dc5	0.104	0.18	21	0.581	0.567	1	9	14
	dd	-0.113	0.362	16.074	-0.311	0.759	1	7	12
	ddd	0.144	0.336	14.23	0.43	0.674	1	8	11
	dld1	-0.149	0.169	18.831	-0.878	0.391	1	10	13
	dlg1	0.147	0.209	21	0.7	0.492	1	9	14
	dlg2	-0.003	0.226	21	-0.014	0.989	1	9	14
	dlv1	-0.803	0.421	22	-1.909	0.069	1	10	14

Table 3.4: Full results of models testing the treatment effects on COX levels in each brain area. Continued on the next page.

dlv2	- 0.048	0.19	22	- 0.254	0.802	1	10	14
dm1	0.043	0.242	22	0.178	0.86	1	10	14
dm2c	0.174	0.371	18	0.469	0.645	1	8	12
dm2r	0.286	0.307	20	0.934	0.362	1	10	12
dm3	0.254	0.13	19.898	1.957	0.064	1	10	14
dp	0.266	0.219	20	1.215	0.238	1	9	13
nt	- 0.292	0.395	16.85	- 0.739	0.47	1	9	11
pag	0.254	0.324	17.139	0.782	0.445	1	9	13
poa	- 0.046	0.184	18.15	- 0.249	0.806	1	9	14
tpp	- 0.191	0.291	19	- 0.655	0.521	1	9	12
vc	0.186	0.277	15.57	0.67	0.513	1	8	12
vdc	0.089	0.301	14.449	0.295	0.772	1	6	12
vdr	0.461	0.314	19.432	1.469	0.158	1	10	14
vl	- 0.382	0.211	17.262	- 1.811	0.088	1	9	13
vp	0.289	0.253	20	1.14	0.268	1	9	13
vsl	0.038	0.278	15.726	0.136	0.893	1	7	11
vsm	0.274	0.221	21	1.239	0.229	1	9	14
vv	0.379	0.295	19.52	1.285	0.214	1	10	14

Table 3.4: Continued on the next page.

Flutamid e	ah	- 0.495	0.613	14	- 0.807	0.433	1	8	8
	atn	0.023	0.62	16	0.037	0.971	1	9	9
	dc1	- 0.362	0.278	18	-1.3	0.21	1	9	11
	dc2	0.156	0.342	15.68 7	0.456	0.654	1	9	11
	dc3	0.486	0.667	15.32 4	0.728	0.478	1	9	10
	dc4	- 0.248	0.259	18	- 0.959	0.35	1	9	11
	dc5	- 0.523	0.313	14.79	- 1.669	0.116	1	9	11
	dd	- 0.148	0.384	17	- 0.384	0.706	1	9	10
	ddd	0.065	0.479	13	0.135	0.895	1	7	8
	dld1	- 0.512	0.481	17	- 1.064	0.302	1	9	10
	dlg1	0.224	0.294	19	0.762	0.455	1	9	12
	dlg2	- 0.102	0.281	15.07 8	- 0.363	0.722	1	9	10
	dlv1	-0.62	0.607	16	- 1.022	0.322	1	9	9
	dlv2	0.204	0.264	18	0.77	0.451	1	9	11
	dm1	0.023	0.276	17	0.084	0.934	1	9	10
	dm2c	- 0.218	0.502	18	- 0.434	0.67	1	9	11

Table 3.4: Continued on the next page.

	dm2r	0.011	0.286	14.264	0.04	0.969	1	9	10
	dm3	0.044	0.324	18	0.136	0.893	1	9	11
	dp	0.319	0.506	14.843	0.631	0.538	1	9	11
	nt	0.36	0.467	15.514	0.771	0.452	1	9	11
	pag	0.298	0.357	18	0.834	0.415	1	9	11
	poa	- 0.074	0.251	18	- 0.294	0.772	1	9	11
	tpp	0.266	0.477	15.349	0.557	0.585	1	9	10
	vc	0.224	0.482	12.867	0.465	0.65	1	8	8
	vdc	0.066	0.509	18	0.13	0.898	1	9	11
	vdr	- 0.204	0.265	15.16	- 0.771	0.452	1	9	11
	vl	- 0.005	0.518	13.931	- 0.009	0.993	1	9	10
	vp	0.416	0.542	18	0.768	0.453	1	9	11
	vsl	0.254	0.727	15	0.349	0.732	1	8	9
	vsm	0.054	0.301	18	0.179	0.86	1	9	11
	vv	- 0.232	0.358	18	- 0.648	0.525	1	9	11

Table 3.4: Continued.

Experiment	Brain Area	Estimate	Std. Error	degrees freedom	T-value	P-value	Holm Adjusted P	Sample Size Control	Sample Size Treated
Fadrozole	dc1	-0.156	0.319	17	-0.488	0.632	1	8	11
	dc2	-0.304	0.291	16	-1.044	0.312	1	7	11
	dc4	0.115	0.178	16.992	0.644	0.528	1	8	11
	dc5	0.231	0.249	14.724	0.929	0.368	1	7	10
	dd	-0.826	0.447	10	-1.849	0.094	1	5	7
	ddd	0.581	0.351	12	1.655	0.124	1	6	8
	dld1	0.261	0.33	17	0.792	0.439	1	8	11
	dlg1	-0.057	0.305	16	-0.188	0.853	1	7	11
	dlg2	0.019	0.395	15.161	0.049	0.961	1	7	11
	dlv1	-0.044	0.449	17	-0.099	0.922	1	8	11

Table 3.5: Full results of models testing the treatment effects on *egr-1* levels in each brain area.

	dlv2	-0.184	0.285	17	- 0.64 7	0.52 6	1	8	11
	dm1	-0.22	0.312	15.98 6	- 0.70 6	0.49 1	1	8	11
	dm2c	-0.13	0.394	16	- 0.33 1	0.74 5	1	8	10
	dm2r	0.356	0.345	14	1.03 4	0.31 9	1	8	8
	dm3	0.176	0.246	17	0.71 6	0.48 3	1	8	11
	dp	0.259	0.438	14.82 5	0.59 1	0.56 4	1	7	10
	nt	0.594	0.383	13	1.55 3	0.14 4	1	6	9
	poa	0.046	0.269	15	0.17	0.86 8	1	8	9
	vc	-0.573	0.501	9	- 1.14 5	0.28 2	1	6	5
	vdc	-0.255	0.496	15.83 7	- 0.51 3	0.61 5	1	8	10
	vdr	0.393	0.324	14.90 1	1.21 3	0.24 4	1	8	10

Table 3.5: Continued on the next page.

	vl	-0.778	0.362	5.268	- 2.14 7	0.08 2	1	7	5
	vp	-0.149	0.352	13.7	- 0.42 3	0.67 9	1	7	9
	vsl	0.037	0.31	14	0.11 8	0.90 8	1	7	9
	vsm	-0.138	0.255	12.61 8	- 0.54 3	0.59 7	1	7	11
	vv	0.109	0.206	17	0.52 8	0.60 4	1	8	11
Flutamid e	ah	-0.761	0.69	10.59 8	- 1.10 3	0.29 5	1	7	6
	dc1	0.114	0.448	17	0.25 5	0.80 2	1	9	10
	dc2	0.254	0.219	18	1.15 7	0.26 2	1	9	11
	dc4	0.286	0.204	15.93 4	1.40 2	0.18	1	9	11
	dc5	0.253	0.337	17.17 9	0.75	0.46 3	1	9	11
	dd	-0.8	0.323	12.55 5	- 2.47 8	0.02 8	0.736	8	9

Table 3.5: Continued on the next page

ddd	-0.597	0.586	11	- 1.01 8	0.33	1	6	7
dld1	0.429	0.413	18	1.03 7	0.31 3	1	9	11
dlg1	0.104	0.246	18	0.42 5	0.67 6	1	9	11
dlg2	0.266	0.345	18	0.77 1	0.45	1	9	11
dlv1	0.552	0.446	15.41 2	1.23 8	0.23 4	1	9	10
dlv2	0.217	0.287	17.21 6	0.75 7	0.45 9	1	9	11
dm1	-0.053	0.246	18	- 0.21 4	0.83 3	1	9	11
dm2c	-0.006	0.268	16	- 0.02 2	0.98 3	1	8	10
dm2r	-0.191	0.276	18	- 0.69 1	0.49 9	1	9	11
dm3	-0.001	0.191	18	- 0.00 4	0.99 7	1	9	11
dp	-0.135	0.32	17	- 0.42 4	0.67 7	1	9	10

Table 3.5: Continued on the next page.

	nt	-0.301	0.421	17.355	-0.715	0.484	1	9	11
	poa	-0.567	0.291	16.77	-1.945	0.069	1	9	11
	vc	0.564	0.355	13	1.59	0.136	1	8	7
	vdc	0.1	0.267	16	0.375	0.713	1	7	11
	vdr	-0.262	0.346	17	-0.756	0.46	1	9	10
	vl	0.454	0.419	9.819	1.084	0.304	1	6	6
	vp	-0.443	0.255	13.837	-1.736	0.105	1	8	10
	vsl	-0.885	0.346	16.963	-2.56	0.02	0.549	8	11
	vsm	-0.078	0.302	18	-0.258	0.799	1	9	11
	vv	-0.353	0.225	16.736	-1.572	0.135	1	9	10

Table 3.5: Continued.

Area	AR	ER α	ER β
dm1	light	heavy	light
dld1	absent	absent	cytosolic
dlv1	medium	medium	medium
dm2r	heavy	absent	cytosolic
dc2	absent	heavy	medium
dlg1	heavy	medium	heavy
dlg2	heavy	heavy	heavy
dc4	medium	medium	cytosolic
dc5	medium	medium	cytosolic
nt	heavy	medium	medium
dlv2	medium	medium	medium
vsm	heavy	heavy	heavy
dm3	light	light	light
vdr	heavy	heavy	heavy
vv	heavy	heavy	heavy
vc	medium	medium	heavy
vl	light	absent	light
vdc	heavy	heavy	heavy
dm2c	heavy	light	cytosolic
poa	heavy	heavy	heavy
vsl	heavy	heavy	heavy
ddd	light	heavy	medium
dd	light	absent	light
tpp	heavy	heavy	heavy
atn	heavy	heavy	medium
ah	light	heavy	heavy
dp	medium	medium	medium
vp	light	heavy	medium
pag	medium	light	medium

Table 3.6: Receptor density categories of each brain area based on Munchrath and Hofmann (2010).

Experiment	Dataset	Cluster 1	Cluster 2	Cluster 3	Cluster 4	Cluster 5
Flutamide	COX	dc2, dm1, dc1, dld1, dlg1, dlg2, dlv1, dc4, dc5	vsl, dm3, vsm	dp, vp	dlv2, vc	NA
	<i>egr-1</i>	dc4, dc5	dm3, dlg2, dlg1, dm2c, vdc	nt, vsm, dp, vp, dd, poa	dm2r, vdr, vsl, vv	NA
Fadrozole	COX	dm2r, dm1, dc1, vdr, dlv2, vv	dc4, vl, dm2c, vdc	dm3, vp, dp, dd, poa, nt, vsm, dc5, dlg2	NA	NA
	<i>egr-1</i>	dc2, dlg1, dc4, dlv2, vc	dm2c, vdc, dd, dm3	nt, ddd,vsl,p oa,vsm	dm2r,vdr, vv	dc1,vl

Table 3.7: Significant clusters of correlated brain areas identified by multiscale bootstrapping of the correlation matrix. Clusters were ordered to highlight similarities across datasets.

Matrix A	Matrix B	Observed Correlation	Simulated p-value
FLUT - COX	FAD - COX	0.206	0.0017
FLUT - COX	FLUT - <i>egr-1</i>	0.244	0.0004
FLUT - COX	FAD - <i>egr-1</i>	0.207	0.0008
FAD - COX	FLUT - <i>egr-1</i>	0.234	0.0008
FAD - COX	FAD - <i>egr-1</i>	0.196	0.0016
FLUT - <i>egr-1</i>	FAD - <i>egr-1</i>	0.265	0.0004

Table 3.8: Mantel test results for each covariance matrix comparison.

Conclusion:

A. burtoni represents a powerful model for studying how the SDMN generates socially regulated behavioral phenotypes and the emergent properties of complex social groups. In chapter 1, I examined the effects of social context using a social network approach to look at direct and indirect peer effects and community effects on hormones and behavior. In chapter 2, I examined brain activity patterns, hormones and behavior of stable DOM and SUB males from naturalistic community settings and also ascending males, which were given an opportunity to transition to DOM status in a more reduced setting. In chapter 3, I utilized the same social opportunity paradigm and gave the focal animals either an androgen receptor antagonist to block nuclear androgen signaling or an aromatase inhibitor to reduce estradiol production. The main findings of each chapter are summarized below.

CHAPTER 1: *A. BURTONI* SOCIAL INTERACTION NETWORKS

I examined 8 replicate communities of *A. burtoni* and looked at the effects of social network position. I found that DOM *A. burtoni* males form the hubs of the network and that social interactions are strongly correlated across time. Furthermore, I found that individuals can have direct and indirect effects on their social partners. For example, among DOM males, receiving aggression from other DOMs is correlated to increased courtship and decreased aggression towards SUB males. This is an example of a direct effect since the amount of aggression received by an individual correlates to the behavior they display toward others. I also found evidence of indirect effects, these are correlations that aren't explained by direct interactions between individuals. For example, among SUB males, total aggression is correlated to the amount of aggression directed from DOM males towards females in the community. This effect is not explained by direct interactions between

DOMs and SUBs. There were also indirect effects on hormones, for example increased connections between DOMs correlated to lower testosterone in SUB males. Finally, there were strong community effects on hormones. This is perhaps the most important aspect of the study since the full extent of this community effect has not been studied before. Both testosterone and cortisol have been measured many times in this species and there is a well-known effect of social status on these hormones. However, with complete sampling of communities it becomes clear that the community effect is equally important. In terms of the variance in hormone levels that each explains, in both the testosterone and cortisol data the status and community effects are nearly equal and in both cases the community effect is actually slightly more important than the much more widely studied effect of status. In the testosterone data for example, the residual sum of squares is 123.60 with a model that only includes the community effect and 131.29 with a model that only includes the status effect. We found that the community effect in the testosterone data could be explained by the stability of the social network, with stable communities having a strong difference between DOM and SUB males. The community effect on cortisol was not explained by stability or any other community level property that we measured. Future work could measure more properties of the community and manipulative experiments could help to hone in on the drivers of correlated cortisol levels within a community. For example, it may have something to do with the environment of the tank itself such as the position within the aquarium facility or light levels among many other environmental and social factors.

This chapter establishes *A. burtoni* as a tractable model for studying complex community dynamics and the neurobiology of social cognition in a naturalistic community. All of the associations described in the chapter are purely correlational, therefore manipulative experiments will be needed in the future to determine which of the

relationships are casual and which are correlated due to other latent factors. Possible future directions include social engineering experiments where a male is removed from the community or drug manipulation experiments where a particular male could be manipulated to increase or decrease aggressive output.

CHAPTER 2: BRAIN ACTIVITY PATTERNS IN DOM, SUB AND ASCENDING MALES.

I examined DOM and SUB males from communities as well as ascending males. I designed a novel enclosure that allows for controlled social ascension and has many advantages over previous designs. It allows for males to be subordinated in the enclosure for at least 9 days and allows for the presentation of a stimulus male to a SUB or ascending animals. I found that the paradigm allowed for robust transition from SUB to DOM status when males were given a social opportunity. I found expected trends of increases in growth rate, gonad size, testosterone and estradiol levels. I measured COX across the forebrain of the stable and ascending animals. This is the first study to comprehensively map COX levels in a teleost fish. As part of that process I discovered a new parcellation of the dorsal lateral telencephalon dl₂. Dlg₂ stains much lighter in cytochrome oxidase and has a distinct cytoarchitecture. Dlg is a hypertrophied region of the dorsal part of dl that is unique to the cichlid lineage. Hypertrophy of dl is found in other species such as the squirrel fish and the electric fish, and has been proposed to be a visual specialization, although it probably has a different role in the electric fish and may be related to elaborated hippocampal circuitry (Elliott et al. 2017; Demski 2013; Burmeister, Munshi, and Fernald 2009). The lower levels of cytochrome oxidase in dl₂ indicate a different organization of the neuropil in that region, future studies should address the connectivity profile of the neurons in each dl₂ parcellation which may explain this difference and may shed light on the function and evolution of teleost pallial circuitry.

There was an effect of social status on COX patterns, which was stronger in the comparison between stable DOM and SUB males than it was in the comparison between ascending and control males. This may reflect the different timing of the two experiments, in the community experiment males were in the same social status for over 40 days, whereas ascending males were only DOM for 7 days. I did not find any status effect on the *egr-1* levels, which is consistent with the fact that both SUB and ascending males had the same reaction to the intruder stimulus. Interestingly in SUB males the intruder response was not correlated to circulating hormone levels the way that it was in ascending males in both chapters 2 and 3. This indicates that SUB male responses may be less tied to circulating hormones, similar to the situation in seasonal birds where non-breeding season aggression is regulated by different mechanisms, and not tied to circulating steroid hormones the way it is during the breeding season (Wingfield and Hahn 1994; Soma et al. 2008). Future studies could address the neural mechanisms of SUB male aggression using my enclosure design and treating the SUB and ascending males with various receptor antagonists prior to stimulus exposure.

CHAPTER 3: PERTURBING ANDROGEN AND ESTROGEN SIGNALING DURING SOCIAL ASCENSION

To test the role of androgen and estrogen signaling in social ascension, I treated ascending males with either flutamide, which is an androgen receptor antagonist, or fadrozole, which is an aromatase inhibitor and thus blocks the conversion of androgens to estrogens. I found that neither inhibited the behaviors associated with social ascension. This suggests that the sharp increase of steroid hormones associated with transition are not directly tied to the behavioral changes, although androgen signaling not tied to the nuclear androgen receptor was not affected by these treatments. Future studies could address this by treating ascending animals with drugs that block the production of androgen, either by

blocking the gonadotropins, inhibiting the enzymes necessary for androgen production or castration, with or without estrogen implants.

Fadrozole treatment drastically affected hormone levels, as expected based on previous studies in this species (Huffman, O'Connell, and Hofmann 2013). I found that in ascending males FAD treatment results in increased aggression. This was not expected because previous studies on DOM males indicated a positive correlation between estrogen signaling and aggression, so we would have expected a decrease in aggression with FAD treatment. This finding establishes *A. burtoni* as a unique and powerful model for understanding the impact of estrogen on male aggression. Across vertebrates, male aggression is usually positively associated with estrogen signaling as it is in DOM male *A. burtoni*. However, in some species the opposite association is found. The neural mechanism behind this difference is not understood and studies have been hampered by the difficulties of comparing across species and the developmental side-effects of using transgenic knockout animals (Trainor, Kyomen, and Marler 2006). *A. burtoni* is the only species yet reported that shows either a positive or negative correlation between aggression and estrogen signaling depending on social status. Future studies can be conducted to uncover the differences between the ascending male's brain and the DOM male brain that cause this opposite reaction to FAD treatment and whether DOM/SUB males of other unrelated species also show this pattern with FAD treatment. We identified a candidate brain region that such a study could target, VL. VL is the putative partial homolog to the subpallial portion of the lateral septum. The lateral septum has been identified in mice to be the area most affected by FAD treatment in relation to IEG induction in aggressive encounters (Trainor, Greiwe, and Nelson 2006). Based on this I hypothesize that inhibitory input from the VL is modulated by estrogen signaling and results in altered aggressive drive, possibly through GABAergic inputs to the ATN (Falkner et al. 2016; Wong et al. 2016; Falkner et

al. 2014). Consistent with this we found a fairly strong trend of FAD treatment lowering activity in VL and a strong correlation between intruder directed aggression and *egr-1* levels in VL. Future studies could follow up on these results by comparing COX levels in the VL of DOM, SUB and ascending males treated with FAD or not. It would be interesting to see if the VL response of DOM males is the same or opposite of ascending males.

THE NEUROMODULATORY PATTERNING HYPOTHESIS AND ALTERNATIVE FRAMEWORKS

In order to address the neuromodulatory patterning hypothesis I looked at pairwise correlations of COX or *egr-1* levels between each brain area. I hypothesized that if functional connectivity is the primary factor that shapes the differences between DOM and SUB behavioral phenotypes, then I would find strong differences in the correlation patterns. Furthermore, I hypothesized that steroid hormones would be at least part of the driving force behind the patterning effect based on studies showing the effects of steroid hormones on behavior, the strong link between social status and steroid hormones and studies showing that steroids can change the neural representation of a stimulus as reflected by IEG induction. Therefore, I hypothesized that perturbing the steroid hormone pathways with flutamide and fadrozole would cause a change to status specific covariance patterns. My permutation analyses did not show a treatment effect on the correlation patterns, at least not one which was detectable above differences that could be due to random sampling effects. While this would seem to argue against the neuromodulatory patterning hypothesis, estimating covariance networks is a difficult statistical problem especially when a large number of variables are measured on a small number of individuals, as is the case in many biological datasets, because the number of parameters grows quadratically with the number of variables. My studies may be underpowered and over-described for this type of analysis and I may not be able to detect a strong patterning effect because of that. Future studies

could improve the situation by utilizing high throughput mapping technologies such as tissue clearing technologies paired with lightsheet microscopy to increase the number of brains included and the quality of the data (Ye et al. 2016). There are also alternative frameworks which I will discuss below.

One alternative theory is that sub-circuits within brain areas, rather than whole nuclei are more relevant to behavioral phenotypes. In a ground breaking study utilizing tissue clearing technology, (Ye et al. 2016) exposed mice to either an adverse (footshock) or rewarding (cocaine) experience. They examined immediate early gene induction in 7 limbic and cortical areas and found that in almost all brain areas the same amount of cells were activated in these two very different experiences. Further experiments revealed that cell populations with distinct molecular and wiring characteristics were recruited in each type of experience and that selectively activating these populations had different impacts on behavior. Future studies could utilize similar technologies within the fish brain to map not only immediate early genes but also molecular markers of cell types to get a better understanding of the impacts of social status on the activity of circuits within particular brain areas.

Another alternative framework is to examine these studies in light of the findings in human functional magnetic resonance imaging (fMRI). fMRI is a technology that can measure brain activity in living human subjects by tracking blood oxygen levels. fMRI studies of various cognitive tasks have revealed correlated networks of brain activity responsible for motivation, attention and task performance (task-FC; Hutchison et al. 2013). Brain area activity correlations persist even when people are not performing a particular task, known as resting state functional connectivity (rs-FC; Guerra-Carrillo, Mackey, and Bunge 2014; Hutchison et al. 2013). In studies of healthy subjects, these correlation patterns are largely consistent across experiments and individuals. Some of

these correlations reflect structural connections but there is also robust rs-FC between brain areas that are not directly connected. Many of the patterns of rs-FC represent known functional pathways (Guerra-Carrillo, Mackey, and Bunge 2014). For example, rs-FC has been observed in the somatomotor pathway and visual network (Guerra-Carrillo, Mackey, and Bunge 2014). The strength of correlations within and between resting state networks is predictive of task performance (Baldassarre et al. 2012; Cole et al. 2012). For example, visual discrimination ability is predicted by the rs-FC of the visual network (Baldassarre et al. 2012). Moreover, training specific tasks increases rs-FC of the relevant networks (Powers, Hevey, and Wallace 2012; Klingner et al. 2013; Vahdat et al. 2011; Ma et al. 2011). It is thought that rs-FC reflects patterns of repeated co-activation which results in strengthening of synapses in those pathways (Hutchison et al. 2013). In some ways rs-FC may be similar to functional connectivity of COX, whereas task-FC may be similar to *egr-1*. COX changes slowly and functional connectivity between brain areas would reflect a history of repeated co-activation between brain areas similar to rs-FC. Task-FC is remodeled as the different brain areas are engaged in attention, motivation and task performance. This may be analogous to the IEG signal which responds to the stimulus more or less in real time. Based on what happens in rs-FC after training, I hypothesize that there would be increased correlations between brain areas recruited in training of a task when measured by cytochrome oxidase after learning has occurred. Future studies could test this by training animals to a particular task and measuring IEG induction and COX prior to learning and after learning has occurred. I hypothesize that the IEG response to early training (prior to learning) will predict changes in to the functional connectivity networks measured by COX. To my knowledge such a study has not yet been conducted. Given that I found some consistent correlations across various datasets, these could be related to functional networks that have a strong likelihood of co-activation both in IEG responses

and COX. Consistent with the interpretation that the COX signal is similar to rs-FC, and the *egr-1* signal is similar to task-FC, a larger effect of social status on COX than on *egr-1* would be expected because changes associated with social status represent a long-term condition, whereas the same brain areas may be activated regardless of social status in response to a stimulus. This directly conflicts with the neuromodulatory patterning hypothesis, which predicts that neural representation of the stimulus in the limbic system would vary depending on behavioral phenotype. While not conclusive, my data are more consistent with the interpretation that the COX signal is similar to rs-FC, and the *egr-1* signal is similar to task-FC, rather than the predictions of the neuromodulatory patterning hypothesis.

FROM SOCIAL CONTEXT TO NEUROMODULATORY PATTERNING: LINKS ACROSS THE STUDIES

My studies show that community dynamics, internal hormonal signaling and individual behavior form an integrated system. A conceptual diagram linking connections between the studies is shown in figure 1. Group level properties are correlated to the behavior and hormone levels of individuals. The interactions that an individual receives from other group members is correlated to the behavior that they direct towards others. Furthermore, third party interactions in the community are correlated to individual behavior and hormones as well. We refer to these as direct and indirect peer effects respectively. The outcome of these peer and community effects can depend on the social status of the individual. For example, stable networks are associated with higher testosterone and DOM males and lower in SUB males. Social status is strongly associated with differences in steroid hormone levels, and these hormones surge during social ascension. I hypothesized that blocking estrogen or androgen signaling would have an impact on social ascension and brain activity patterns associated with status. Perturbing

these hormonal pathways did not block social ascension, however blocking estrogen signaling caused males to become hyperaggressive. This hyperaggressive phenotype depends on social status, presumably because of status dependent changes in neural network activity or steroid hormone sensitivity. Future experiments could utilize this type of manipulation to directly test the link between individual behavior and social network properties. By manipulating the behavior of an individual, making a DOM male less aggressive or an intermediate or ascending male more aggressive, I would expect to see cascading effects on the behavior and hormones of the other individuals as well as effects on group properties.

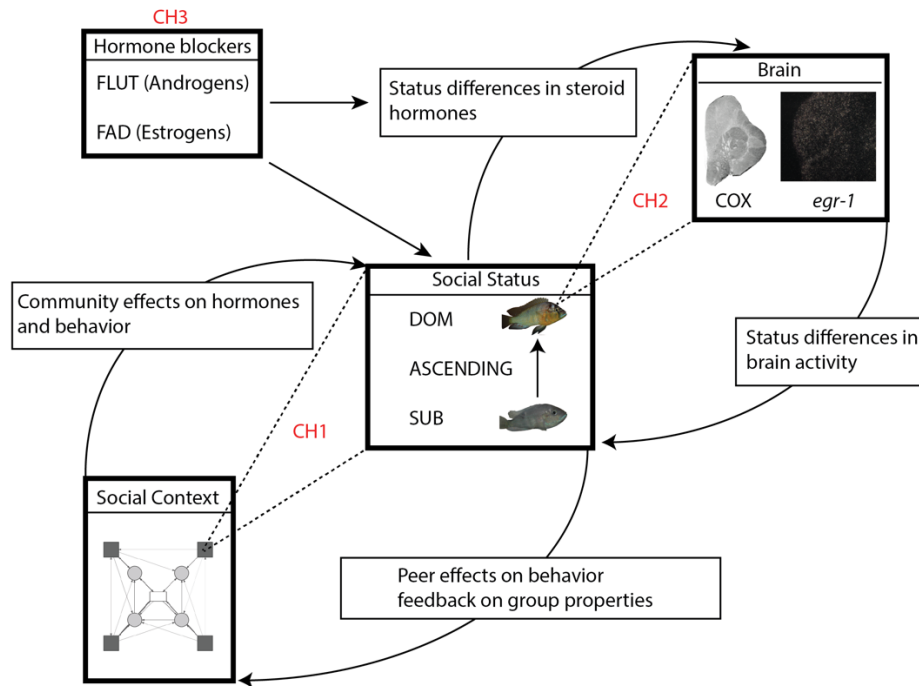
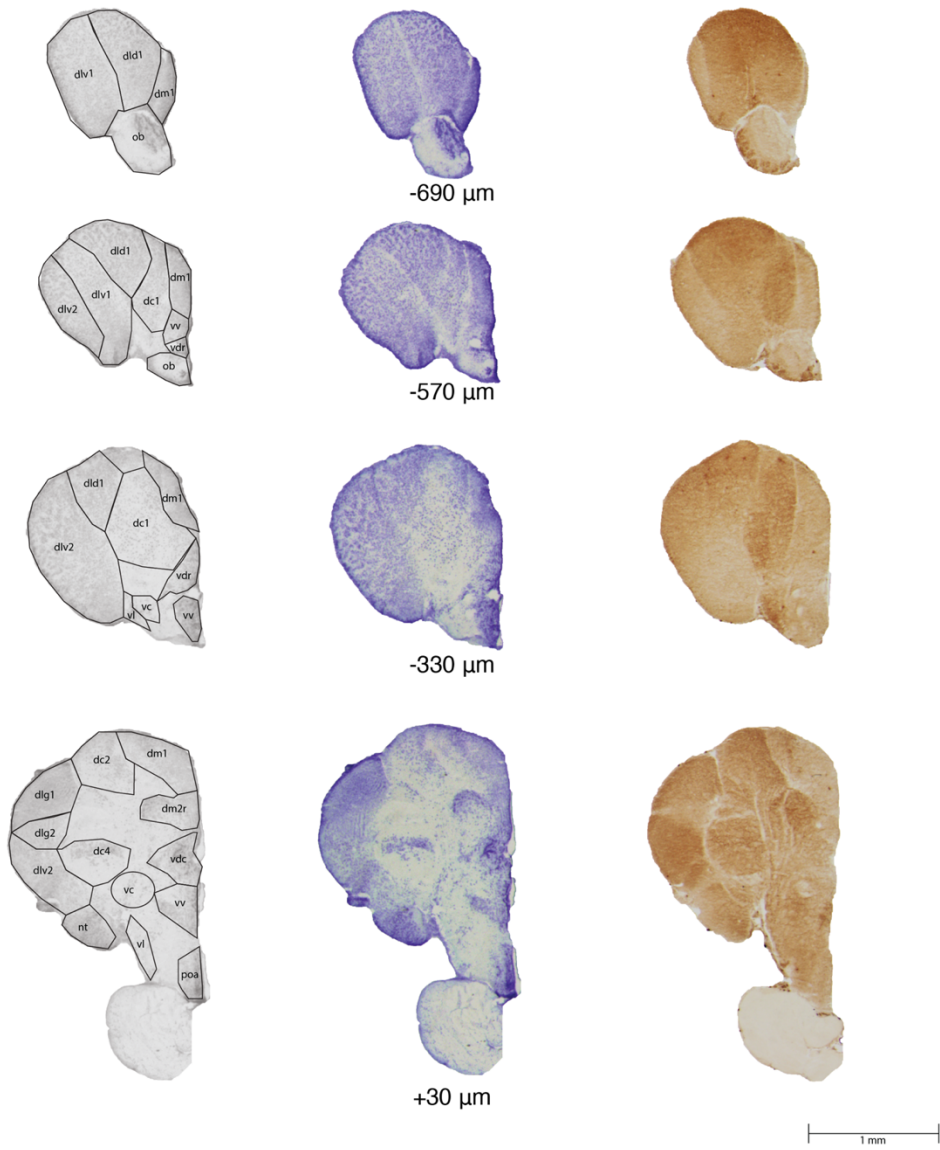
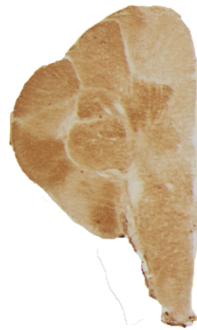
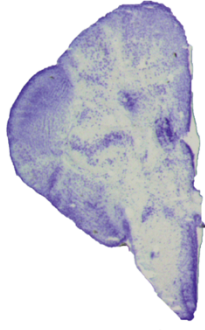
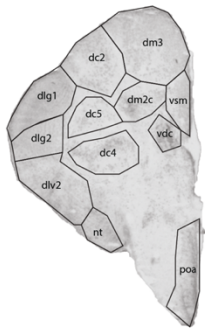


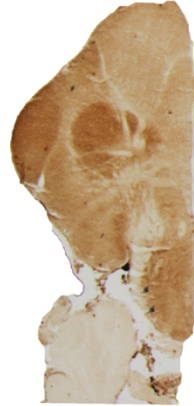
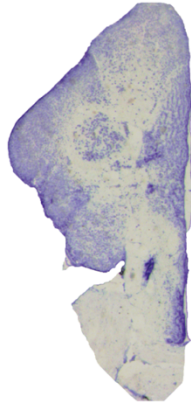
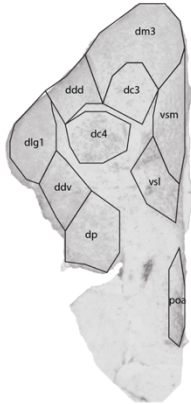
Figure 4.1: Conceptual diagram illustrating possible links between the three chapters. Social context (chapter 1) has effects on hormones as well as behavior of individuals and those effects depend on social status. Social status is linked to differences in brain activity and steroid hormone levels. Blocking the nuclear androgen pathway with flutamide or estrogen signaling with fadrozole did not block social ascension. It did however have effects on circulating hormones but only weakly effected brain activity patterns. The effect of fadrozole depended on social status. All of these processes form an integrated system, whereby changes in the brain activity networks, hormones and behavior of an individual can feedback on group properties and group properties can affect individual's hormone levels and behavior.

Appendix A: Cytochrome Oxidase Atlas

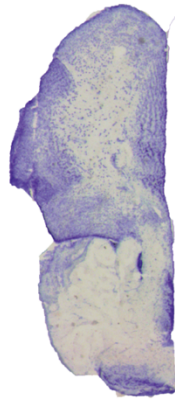
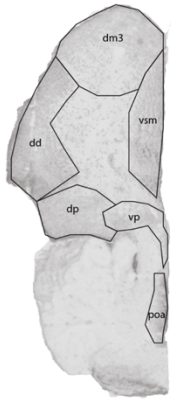




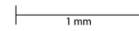
+150 μ m

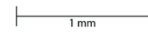
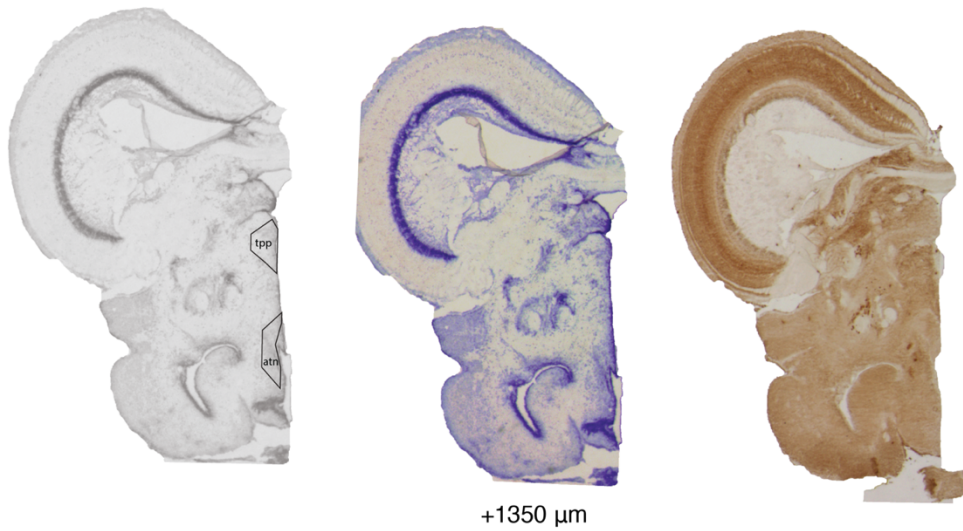
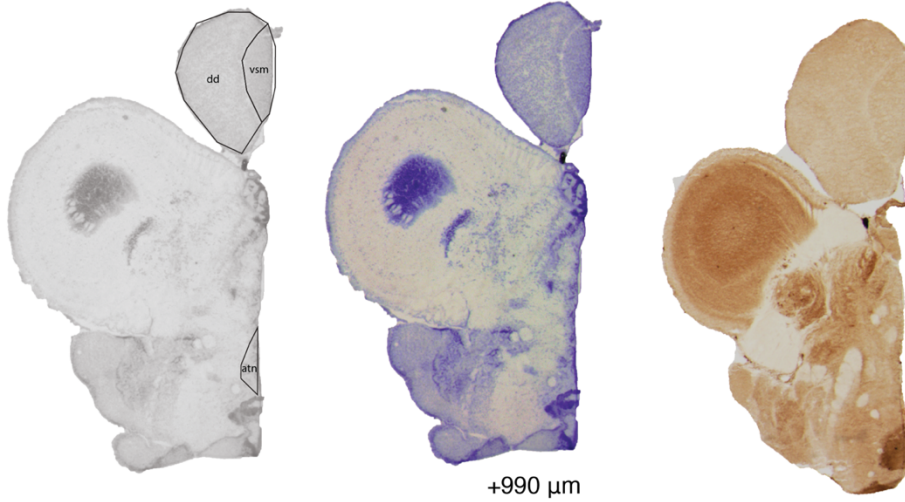


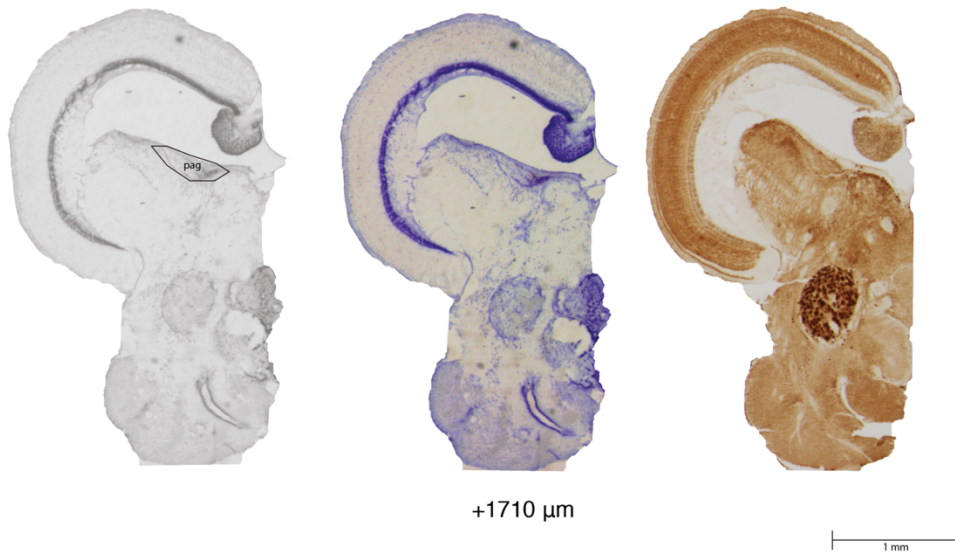
+390 μ m



+510 μ m







Appendix A: COX brain atlas. Coordinates are measured based on their distance in relation to location of the anterior commissure (AC), with negative coordinates rostral to the AC and positive coordinates caudal to the AC. Left hand sections are a schematic showing outlines of the brain areas, center sections show the Nissl stained cell bodies and right hand sections show an alternative section of the same brain stained for COX.

References

- Afonso, L.O., G.K. Iwama, J. Smith, and E.M. Donaldson. 1999. "Effects of the Aromatase Inhibitor Fadrozole on Plasma Sex Steroid Secretion and Ovulation Rate in Female Coho Salmon, *Oncorhynchus Kisutch*, close to Final Maturation." *General and Comparative Endocrinology* 113 (2): 221–29. doi:10.1006/gcen.1998.7198.
- Albert, D. J., and G. L. Chew. 1980. "The Septal Forebrain and the Inhibitory Modulation of Attack and Defense in the Rat. A Review." *Behavioral and Neural Biology*. doi:10.1016/S0163-1047(80)91247-9.
- Ankley, G.T., M.D. Kahl, K.M. Jensen, M.W. Hornung, J. J. Korte, E.A. Makynen, and R.L. Leino. 2002. "Evaluation of the Aromatase Inhibitor Fadrozole in a Short-Term Reproduction Assay with the Fathead Minnow (*Pimephales Promelas*)." *Toxicological Sciences* 67 (1): 121–30. doi:10.1093/toxsci/67.1.121.
- Aplin, L.M., D.R. Farine, R.P. Mann, and B.C. Sheldon. 2014. "Individual-Level Personality Influences Social Foraging and Collective Behaviour in Wild Birds." *Proc. Roc. Soc. B.* 281 (July): 20141016. doi:10.1098/rspb.2014.1016.
- Aranda, P.S., D.M. LaJoie, and C.L. Jorcyk. 2012. "Bleach Gel: A Simple Agarose Gel for Analyzing RNA Quality." *Electrophoresis* 33 (2): 366–69. doi:10.1002/elps.201100335.Bleach.
- Arnold, A.P. 2009. "The Organizational-Activational Hypothesis as the Foundation for a Unified Theory of Sexual Differentiation of All Mammalian Tissues." *Hormones and Behavior* 55 (5): 570–78. doi:10.1016/j.yhbeh.2009.03.011.
- Baldassarre, A., C.M. Lewis, G. Comitteri, A.Z. Snyder, G.L. Romani, and M. Corbetta. 2012. "Individual Variability in Functional Connectivity Predicts Performance of a Perceptual Task." *PNAS* 109 (9): 3516–21. doi:10.1073/pnas.1113148109.
- Balthazart, J., M. Baillien, C.A. Cornil, and G.F. Ball. 2004. "Preoptic Aromatase Modulates Male Sexual Behavior: Slow and Fast Mechanisms of Action." *Physiology and Behavior*. doi:10.1016/j.physbeh.2004.08.025.
- Barrett, L., S.P. Henzi, and D. Lusseau. 2012. "Taking Sociality Seriously: The Structure of Multi-Dimensional Social Networks as a Source of Information for Individuals." *Phil. Trans. Roc. Soc. B.* 367 (1599): 2108–18. doi:10.1098/rstb.2012.0113.
- Bates, Douglas, M. Mächler, B.M. Bolker, and S. C. Walker. 2015. "Fitting Linear Mixed-Effects Models Using lme4." *Journal of Statistical Software* 67 (1): 1–48. doi:10.18637/jss.v067.i01.
- Beach, F.A. 1983. "Daniel Berlyne Memorial Lecture. Hormones and Psychological Processes." *Canadian Journal of Psychology* 37 (2): 193–210.

- Beletsky, L.D., G.H. Orians, and J.C. Wingfield. 1990. "Effects of Exogenous Androgen and Antiandrogen on Territorial and Nonterritorial Red-winged Blackbirds (Aves: Icterinae)." *Ethology* 85 (1): 58–72. doi:10.1111/j.1439-0310.1990.tb00386.x.
- Black, M.P, J. Balthazart, M. Baillien, M.S. Grober. 2005. "Socially Induced and Rapid Increases in Aggression Are Inversely Related to Brain Aromatase Activity in a Sex-Changing Fish, *Lythrypnus Dalli*." *Proc. Roc. Soc. B.* 272 (1579): 2435–40. doi:10.1098/rspb.2005.3210.
- Bradski, G. 2000. "The OpenCV Library." *Dr Dobbs Journal of Software Tools* 25: 120–25. doi:10.1111/0023-8333.50.s1.10.
- Bressler, S.L., and A.R. Mcintosh. 2007. "The Role of Neural Context in Large-Scale Neurocognitive Network Operations." *Understanding Complex Systems* 2007: 403–19. doi:10.1007/978-3-540-71512-2_14.
- Burmeister, S.S., E.D. Jarvis, and R.D. Fernald. 2005. "Rapid Behavioral and Genomic Responses to Social Opportunity." *PLoS Biology* 3 (11): 1996–2004. doi:10.1371/journal.pbio.0030363.
- Burmeister, S.S., V. Kailasanath, and R.D. Fernald. 2007. "Social Dominance Regulates Androgen and Estrogen Receptor Gene Expression." *Hormones and Behavior* 51 (1): 164–70. doi:10.1016/j.yhbeh.2006.09.008.
- Burmeister, S.S., R.G. Munshi, and R.D. Fernald. 2009. "Cytoarchitecture of a Cichlid Fish Telencephalon." *Brain, Behavior and Evolution* 74 (2): 110–20. doi:10.1159/000235613.
- Butts, C.T. 2014. *Sna: Tools for Social Network Analysis. R Package Version 2-3.2.* <http://cran.r-project.org/package=sna>.
- Canoine, V., and Eberhard Gwinner. 2002. "Seasonal Differences in the Hormonal Control of Territorial Aggression in Free-Living European Stonechats." *Hormones and Behavior* 41 (1): 1–8. doi:10.1006/hbeh.2001.1720.
- Chase, I.D., and K. Seitz. 2011. "Self-Structuring Properties of Dominance Hierarchies. A New Perspective." *Advances in Genetics* 75: 51–81. doi:10.1016/B978-0-12-380858-5.00001-0.
- Chen, C., K. Wada, and E.D. Jarvis. 2012. "Radioactive *in situ* Hybridization for Detecting Diverse Gene Expression Patterns in Tissue." *Journal of Visualized Experiments*, no. 62: 1–7. doi:10.3791/3764.
- Christakis, N.A., and Fowler, J.H. 2008. "The Collective Dynamics of Smoking in a Large Social Network." *New England Journal of Medicine* 358 (21): 2249–58. doi:10.1056/NEJMsa0706154.
- Christakis, N.A., and J.H. Fowler. 2007. "The Spread of Obesity in a Large Social Network over 32 Years." *The New England Journal of Medicine* 357 (4): 370–79. doi:10.1056/NEJMsa066082.

- Clutton-Brock, T.H., and P.H. Harvey. 1977. "Primate Ecology and Social Organization." *Journal of Zoology* 183: 1–39. <http://dx.doi.org/10.1111/j.1469-7998.1977.tb04171.x>.
- Cole, M.W., T. Yarkoni, G. Repovš, A. Anticevic, and T.S. Braver. 2012. "Global Connectivity of Prefrontal Cortex Predicts Cognitive Control and Intelligence." *The Journal of Neuroscience* 32 (26): 8988–99. doi:10.1523/JNEUROSCI.0536-12.2012.
- Craft, M.E., E. Volz, C. Packer, and L.A. Meyers. 2011. "Disease Transmission in Territorial Populations: The Small-World Network of Serengeti Lions." *Journal of the Royal Society, Interface* 8 (59): 776–86. doi:10.1098/rsif.2010.0511.
- Crews, D. 2003. "The Development of Phenotypic Plasticity: Where Biology and Psychology Meet." *Developmental Psychobiology*. 43 (1):1-10. doi:10.1002/dev.10115.
- Croft, D.P., J. Krause, and R. James. 2004. "Social Networks in the Guppy (*Poecilia Reticulata*)." *Proc. Roc. Soc. B.* 271 Suppl: S516–19. doi:10.1098/rsbl.2004.0206.
- Csárdi, G., and T. Nepusz. 2006. "The Igraph Software Package for Complex Network Research." *InterJournal Complex Systems*. 1695. <http://igraph.org>.
- Davis, M., and P.J. Whalen. 2001. "The Amygdala: Vigilance and Emotion." *Molecular Psychiatry* 6 (1): 13–34. doi:10.1038/sj.mp.4000812.
- Demski, L.S. 2013. "The Pallium and Mind/behavior Relationships in Teleost Fishes." *Brain, Behavior and Evolution* 82 (1): 31–44. doi:10.1159/000351994.
- Demski, L.S., and K.M. Knigge. 1971. "The Telencephalon and Hypothalamus of the Bluegill (*Lepomis Macrochirus*): Evoked Feeding, Aggressive and Reproductive Behavior with Representative Frontal Sections." *The Journal of Comparative Neurology* 143 (1):1–16. doi:10.1002/cne.901430102.
- Desjardins, J.K., H.A. Hofmann, and R.D. Fernald. 2012. "Social Context Influences Aggressive and Courtship Behavior in a Cichlid Fish." *PLoS ONE* 7 (7). doi:10.1371/journal.pone.0032781.
- Dijkstra, P.D., S.M. Maguire, R.M. Harris, A.A. Rodriguez, R.S. DeAngelis, S.A. Flores, and H.A. Hofmann. 2017. "The melanocortin system regulates body pigmentation and social behaviour in a colour polymorphic cichlid fish." *Proc. Roc. Soc. B.* 284 (1851). doi:10.1098/rspb.2016.2838
- Dray, S., and A.B. Dufour. 2007. "The ade4 Package: Implementing the Duality Diagram for Ecologists." *Journal of Statistical Software* 22 (4): 1–20. doi:10.1.1.177.8850.
- Elliott, S.B., E. Harvey-Girard, A.C.C. Giassi, and L. Maler. 2017. "Hippocampal-like Circuitry in the Pallium of an Electric Fish: Possible Substrates for Recursive Pattern Separation and Completion." *Journal of Comparative Neurology* 525 (1): 8–46. doi:10.1002/cne.24060.

- Elston, D.A., R. Moss, T. Boulinier, C. Arrowsmith, and X. Lambin. 2001. "Analysis of Aggregation, a Worked Example: Numbers of Ticks on Red Grouse Chicks." *Parasitology* 122 (5): 563–69. doi:10.1017/S0031182001007740.
- Ervin, K.S., J.M. Lymer, R. Matta, A.E. Clipperton-Allen, M. Kavaliers, and E. Choleris. 2015. "Estrogen Involvement in Social Behavior in Rodents: Rapid and Long-Term Actions." *Hormones and Behavior* (74): 53-76. doi:10.1016/j.yhbeh.2015.05.023.
- Falkner, A.L., P. Dollar, P. Perona, D.J. Anderson, and D. Lin. 2014. "Decoding Ventromedial Hypothalamic Neural Activity during Male Mouse Aggression." *The Journal of Neuroscience* 34 (17): 5971–84. doi:10.1523/JNEUROSCI.5109-13.2014.
- Falkner, A.L., L. Grosenick, T.J. Davidson, K. Deisseroth, and D. Lin. 2016. "Hypothalamic Control of Male Aggression-Seeking Behavior." *Nature Neuroscience* 19 (4): 596–604. doi:10.1038/nn.4264.
- Fernald, R.D., and N.R. Hirata. 1977. "Field Study Of Haplochromis-Burtoni Quantitative Behavioral Observations." *Animal Behaviour* 25: 964–75.
- Fernald, R.D., and N.R. Hirata. 1977. "Field Study of Haplochromis Burtoni: Habitats and Co-Habitant." *Environmental Biology of Fishes* 2 (3): 299–308. doi:10.1007/BF00005997.
- Flack, J.C., M. Girvan, F.B. de Waal, and D.C. Krakauer. 2006. "Policing Stabilizes Construction of Social Niches in Primates." *Nature* 439 (7075): 426–29. doi:10.1038/nature04326.
- Fontanini, A., and D.B. Katz. 2008. "Behavioral States, Network States, and Sensory Response Variability." *J. Neurophysiol.* 100 (3): 1160–68. doi:10.1152/jn.90592.2008.
- Foradori, C.D., M.J. Weiser, and R.J. Handa. 2008. "Non-Genomic Actions of Androgens." *Frontiers in Neuroendocrinology.* 29(2):169-81 doi:10.1016/j.yfrne.2007.10.005.
- Forlano, P.M., B.A. Schlinger, and A.H. Bass. 2006. "Brain Aromatase: New Lessons from Non-Mammalian Model Systems." *Frontiers in Neuroendocrinology* 27 (3): 247–74. doi:10.1016/j.yfrne.2006.05.002.
- Fouse, A., N. Weibel, E. Hutchins, and J.D. Hollan. 2011. "ChronoViz: A System for Supporting Navigation of Time-Coded Data." In *CHI'11 Extended Abstracts on Human Factors in Computing Systems*, 299–304.
- Fox, H.E., S.A. White, M.H. Kao, and R.D. Fernald. 1997. "Stress and Dominance in a Social Fish." *The Journal of Neuroscience* 17 (16): 6463–69.
- Fox, J., and S. Weisberg. 2011. *An R Companion to Applied Regression*. Second. Thousand Oaks CA: Sage. <http://socserv.socsci.mcmaster.ca/jfox/Books/Companion>.

- Friston, K.J. 2011. "Functional and Effective Connectivity: A Review." *Brain Connectivity* 1 (1): 13–36. doi:10.1089/brain.2011.0008.
- Gillebert, C.R., and D. Mantini. 2013. "Functional Connectivity in the Normal and Injured Brain." *The Neuroscientist : A Review Journal Bringing Neurobiology, Neurology and Psychiatry* 19 (5): 509–22. doi:10.1177/1073858412463168.
- Godfrey, S.S., J.A. Moore, N.J. Nelson, and C. M. Bull. 2010. "Social Network Structure and Parasite Infection Patterns in a Territorial Reptile, the Tuatara (*Sphenodon Punctatus*)." *International Journal for Parasitology* 40 (13): 1575–85. doi:10.1016/j.ijpara.2010.06.002.
- Gonzalez-Lima, F., and M. Garrosa. 1991. "Quantitative Histochemistry of Cytochrome Oxidase in Rat Brain." *Neuroscience Letters* 123 (2): 251–53. doi:10.1016/0304-3940(91)90943-N.
- Goodson, J.L. 2005. "The Vertebrate Social Behavior Network: Evolutionary Themes and Variations." *Hormones and Behavior* 48 (1): 11–22. doi:10.1016/j.yhbeh.2005.02.003.
- Goodson, J.L., and D. Kabelik. 2009. "Dynamic Limbic Networks and Social Diversity in Vertebrates: From Neural Context to Neuromodulatory Patterning." *Frontiers in Neuroendocrinology* 30 (4): 429–41. doi:10.1016/j.yfrne.2009.05.007.
- Goodson, J.L., A.K. Evans, and K.K. Soma. 2005. "Neural Responses to Aggressive Challenge Correlate with Behavior in Non-Breeding Sparrows." *Neuroreport* 16 (15): 1719–23. doi:10.1016/j.biotechadv.2011.08.021.Secreted.
- Grear, D.A., S.E. Perkins, and P.J. Hudson. 2009. "Does Elevated Testosterone Result in Increased Exposure and Transmission of Parasites?" *Ecology Letters* 12 (6): 528–37. doi:10.1111/j.1461-0248.2009.01306.x.
- Grosenick, L., T.S. Clement, and R.D. Fernald. 2007. "Fish Can Infer Social Rank by Observation Alone." *Nature* 445 (7126): 429–32. doi:10.1038/nature05646.
- Guerra-Carrillo, B., A.P. Mackey, and S.A. Bunge. 2014. "Resting-State fMRI: A Window into Human Brain Plasticity." *Neuroscientist* 20 (5): 522–33. doi:10.1177/1073858414524442.
- Handa, R.J., L.H. Burgess, J.E. Kerr, and J.A. O'Keefe. 1994. "Gonadal Steroid Hormone Receptors and Sex Differences in the Hypothalamo-Pituitary-Adrenal Axis." *Hormones and Behavior* 35 (2): 197-220. doi:10.1006/hbeh.1994.1044.
- Hasen, N.S., and S.C. Gammie. 2005. "Differential Fos Activation in Virgin and Lactating Mice in Response to an Intruder." *Physiology and Behavior* 84 (5): 681–95. doi:10.1016/j.physbeh.2005.02.010.
- Hau, M., and K. Beebe. 2011. "Plastic Endocrine Regulation of Year-Round Territorial Aggression in Tropical Male Spotted Antbirds." *General and Comparative Endocrinology* 172 (2): 305–13. doi:10.1016/j.ygcen.2011.03.016.

- Hau, M., S.T. Stoddard, and K.K. Soma. 2004. "Territorial Aggression and Hormones during the Non-Breeding Season in a Tropical Bird." *Hormones and Behavior* 45 (1): 40–49. doi:10.1016/j.yhbeh.2003.08.002.
- Hegner, R.E., and J.C. Wingfield. 1987. "Effects of Experimental Manipulation of Testosterone Levels on Parental Investment and Breeding Success in Male House Sparrows." *The Auk* 104 (3): 462–69. doi:10.2307/4087545.
- Hellman, L., H. L. Bradlow, S. Freed, J. Levin, R. S. Rosenfeld, W. F. Whitmore, and B. Zumoff. 1977. "The Effect of Flutamide on Testosterone Metabolism and the Plasma Levels of Androgens and Gonadotropins." *Journal of Clinical Endocrinology and Metabolism* 45 (6): 1224–29. doi:10.1210/jcem-45-6-1224.
- Herbert, A.D., A.M. Carr, E. Hoffmann, and M. Lichten. 2014. "FindFoci: A Focus Detection Algorithm with Automated Parameter Training That Closely Matches Human Assignments, Reduces Human Inconsistencies and Increases Speed of Analysis." *PLoS ONE* 9 (12): 1–33. doi:10.1371/journal.pone.0114749.
- Hesselmann, G., C.A. Kell, E. Eger, and A. Kleinschmidt. 2008. "Spontaneous Local Variations in Ongoing Neural Activity Bias Perceptual Decisions." *PNAS* 105 (31): 10984–89. doi:10.1073/pnas.0712043105.
- Hevner, R.F. 1998. "Cytochrome Oxidase and Neuroanatomical Patterns: What Is the Connection?" In *Cytochrome Oxidase in Neuronal Metabolism and Alzheimer's Disease*, 91–108. New York: Plenum Press.
- Hirschenhauser, K., M. Taborsky, T. Oliveira, A.V.M. Canário, and R. F. Oliveira. 2004. "A Test of the 'Challenge Hypothesis' in Cichlid Fish: Simulated Partner and Territory Intruder Experiments." *Animal Behaviour* 68 (4): 741–50. doi:10.1016/j.anbehav.2003.12.015.
- Hirschenhauser, K., and R.F. Oliveira. 2006. "Social Modulation of Androgens in Male Vertebrates: Meta-Analyses of the Challenge Hypothesis." *Animal Behaviour*. doi:10.1016/j.anbehav.2005.04.014.
- Hobson, E.A., M.L. Avery, and T.F. Wright. 2013. "An Analytical Framework for Quantifying and Testing Patterns of Temporal Dynamics in Social Networks." *Animal Behaviour* 85 (1): 83–96. doi:10.1016/j.anbehav.2012.10.010.
- Hofmann, H.A. 2010. "The Neuroendocrine Action Potential." *Hormones and Behavior* 58 (4): 555–62. doi:10.1016/j.yhbeh.2010.06.012.
- Hofmann, H.A., A.K. Beery, D.T. Blumstein, I.D. Couzin, R.L. Earley, L.D. Hayes, P.L. Hurd, E.A. Lacey, S.M. Phelps, N.G. Solomon, M. Taborsky, L.J. Young, D.R. Rubenstein. 2014. "An Evolutionary Framework for Studying Mechanisms of Social Behavior." *Trends in Ecology and Evolution* 29 (10): 581–589. doi:10.1016/j.tree.2014.07.008.
- Hofmann, H.A., M.E. Benson, and R.D. Fernald. 1999. "Social Status Regulates Growth

- Rate: Consequences for Life-History Strategies.” *PNAS* 96 (24): 14171–76.
doi:10.1073/pnas.96.24.14171.
- Hoke, K.L., S.S. Burmeister, R.D. Fernald, A.S. Rand, M.J. Ryan, and W. Wilczynski. 2004. “Functional Mapping of the Auditory Midbrain during Mate Call Reception.” *Journal of Neuroscience* 24 (50): 11264–72. doi:10.1523/JNEUROSCI.2079-04.2004.
- Hoke, K.L., M.J. Ryan, and W. Wilczynski. 2005. “Social Cues Shift Functional Connectivity in the Hypothalamus.” *PNAS* 102 (30): 10712–17.
doi:10.1073/pnas.0502361102.
- Huffman, L.S., F.I. Hinz, S. Wojcik, N. Aubin-Horth, and H.A. Hofmann. 2015. “Arginine Vasotocin Regulates Social Ascent in the African Cichlid Fish *Astatotilapia Burtoni*.” *General and Comparative Endocrinology* 212: 106–13.
doi:10.1016/j.ygcen.2014.03.004.
- Huffman, L.S., M.M. Mitchell, L.A. O’Connell, and H.A. Hofmann. 2012. “Rising StARs: Behavioral, Hormonal, and Molecular Responses to Social Challenge and Opportunity.” *Hormones and Behavior* 61 (4): 631–41.
doi:10.1016/j.yhbeh.2012.02.016.
- Huffman, L.S., L.A. O’Connell, and H.A. Hofmann. 2013. “Aromatase Regulates Aggression in the African Cichlid Fish *Astatotilapia Burtoni*.” *Physiology and Behavior* 112–113: 77–83. doi:10.1016/j.physbeh.2013.02.004.
- Hutchison, R.M., T. Womelsdorf, E.A. Allen, P.A. Bandettini, V.D. Calhoun, M. Corbetta, S.D. Penna, J.H. Duyn, G.H. Glover, J. Gonzalez-Castillo, D.A. Handwerker, S. Keilholz, V. Kiviniemi, D.A. Leopold, F. de Pasquale, O. Sporns, M. Walter and C. Chang. 2013. “Dynamic Functional Connectivity: Promise, Issues, and Interpretations.” *NeuroImage* 80: 360–78.
doi:10.1016/j.neuroimage.2013.05.079.
- Jacobs, A., and O. Petit. 2011. “Social Network Modeling: A Powerful Tool for the Study of Group Scale Phenomena in Primates.” *American Journal of Primatology*.
doi:10.1002/ajp.20932.
- Jarvis, E.D. 2004. “Learned Birdsong and the Neurobiology of Human Language.” *Annals of the New York Academy of Sciences* 1016: 749–77.
doi:10.1196/annals.1298.038.
- Jensen, K.M., M.D. Kahl, E.A. Makynen, J.J. Korte, R. L. Leino, B.C. Butterworth, and G.T. Ankley. 2004. “Characterization of Responses to the Antiandrogen Flutamide in a Short-Term Reproduction Assay with the Fathead Minnow.” *Aquatic Toxicology* 70 (2): 99–110. doi:10.1016/j.aquatox.2004.06.012.
- Jordan, L.A., S.M. Maguire, H.A. Hofmann, and M. Kohda. 2016. “The Social and Ecological Costs of an ‘over-Extended’ Phenotype.” *Proc. Roc. Soc. B.* 283 (1822): 20152359-. doi:10.1098/rspb.2015.2359.

- Kempenaers, B., A. Peters, and K. Foerster. 2008. "Sources of Individual Variation in Plasma Testosterone Levels." *Philosophical Transactions of the Royal Society of London. Series B, Biological Sciences* 363 (1497): 1711–23.
doi:10.1098/rstb.2007.0001.
- Kidd, C.E., M.R. Kidd, and H.A. Hofmann. 2010. "Measuring Multiple Hormones from a Single Water Sample Using Enzyme Immunoassays." *General and Comparative Endocrinology* 165 (2): 277–85. doi:10.1016/j.ygcen.2009.07.008.
- Klingner, C.M., C. Hasler, S. Brodoehl, H. Axer, and O.W. Witte. 2013. "Perceptual Plasticity Is Mediated by Connectivity Changes of the Medial Thalamic Nucleus." *Human Brain Mapping* 34 (9): 2343–52. doi:10.1002/hbm.22074.
- Krause, J., and G. D. Ruxton. 2002. "Living in Groups." *Living in Groups* I (4): 210.
doi:10.1093/sysbio/sys022.
- Laming, P.R. 1987. "Behavioural Arousal and Its Habituation in the Squirrel Fish, *Holocentrus Rufus*: The Role of the Telecephalon." *Behavioral and Neural Biology* 47 (1): 80–104. <http://www.ncbi.nlm.nih.gov/pubmed/3566695>.
- Landau, H.G. 1951a. "On Dominance Relations and the Structure of Animal Societies: I. Effect of Inherent Characteristics." *Bulletin of Mathematical Biology* 13 (1).
Springer: 1–19.
- Landau, H.G. 1951b. "On Dominance Relations and the Structure of Animal Societies: II. Some Effects of Possible Social Factors." *Bulletin of Mathematical Biology* 13 (4).
Springer: 245–62.
- Leatherland, J.F. 1985. "Effects of 17 Beta-Estradiol and Methyl Testosterone on the Activity of the Thyroid Gland in Rainbow Trout, *Salmo Gairdneri* Richardson." *General and Comparative Endocrinology* 60 (3): 343–52.
- Liang, H. L., S. Ongwijitwat, and M.T.T. Wong-Riley. 2006. "Bigenomic Functional Regulation of All 13 Cytochrome c Oxidase Subunit Transcripts in Rat Neurons in Vitro and in Vivo." *Neuroscience* 140 (1): 177–90.
doi:10.1016/j.neuroscience.2006.01.056.
- Lusseau, D. 2003. "The Emergent Properties of a Dolphin Social Network." *Proc. Roc. Soc. B.* 270 Suppl: S186-8. doi:10.1098/rsbl.2003.0057.
- Lusseau, D. and M. E. J. Newman. 2004. "Identifying the Role That Animals Play in Their Social Networks." *Proc. Roc. Soc. B.* 271 (Supplement 6): S477–81.
doi:10.1098/rsbl.2004.0225.
- Lusseau, D., K. Schneider, O.J. Boisseau, P. Haase, E. Slooten, and S.M. Dawson. 2003. "The Bottlenose Dolphin Community of Doubtful Sound Features a Large Proportion of Long-Lasting Associations: Can Geographic Isolation Explain This Unique Trait?" *Behavioral Ecology and Sociobiology* 54 (4): 396–405.
doi:10.1007/s00265-003-0651-y.

- Ma, L., S. Narayana, D.A. Robin, P.T. Fox, and J. Xiong. 2011. "Changes Occur in Resting State Network of Motor System during 4 Weeks of Motor Skill Learning." *NeuroImage* 58 (1): 226–33. doi:10.1016/j.neuroimage.2011.06.014.
- Maney, D.L., C.T. Goode, H.S. Lange, S.E. Sanford, and B.L. Solomon. 2008. "Estradiol Modulates Neural Responses to Song in a Seasonal Songbird." *Journal of Comparative Neurology* 511 (2): 173–86. doi:10.1002/cne.21830.
- Maruska, K.P. 2015. "Social Transitions Cause Rapid Behavioral and Neuroendocrine Changes." *Integrative and Comparative Biology* 55 (2): 294–306. doi:10.1093/icb/icv057.
- Maruska, K.P., R.E. Carpenter, and R.D. Fernald. 2012. "Characterization of Cell Proliferation throughout the Brain of the African Cichlid Fish *Astatotilapia Burtoni* and Its Regulation by Social Status." *Journal of Comparative Neurology* 520 (15): 3471–91. doi:10.1002/cne.23100.
- Maruska, K.P., and R.D. Fernald. 2010. "Behavioral and Physiological Plasticity: Rapid Changes during Social Ascent in an African Cichlid Fish." *Hormones and Behavior* 58 (2): 230–40. doi:10.1016/j.yhbeh.2010.03.011.
- Maruska, K.P., and R.D. Fernald. 2011. "Plasticity of the Reproductive Axis Caused by Social Status Change in an African Cichlid Fish: II. Testicular Gene Expression and Spermatogenesis." *Endocrinology* 152 (1): 291–302. doi:10.1210/en.2010-0876.
- Maruska, K.P., and R.D. Fernald. 2013. "Social Regulation of Male Reproductive Plasticity in an African Cichlid Fish." *Integrative and Comparative Biology* 53 (6): 938–50. doi:10.1093/icb/ict017.
- Maruska, K.P., B. Levavisivan, J. Biran, and R.D. Fernald. 2011. "Status Change in an African Cichlid Fish: I. Pituitary." *Endocrinology* 152 (1): 281–90. doi:10.1210/en.2010-0875.
- Maruska, K.P., A. Zhang, A. Neboori, and R. D. Fernald. 2013. "Social Opportunity Causes Rapid Transcriptional Changes in the Social Behaviour Network of the Brain in an African Cichlid Fish." *Journal of Neuroendocrinology* 25 (2): 145–57. doi:10.1111/j.1365-2826.2012.02382.x.
- McDonald, M.M., C.M. Markham, A. Norvelle, H. E. Albers, and K.L. Huhman. 2012. "GABA A Receptor Activation in the Lateral Septum Reduces the Expression of Conditioned Defeat and Increases Aggression in Syrian Hamsters." *Brain Research* 1439: 27–33. doi:10.1016/j.brainres.2011.12.042.
- Michels, G., and U.C. Hoppe. 2008. "Rapid Actions of Androgens." *Frontiers in Neuroendocrinology* 29 (2): 182–98. doi:10.1016/j.yfrne.2007.08.004.
- Mueller, T., Z. Dong, M.A. Berberoglu, and S. Guo. 2011. "The Dorsal Pallium in Zebrafish, *Danio rerio* (Cyprinidae, Teleostei)." *Brain Research* 49: 95–105. doi:10.1016/j.brainres.2010.12.089.The.

- Munchrath, L.A., and H.A. Hofmann. 2010. "Distribution of Sex Steroid Hormone Receptors in the Brain of an African Cichlid Fish, *Astatotilapia Burtoni*." *Journal of Comparative Neurology* 518 (16): 3302–26. doi:10.1002/cne.22401.
- Neumeister, H., K.W. Whitaker, H.A. Hofmann, and T. Preuss. 2010. "Social and Ecological Regulation of a Decision-Making Circuit." *Journal of Neurophysiology* 104: 3180–88. doi:10.1152/jn.00574.2010.
- Newman, S.W. 1999. "The Medial Extended Amygdala in Male Reproductive Behavior. A Node in the Mammalian Social Behavior Network." *Annals of the New York Academy of Sciences* 877: 242–57. doi:10.1111/j.1749-6632.1999.tb09271.x.
- Northcutt, R. G. 2011. "Do Teleost Fishes Possess a Homolog of Mammalian Isocortex?" *Brain, Behavior and Evolution* 78 (2): 136–38. doi:10.1159/000330830.
- O'Connell, L.A., M.M. Rigney, D.W. Dykstra, and H.A. Hofmann. 2013. "Neuroendocrine Mechanisms Underlying Sensory Integration of Social Signals." *Journal of Neuroendocrinology* 25 (7): 644–54. doi:10.1111/jne.12045.
- O'Connell, L.A., J.H. Ding, and H.A. Hofmann. 2013. "Sex Differences and Similarities in the Neuroendocrine Regulation of Social Behavior in an African Cichlid Fish." *Hormones and Behavior* 64 (3): 468–76. doi:10.1016/j.yhbeh.2013.07.003.
- O'Connell, L.A., and H.A. Hofmann. 2011. "The Vertebrate Mesolimbic Reward System and Social Behavior Network: A Comparative Synthesis." *Journal of Comparative Neurology* 519 (18): 3599–3639. doi:10.1002/cne.22735.
- O'Connell, L.A., and H.A. Hofmann. 2012. "Evolution of a Vertebrate Social Decision-Making Network." *Science* 336 (6085): 1154–57. doi:10.1126/science.1218889.
- O'Connell, L.A., and H.A. Hofmann. 2012. "Social Status Predicts How Sex Steroid Receptors Regulate Complex Behavior across Levels of Biological Organization." *Endocrinology* 153 (3): 1341–51. doi:10.1210/en.2011-1663.
- Oh, K.P., and A.V. Badyaev. 2010. "Structure of Social Networks in a Passerine Bird: Consequences for Sexual Selection and the Evolution of Mating Strategies." *The American Naturalist* 176 (3): 80–89. doi:10.1086/655216.
- Okuno, H. 2011. "Regulation and Function of Immediate-Early Genes in the Brain : Beyond Neuronal Activity Markers." *Neuroscience Research* 69 (3): 175–86. doi:10.1016/j.neures.2010.12.007.
- Parikh, V.N., T. Clement, and R.D. Fernald. 2006a. "Physiological Consequences of Social Descent: Studies in *Astatotilapia Burtoni*." *Journal of Endocrinology* 190 (1): 183–90. doi:10.1677/joe.1.06755.
- Parikh, V.N., T.S. Clement, and R.D. Fernald. 2006b. "Androgen Level and Male Social Status in the African Cichlid, *Astatotilapia Burtoni*." *Behavioural Brain Research* 166 (2): 291–95. doi:10.1016/j.bbr.2005.07.011.

- Pohlert, T. 2014. "The Pairwise Multiple Comparison of Mean Ranks Package (PMCMR)." *R Package*, 27.
doi:<http://cran.ms.unimelb.edu.au/web/packages/PMCMR/vignettes/PMCMR.pdf>.
- Potegal, M., A. Blau, and M. Glusman. 1981. "Effects of Anteroventral Septal Lesions on Intraspecific Aggression in Male Hamsters." *Physiology and Behavior* 26 (3): 407–12. doi:10.1016/0031-9384(81)90167-0.
- Powers, A.R., M.A. Hevey, and M.T. Wallace. 2012. "Neural Correlates of Multisensory Perceptual Learning." *Journal of Neuroscience* 32 (18): 6263–74.
doi:10.1523/JNEUROSCI.6138-11.2012.
- Poyet, P., and F. Labrie. 1985. "Comparison of the Antiandrogenic/androgenic Activities of Flutamide, Cyproterone Acetate and Megestrol Acetate." *Molecular and Cellular Endocrinology* 42 (3): 283–88. doi:10.1016/0303-7207(85)90059-0.
- R Core Team. 2016. "R: A Language and Environment for Statistical Computing." Vienna, Austria. <https://www.r-project.org/>.
- Remage-Healey, L., and A.H. Bass. 2006. "A Rapid Neuromodulatory Role for Steroid Hormones in the Control of Reproductive Behavior." *Brain Research* 1126 (1): 27–35. doi:10.1016/j.brainres.2006.06.049.
- Renn, S.C.P., N. Aubin-Horth, and H.A. Hofmann. 2008. "Fish and Chips: Functional Genomics of Social Plasticity in an African Cichlid Fish." *Journal of Experimental Biology* 211 (18): 3041–56. doi:10.1242/jeb.018242.
- Renn, S.C.P., J.B. Carleton, H. Magee, M.L.T. Nguyen, and A.C.W. Tanner. 2009. "Maternal Care and Altered Social Phenotype in a Recently Collected Stock of *Astatotilapia Burtoni* Cichlid Fish." *Integrative and Comparative Biology* 49 (6): 660–73. doi:10.1093/icb/icp085.
- Rooney, D.J., and P.R. Laming. 1986. "Localization of Telencephalic Regions Concerned with Habituation of Cardiac and Ventilatory Responses Associated with Arousal in the Goldfish (*Carassius Auratus*)." *Behavioral Neuroscience* 100 (1): 45–50.
<http://www.ncbi.nlm.nih.gov/pubmed/3954879>.
- Rose, G.J. 2004. "Insights into Neural Mechanisms and Evolution of Behaviour from Electric Fish." *Nature Reviews. Neuroscience* 5 (12): 943–51. doi:10.1038/nrn1558.
- Rosenquist, J.N., J.H. Fowler, and N.A. Christakis. 2011. "Social Network Determinants of Depression." *Molecular Psychiatry* 16 (3): 273–81. doi:10.1038/mp.2010.13.
- Royle, N.J., T.W. Pike, P. Heeb, H. Richner, and M. Kölliker. 2012. "Offspring Social Network Structure Predicts Fitness in Families." *Proc. Roc. Soc. B.* 279 (1749): 4914–22. doi:10.1098/rspb.2012.1701.
- Rozen, S., and H.J. Skaletsky. 1998. "Primer3." *Bioinformatics Methods and Protocols Methods in Molecular Biology*.

http://www-genome.wi.mit.edu/genome_software/other/primer3.html.

- Rubin, R.D, P.D. Watson, M.C. Duff, and N.J. Cohen. 2014. "The Role of the Hippocampus in Flexible Cognition and Social Behavior." *Front Hum Neurosci* 8: 742. doi:10.3389/fnhum.2014.00742.
- Ryder, T.B., D.B. McDonald, J.G. Blake, P.G. Parker, and B.A. Loiselle. 2008. "Social Networks in the Lek-Mating Wire-Tailed Manakin (*Pipra Filicauda*)." *Proc. Roc. Soc. B.* 275 (1641): 1367–74. doi:10.1098/rspb.2008.0205.
- Ryder, T.B., P.G. Parker, J.G. Blake, and B.A. Loiselle. 2009. "It Takes Two to Tango: Reproductive Skew and Social Correlates of Male Mating Success in a Lek-Breeding Bird." *Proc. Roc. Soc. B.* 276 (1666): 2377–84. doi:10.1098/rspb.2009.0208.
- Sakata, J.T., P. Coomber, F. Gonzalez-Lima, and D. Crews. 2000. "Functional Connectivity among Limbic Brain Areas: Differential Effects of Incubation Temperature and Gonadal Sex in the Leopard Gecko, *Eublepharis Macularius*." *Brain, Behavior and Evolution* 55 (3): 139–51. doi:6648.
- Sakata, J.T., and D. Crews. 2004. "Cytochrome Oxidase Activity in the Preoptic Area Correlates with Differences in Sexual Behavior of Intact and Castrated Male Leopard Geckos (*Eublepharis Macularius*)." *Behav Neurosci* 118 (4): 857–62. doi:10.1037/0735-7044.118.4.857.
- Sakata, J.T., and D. Crews. 2004. "Developmental Sculpting of Social Phenotype and Plasticity." *Neuroscience and Biobehavioral Reviews*. 28(2):95-112. doi:10.1016/j.neubiorev.2004.01.001.
- Sapolsky, R.M. 2005. "The Influence of Social Hierarchy on Primate Health." *Science* 308 (5722): 648–52. doi:10.1126/science.1106477.
- Schafer, J.L., and J.W. Graham. 2002. "Missing Data: Our View of the State of the Art." *Psychological Methods* 7 (2): 147–77. doi:10.1037//1082-989X.7.2.147.
- Schindelin, J., I. Arganda-Carreras, E. Frise, V. Kaynig, M. Longair, T. Pietzsch, Stephan Preibisch, et al. 2012. "Fiji: An Open Source Platform for Biological Image Analysis." *Nature Methods* 9 (7): 676–82. doi:10.1038/nmeth.2019.Fiji.
- Schlinger, B.A., and G.V. Callard. 1989. "Aromatase Activity in Quail Brain: Correlation with Aggressiveness." *Endocrinology* 124 (1): 437–43. doi:10.1210/endo-124-1-437.
- Schürch, R., S. Rothenberger, and D. Heg. 2010. "The Building-up of Social Relationships: Behavioural Types, Social Networks and Cooperative Breeding in a Cichlid." *Phil. Tran. Roc. Soc. B* 365 (1560): 4089–98. doi:10.1098/rstb.2010.0177.
- Silverin, B., M. Baillien, and J. Balthazart. 2004. "Territorial Aggression, Circulating Levels of Testosterone, and Brain Aromatase Activity in Free-Living Pied Flycatchers." *Hormones and Behavior* 45 (4): 225–34.

doi:10.1016/j.yhbeh.2003.10.002.

- Simões, J.M., E.N. Barata, R.M. Harris, L.A. O'Connell, and H.A. Hofmann. 2015. "Social Odors Conveying Dominance and Reproductive Information Induce Rapid Physiological and Neuromolecular Changes in a Cichlid Fish" *BMC Genomics* 16:114. doi:10.1186/s12864-015-1255-4.
- Simon, Neal G, and Richard E Whalen. 1986. "Hormonal Regulation of Aggression: Evidence for a Relationship among Genotype, Receptor Binding, and Behavioral Sensitivity to Androgen and Estrogen." *Aggressive Behavior* 12 (4): 255–66.
- Soma, K.K., M.A.L. Scotti, A.E.M. Newman, T.D. Charlier, and G.E. Demas. 2008. "Novel Mechanisms for Neuroendocrine Regulation of Aggression." *Frontiers in Neuroendocrinology*. doi:10.1016/j.yfrne.2007.12.003.
- Sporns, O. 2009. "Networks of the Brain." *MIT Press, Cambridge, MA*.
- Suzuki, R., and H. Shimodaira. 2015. "Pvclust: Hierarchical Clustering with P-Values via Multiscale Bootstrap Resampling." <https://cran.r-project.org/package=pvclust>.
- Taborsky, B., and R.F. Oliveira. 2012. "Social Competence: An Evolutionary Approach." *Trends in Ecology and Evolution* 27 (12): 679–88. doi:10.1016/j.tree.2012.09.003.
- Teles, M.C., and R.F. Oliveira. 2016. "Androgen Response to Social Competition in a Shoaling Fish." *Hormones and Behavior* 78: 8–12. doi:10.1016/j.yhbeh.2015.10.009.
- Teles, M.C., O. Almeida, J.S. Lopes, R.F. Oliveira. 2015. "Social Interactions Elicit Rapid Shifts in Functional Connectivity in the Social Decision-Making Network of Zebrafish." *Proc. Roc. Soc. B.* 282 (1816): 20151099. doi:10.1098/rspb.2015.1099.
- Thompson, A., D. Vo, C. Comfort, and H.H. Zakon. 2014. "Expression Evolution Facilitated the Convergent Neofunctionalization of a Sodium Channel Gene." *Molecular Biology and Evolution* 31 (8): 1941–55. doi:10.1093/molbev/msu145.
- Toda, K., T. Saibara, T. Okada, S. Onishi, and Y. Shizuta. 2001. "A Loss of Aggressive Behaviour and Its Reinstatement by Oestrogen in Mice Lacking the Aromatase Gene (Cyp19)." *Journal of Endocrinology* 168 (2): 217–20. doi:10.1677/joe.0.1680217.
- Torchiano, M. 2016. "Effsize: Efficient Effect Size Computation." <https://cran.r-project.org/package=effsize>.
- Trainor, B.C., K.M. Greiwe, and R.J. Nelson. 2006. "Individual Differences in Estrogen Receptor α in Select Brain Nuclei Are Associated with Individual Differences in Aggression." *Hormones and Behavior* 50 (2): 338–45. doi:10.1016/j.yhbeh.2006.04.002.
- Trainor, B.C., H.H. Kyomen, and C.A. Marler. 2006. "Estrogenic Encounters: How Interactions between Aromatase and the Environment Modulate Aggression." *Frontiers in Neuroendocrinology* 27 (2): 170–79. doi:10.1016/j.yfrne.2005.11.001.

- Tseng, Q. 2016. "Adaptive Threshold ImageJ Plugin." Accessed January 1. <https://sites.google.com/site/qingzongtseng/adaptivethreshold>.
- Vahdat, S., M. Darainy, T.E. Milner, and D.J. Ostry. 2011. "Functionally Specific Changes in Resting-State Sensorimotor Networks after Motor Learning." *Journal of Neuroscience* 31 (47): 16907–15. doi:10.1523/JNEUROSCI.2737-11.2011.
- Viguié-Martinez, M. C., M. T. H. Reviers, B. Barenton, and C. Perreau. 1983. "Effects of a Non-Steroidal Antiandrogen, Flutamide, on the Hypothalamo-Pituitary Axis, Genital Tract and Testis in Growing Male Rats: Endocrinological and Histological Data." *Acta Endocrinologica* 102 (2): 299–306. doi:10.1530/acta.0.1020299.
- Vullioud, P., R. Bshary, and A.F.H. Ros. 2013. "Intra- and Interspecific Aggression Do Not Modulate Androgen Levels in Dusky Gregories, yet Male Aggression Is Reduced by an Androgen Blocker." *Hormones and Behavior* 64 (3): 430–38. doi:10.1016/j.yhbeh.2013.06.007.
- Wahli, W., and E. Martinez. 1991. "Superfamily of Steroid Nuclear Receptors: Positive and Negative Regulators of Gene Expression." *The FASEB Journal* 5 (9): 2243–49.
- Wang, C., Y. Liu, and J.M.C. 2014. "G Protein-Coupled Receptors: Extranuclear Mediators for the Non-Genomic Actions of Steroids." *International Journal of Molecular Sciences*. doi:10.3390/ijms150915412.
- Ward, A.J.W., M.S. Botham, D.J. Hoare, R. James, M. Broom, J.J. Godin, and J. Krause. 2002. "Association Patterns and Shoal Fidelity in the Three-Spined Stickleback." *Proc. R. Soc. B.* 269 (1508): 2451–55. doi:10.1098/rspb.2002.2169.
- Weitekamp, C.A., and H.A. Hofmann. 2014. "Evolutionary Themes in the Neurobiology of Social Cognition." *Current Opinion in Neurobiology* 28:22-7. doi:10.1016/j.conb.2014.06.005.
- Weitekamp, C.A., and H.A. Hofmann. 2017. "Neuromolecular Correlates of Cooperation and Conflict during Territory Defense in a Cichlid Fish." *Hormones and Behavior* 89: 145–56. doi:10.1016/j.yhbeh.2017.01.001.
- Welsh, T.H., T.H. Bambino, and A.J. Hsueh. 1982. "Mechanism of Glucocorticoid-Induced Suppression of Testicular Androgen Biosynthesis in Vitro." *Biology of Reproduction* 27 (5): 1138–46. doi:10.1095/biolreprod27.5.1138.
- Wendelaar, B.S.E. 1997. "The Stress Response in Fish." *Physiological Reviews* 77 (3): 591–625. doi:stress physiologie comportement cortisol cerveau hypophyse catecholamine osmoregulation branchie.
- White, D.J., A.S Gersick, and N. Snyder-Mackler. 2012. "Social Networks and the Development of Social Skills in Cowbirds." *Philosophical Transactions of the Royal Society of London. Series B, Biological Sciences* 367 (1597): 1892–1900. doi:10.1098/rstb.2011.0223.
- White, S.A., T. Nguyen, and R.D. Fernald. 2002. "Social Regulation of Gonadotropin-

- Releasing Hormone.” *The Journal of Experimental Biology* 205 (17): 2567–81.
- Whitehead, H. 2009. “SOCPROG Programs: Analysing Animal Social Structures.” *Behavioral Ecology and Sociobiology* 63 (5): 765–78. doi:10.1007/s00265-008-0697-y.
- Williams, R., and D. Lusseau. 2006. “A Killer Whale Social Network Is Vulnerable to Targeted Removals.” *Biology Letters* 2 : 497–500. doi:10.1098/rsbl.2006.0510.
- Williamson, C.M., B. Franks, and J.P. Curley. 2016. “Mouse Social Network Dynamics and Community Structure Are Associated with Plasticity-Related Brain Gene Expression.” *Frontiers in Behavioral Neuroscience* 10 : 152. doi:10.3389/fnbeh.2016.00152.
- Wingfield, J.C., and T.P. Hahn. 1994. “Testosterone and Territorial Behaviour in Sedentary and Migratory Sparrows.” *Animal Behaviour* 47 (1): 77–89. doi:10.1006/anbe.1994.1009.
- Wingfield, J.C., R.E. Hegner, A.M. Dufty jr., and G.F. Ball. 1990. “The ‘Challenge Hypothesis’: Theoretical Implications for Patterns of Testosterone Secretion, Mating Systems, and Breeding Strategies.” *The American Naturalist* 136 (6): 829–46. doi:10.1086/285134.
- Wong-Riley, M.T.T 1989. “Cytochrome Oxidase: An Endogenous Metabolic Marker for Neuronal Activity.” *Trends in Neurosciences*. doi:10.1016/0166-2236(89)90165-3.
- Wong-Riley, M.T.T, F. Nie, R.F. Hevner, and S.Y. Liu. 1998. “Brain Cytochrome Oxidase - Functional Significance and Bigenomic Regulation in the CNS.” *Cytochrome Oxidase in Neuronal Metabolism and Alzheimer’s Disease*, 1–53.
- Wong, L.C., L. Wang, J.A. D’Amour, T. Yumita, G. Chen, T. Yamaguchi, B.C. Chang, H. Bernstein, X. You, J.E. Feng, R.C. Froemke and D. Lin. 2016. “Effective Modulation of Male Aggression through Lateral Septum to Medial Hypothalamus Projection.” *Current Biology* 26 (5): 593–604. doi:10.1016/j.cub.2015.12.065.
- Wyart, V., and C. Tallon-Baudry. 2009. “How Ongoing Fluctuations in Human Visual Cortex Predict Perceptual Awareness: Baseline Shift versus Decision Bias.” *Journal of Neuroscience* 29 (27): 8715–25. doi:10.1523/JNEUROSCI.0962-09.2009.
- Yang, E.J., and W. Wilczynski. 2007. “Social Experience Organizes Parallel Networks in Sensory and Limbic Forebrain.” *Developmental Neurobiology* 67 (3): 285–303. doi:10.1002/dneu.20347.
- Ye, L., W.E.E. Allen, K.R.R. Thompson, Q. Tian, B. Hsueh, C. Ramakrishnan, A.C. Wang, J.H. Jennings, A. Adhikari, C.H. Halpern, I.B. Witten, A.L. Barth, L. Luo, J.A. McNab and K. Deisseroth. 2016. “Wiring and Molecular Features of Prefrontal Ensembles Representing Distinct Experiences.” *Cell* 165 (7): 1776–88. doi:10.1016/j.cell.2016.05.010.
- Zar, J.H. 1999. *Biostatistical Analysis*. Prentice Hall.

<https://books.google.com/books?id=edxqAAAAMAAJ>.

Zeman, W., and F.A. King. 1958. "Tumors of the Septum Pellucidum and Adjacent Structures with Abnormal Affective Behavior: An Anterior Midline Structure Syndrome." *The Journal of Nervous and Mental Disease* 127 (6):490–502.

Zumpe, D., R.W. Bonsall, and R.P. Michael. 1993. "Effects of the Nonsteroidal Aromatase Inhibitor, Fadrozole, on the Sexual Behavior of Male Cynomolgus Monkeys (*Macaca Fascicularis*)." *Hormones & Behavior* 27 (2): 200–15.

Vita

Sean Martin Maguire was born and raised in Leyden, Massachusetts. He graduated from the University of Massachusetts - Amherst in 2008, with a degree in biochemistry and molecular biology. After graduation he took a research assistant position under the supervision of Dr. Mark Alkema where he conducted studies on *C. elegans* worms and was first exposed to the amazing study of animal behavior. He enrolled in the Ecology, Evolution and Behavior graduate program at the University of Texas at Austin in 2010 under the supervision of Hans Hofmann where his work focused on the mechanistic basis of behavior in cichlid fish.

Permanent address: smmaguire@gmail.com

This dissertation was typed by the author.